EXPERIMENTAL AND THEORETICAL INVESTIGATION OF THE REACTIVITY OF PARTIALLY FLUORINATED RADICALS

By

MICHAEL DAVID BARTBERGER

A DISSERTATION PRESENTED TO THE GRADUATE SCHOOL
OF THE UNIVERSITY OF FLORIDA IN PARTIAL FULFILLMENT
OF THE REQUIREMENTS FOR THE DEGREE OF
DOCTOR OF PHILOSOPHY

UNIVERSITY OF FLORIDA

1998

ACKNOWLEDGEMENTS

Among the great number of individuals with whom I have interacted throughout the course of my education at the University of Florida and elsewhere, I wish to express my sincere appreciation to the special few that have motivated, challenged, and inspired me.

I extend my deepest gratitude to Prof. William R. Dolbier, Jr., an outstanding scientist and truly exceptional educator, for his excellent guidance, support, and friendship throughout the course of my graduate career. My appreciation for the knowledge he has shared with me, as well as his patience and level of understanding, particularly during periods of difficulty and stress, can not be overstated.

I wish to thank the two finest classroom instructors I have ever had--my first college level chemistry teacher, Dr. Jeanette Madea, for her profound influence in my decision to pursue a career in the chemical sciences, and Prof. Seth Elsheimer, for my initial exposure to the fascinating area of organofluorine chemistry in 1990 and his friendship thereafter.

I am indebted to Dr. Max Muir for introducing me to computational chemistry. The experience I have gained in the use of molecular orbital methods as a tool for the understanding of chemical reactivity is due entirely to him. Special thanks go to Prof. Benjamin Horenstein for his helpful discussions and generosity with regard to computational resources.

I thank my colleagues, past and present, in both the Dolbier group and the Department of Chemistry as a whole. A few bear special mention--Dr. Keith Palmer, for his friendship and advice during my first year in the group; Dr. Xiao Xin Rong and He-Qi

Pan, for their camaraderie and early assistance with radical kinetics; Dr. Conrad Burkholder, for numerous stimulating discussions; and Dr. Henryk Koroniak, Michelle Fletcher, Lian Luo, Feng Tian, and Kevin Ley for their friendship (and tolerance!) throughout the course of my stay in the department.

I wish to thank my graduate committee, particularly the "organic" portion thereof--Profs. Merle Battiste and Kirk Schanze, for their advice and encouragement. Also, special thanks go to Prof. R. J. Bartlett for taking seriously my interest in theoretical methodology and the invitations to participate in his workshops on Applied Molecular Orbital Theory.

I am especially grateful to my very best friend, Cynthia Dawn Zook, for her unrelenting moral support and encouragement over the last several years. Finally, I wish to acknowledge my parents, George Charles and Beverly Jean, for instilling in me the work ethic which has likely had as much to do with the successful completion of this work as any of the chemistry I ever learned.

TABLE OF CONTENTS

ACKNOWLEDGEMENTS ii

ABSTRACT vi

CHAPTER

1 AN OVERVIEW OF ORGANIC FREE RADICAL REACTIONS 1

Introduction 1
Radical Chain Processes. 2
Hydrogen Atom Abstraction Reactions 4
Intermolecular Radical Addition Reactions 9
Intramolecular Addition Reactions: Radical Cyclizations 13
Methods for Determination of Organic Radical Kinetics 22
Conclusion 26

2 THE FLUORINE SUBSTITUENT IN ORGANIC SYSTEMS 28

Introduction 28
Structure, Bonding, and Reactivity in Saturated Systems 29
Structure, Bonding, and Reactivity in Unsaturated Systems 31
Fluorine Non-Bonded Interactions in Reactive Intermediates 33
Fluorine Steric Effects 35
The Fluorine Substituent in Free Radicals 37
Organofluorine Radical Reactivity 40
Conclusion 48

3 THE REACTIVITY OF PARTIALLY FLUORINATED RADICALS IN INTERMOLECULAR ADDITION AND HYDROGEN ABSTRACTION REACTIONS 49

Introduction 49
Precursor Syntheses and Competitive Kinetic Studies. 50
Discussion 61
Conclusion 76

4 THE REACTIVITY OF PARTIALLY FLUORINATED RADICALS IN INTRAMOLECULAR CYCLIZATION REACTIONS 77

Introduction 77
Precursor Syntheses and Competitive Kinetic Studies 78
Discussion 89
Conclusion 100

5 EXPERIMENTAL 102

General Methods- Experimental 102
General Methods- Theoretical. 103
Synthetic Procedures 103
Competitive Kinetic Procedures 129

APPENDIX A: SELECTED ^{19}F NMR SPECTRA 136

APPENDIX B: B3LYP/6-31G(d) TOTAL AND ZERO-POINT ENERGIES FOR DATA IN TABLES 3-3 AND 3-4 172

REFERENCES 175

BIOGRAPHICAL SKETCH 185

Abstract of Dissertation Presented to the Graduate School
of the University of Florida in Partial Fulfillment of the
Requirements for the Degree of Doctor of Philosophy

EXPERIMENTAL AND THEORETICAL INVESTIGATION OF THE REACTIVITY OF PARTIALLY FLUORINATED RADICALS

By

Michael David Bartberger

May 1998

Chairman: William R. Dolbier, Jr.
Major Department: Chemistry

The reactivities of a series of partially-fluorinated radicals towards intermolecular addition, hydrogen abstraction, and intramolecular cyclization have been investigated. Based on competitive kinetic techniques and absolute rate contants for addition of these radicals to styrene obtained by laser flash photolysis, absolute rate constants for abstraction of hydrogen from tributylstannane have been determined for 1,1-difluoroalkyl, 2,2-difluoroalkyl, 1,1,2,2-tetrafluoroalkyl, 3-perfluoroalkyl, and pentafluoroethyl radicals. Fluorination at the 3-position of an alkyl radical was found to exert a negligible effect on the kinetics of hydrogen abstraction. All other systems exhibit rate enhancements relative to non-fluorinated analogues, the magnitudes of which are dependent upon the degree and location of fluorine substitution. A parallel computational study was performed utilizing density functional calculations, providing estimates of carbon-carbon and carbon-hydrogen bond dissociation energies (BDEs) for hydrofluorocarbons. The observed kinetic enhancements were attributed to a combination of structural, charge transfer, and enthalpic effects, due to the pyramidal nature of 1-fluoralkyl radicals, increased electrophilic character induced by successive fluorination, and thermodynamics of carbon-carbon and carbon-hydrogen bond

formation. From the computation of partial atomic charges in fluoroalkanes, the contrasting effect of 1-fluorination on carbon-carbon and carbon-hydrogen BDEs and the consistent strengthening effect of such substitution at the 2-position have been explained on the basis of Coulombic interactions.

Based on the rate constants obtained for hydrogen abstraction, absolute rate constants for *5-exo* and *6-endo* intramolecular cyclization for a series of partially fluorinated 5-hexenyl radicals have been obtained. These observed rates of cyclization may be rationalized by the same combination of effects influencing their bimolecular addition reactions. In some cases, the rate of *6-endo* closure is dramatically accelerated relative to the parent hydrocarbon without the introduction of reversibility of ring closure.

CHAPTER 1

AN OVERVIEW OF ORGANIC FREE RADICAL REACTIONS

Introduction

The discovery of the first free radical, triphenylmethyl, by Moses Gomberg[1] in 1900 initiated considerable effort directed toward the understanding of radical reactivity. However, only after a series of pioneering investigations undertaken more than thirty years later were the primary mechanistic pathways available to organic free radicals well elucidated.[2-6] These studies, most notably those of Kharasch *et al.*,[4-7] demonstrated that most radical processes can be expressed in terms of a small number of elementary steps, or variations thereof, as shown below in Figure 1-1.[8]

$A^{\bullet} + B^{\bullet} \rightleftharpoons A\text{-}B$	coupling / homolysis	(1-1)
$A^{\bullet} + B\text{-}D \rightleftharpoons A\text{-}B + D^{\bullet}$	substitution (S_H2)	(1-2)
$A^{\bullet} + B{=}D \rightleftharpoons A\text{-}B\text{-}D^{\bullet}$	addition / β-fission	(1-3)
$A^{\bullet} + e \rightleftharpoons A^{-}$;	electron transfer	(1-4)
$A^{\bullet} - e \rightleftharpoons A^{+}$		

Figure 1-1. The Elementary Mechanistic Pathways of Free Radical Reactions.

Despite these breakthroughs, organic free radical reactions continued for years to be regarded as unpredictable, unselective, and in general inadaptable to synthetic application. Fortunately, subsequent kinetic and thermochemical studies have served to uncover the factors governing the reactivity of organic radicals, and consequently in recent years sentiment toward the utility of free radicals in synthesis has drastically changed. Indeed, the number of elegant works in the literature based on radical

mediated transformations is a testament to their applicability in the construction of natural products and other complex synthetic targets.[9-15] It is the purpose of this introductory chapter to acquaint the reader with the fundamental types of free radical processes which occur in organic systems, as well as to provide an overview of the wealth of physical studies which have given rise to the current level of understanding of organic radical reactivity.

Radical Chain Processes

Most free radical reactions occur via a sequence of chain events, propagated by intermediate steps during the course of the reaction. An example illustrating a competition between two potential pathways is provided in Figure 1-2.

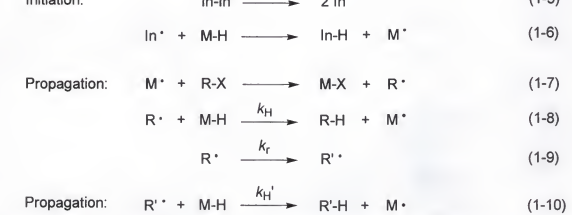

Figure 1-2. Radical Chain Process Involving Competition Between Rearrangement versus Hydrogen Atom Transfer from a Donor Molecule M-H.

Homolysis of an initiator, typically accomplished by thermal or photochemical means, provides a source of (often metal centered) radicals M• (equation 1-6) from which intermediate radicals R• are generated by reaction with a suitable precursor R-X (equation 1-7). This species encounters one of two fates: trapping, in this case by hydrogen atom donor, to yield R-H (equation 1-8) or transformation via a unimolecular or bimolecular process (equation 1-9) to form radical R'•, itself then trapped producing

R'-H. In either case, additional metal radicals are formed and the chain process continued via the propagation steps given in equations 1-7, 1-8 and 1-10.

The distribution of products R-H and R'-H is governed by the relative propensity of R$^{\bullet}$ toward rearrangement versus trapping (that is, k_r and $k_{H,}$) the latter dependent on both the nature of R$^{\bullet}$ and the type of trapping agent employed. In systems where trapping is fast relative to rearrangement ($k_H >> k_r$), the partitioning radical R$^{\bullet}$ is converted to R-H with little or no rearranged product. However, if k_H and k_r are of comparable magnitude, product mixtures result. An understanding of the reactivity of a radical intermediate toward potential competing processes is therefore essential for the design of useful kinetic experiments, as well as for the development of effective synthetic strategies.

For an efficient chain process, it is necessary that the propagation steps are rapid relative to chain termination steps, thereby maintaining a low but constant concentration of radical intermediates. Besides the obvious practical benefit (higher product yields) resulting from such a condition, the occurrence of undesired chain termination side reactions such as disproportionation and radical-radical coupling, possibly complicating kinetic analyses, is minimized. In many cases, this may be achieved by judicious selection of the type and concentrations of precursor R-X and trapping agent.

This procedure enjoys wide application in both kinetic and synthetic studies requiring the controlled generation of radical intermediates. One of its variants, likely the most commonly used procedure for the indirect (competitive) determination of the rates of organic radical reactions, is based on the trialkylstannane reduction of an alkyl halide (the "Tin Hydride Method").[16-18] Other modifications of this general procedure exist, accommodating a variety of radical precursors and trapping agents; a discussion of time-resolved and competitive techniques utilized in radical kinetic measurements is provided later in the chapter.

Finally, it is important to note the implication of *kinetic control* in the above discussion. That is, that the distribution of products R-H and R'-H may be ascribed to the relative values of k_H and k_r hinges on the absence of any thermodynamic equilibration of products under the reaction conditions. This is of vital importance in the design and interpretation of competitive kinetic studies and is discussed in detail in Chapter 3.

Radical reactivity is dependent on the "complex interplay" of thermodynamic, steric, and polar considerations.[19] The relationship between enthalpies of activation and heats of reaction, the basis of the thermochemical kinetic approach of Benson,[20] was recognized early on and holds for a number of radical addition and substitution reactions, where the order of reactivity often parallels exothermicity.[21-23] This relation has led to such overgeneralizations as "radical reactions follow the most exothermic available pathway" or ". . . afford the most stable possible product."[8] However, reaction thermochemistry is not the sole, nor even predominant decisive factor in the outcome of radical reactions. Nonbonding interactions and the electronic influence of substituents in ground and transition states (which may be rationalized in terms of Frontier Molecular Orbital (FMO) theory)[24,25] will also play a role. A discussion of the combination of these effects as manifested in hydrogen atom abstractions and inter- and intramolecular additions, the most commonly occurring and well-characterized reactions of organic free radicals, will now be presented.

Hydrogen Atom Abstraction Reactions

The vast majority of free radical applications involve the use of an organometallic hydride of the type R_3M-H (most commonly, where M = Sn, Si, or Ge) as a hydrogen atom donor and chain propagation agent, the properties of which have been the focus of extensive investigation by kineticists. Metal-hydrogen bond dissociation energies (BDEs) along with activation parameters and associated absolute rate constants for

hydrogen atom transfer to *n*-alkyl hydrocarbon radicals by a series of donors R_3M-H have been determined and are provided below in Table 1-1.[16, 26-32]

Table 1-1. Bond Dissociation Energies with Activation Parameters and Rate Constants for Hydrogen Atom Transfer to Hydrocarbon Radicals by R_3M-H.

R_3M-H	BDE, kcal · mol^{-1}	log A	E_a, kcal · mol^{-1}	k_H, 10^6 M^{-1} s^{-1} (298 K)
nBu_3SnH	73.7	9.06	3.65	2.3
$(TMS)_3SiH$	79.0	8.86	4.47	0.38
nBu_3GeH	82.6	8.44	4.70	0.093
$(TMS)_2Si(CH_3)H$	82.9	8.89	5.98	0.032
Et_3SiH	90.1	8.66	7.98	0.00064

Analysis of the data demonstrates that for hydrogen atom abstraction by structurally similar radicals from this series of donors, a direct relation holds between the rate of transfer and the strength of the metal-hydrogen bond being broken. This is depicted graphically in Figure 1-3. In addition, it is noted that in each case the pre-exponential term in the Arrhenius relation remains relatively constant. Thus, the rate variations within the series are due almost entirely to differences in activation energies.

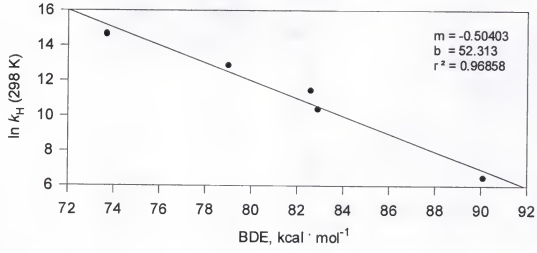

Figure 1-3. Plot of ln k_H for Alkyl Radicals versus M-H Bond Dissociation Energies for Hydrogen Atom Donors R_3M-H in Table 1-1.

However, as previously mentioned, relative thermodynamics is not the only factor which influences the kinetics of hydrogen atom transfer. The fast donor thiophenol (PhSH) reacts with primary alkyl radicals with a rate constant of 1.36×10^8 M^{-1} s^{-1} at 298 K,[33] and has been employed as a trapping agent in competitive kinetic studies involving strained or otherwise highly reactive radicals with rearrangement rates upward of 10^{11} s^{-1} and thus with lifetimes on the picosecond timescale.[34] This enhanced rate of transfer, not commensurate with its S-H BDE of 82.0 kcal · mol^{-1},[35] gives rise to a severe deviation from the plot in Figure 1-3 and indicates the presence of other influences.

Table 1-2. Absolute Rate Constants for Hydrogen Atom Transfer to *tert*-Butoxyl Radicals by R_3M-H.

R_3M-H	k_H, 10^6 M^{-1} s^{-1} (300 K)
nBu_3SnH	220
$(TMS)_3SiH$	110
nBu_3GeH	80
Et_3SiH	5.7

Further evidence may be found in the rates of hydrogen atom transfer to *tert*-butoxyl radicals by the same series of hydrogen atom donors, provided in Table 1-2 and illustrated graphically in Figure 1-4.[36,37] It is observed that for *tert*-butoxyl radicals, rates of hydrogen abstraction are at least two orders of magnitude greater than those of their *n*-alkyl counterparts. Although the relative strengths of the newly formed C-H or O-H bonds will certainly play a role, the difference in BDE between *t*BuO-H and *n*-alkyl C-H bonds (105 and 100 kcal · mol^{-1}, respectively)[38] is not sufficient to explain the increase in reactivity, especially in light of the fact that such rapid hydrogen atom abstractions should proceed with early transition states.[36]

At this time, the absolute rates of reduction of *tert*-butoxyl radicals by thiophenol have yet to be determined. However, a series of competition studies by Hartung and

Gallou[39] involving 4-pentenyl-1-oxy radicals and utilizing naphthalene 2-thiol (NpSH) as a trapping agent have determined a ratio [k_H (NpSH) / k_H (nBu_3SnH)] of 1.4. By comparison, *n*-alkyl radicals afford the ratio [k_H (PhSH) / k_H (nBu_3SnH)] = 59.1. Although a leveling effect may be partly responsible for the compressed ratio of rates for *tert*-butoxyl radicals (which are indeed within an order of magnitude of the diffusion-controlled limit)[40] it is logical to assume based on the aforementioned examples that hydrogen abstraction reactivity will be governed to some extent by factors other than simple relative BDE values of the donor species.

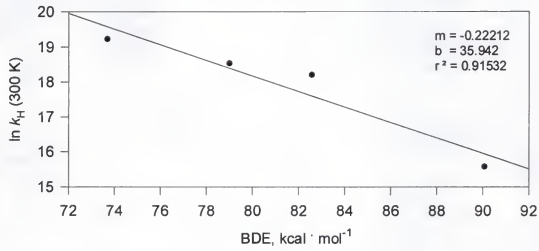

Figure 1-4. Plot of ln k_H for *tert*-Butoxyl Radicals vs. M-H Bond Dissociation Energies for Hydrogen Atom Donors R_3M-H in Table 1-2.

Chatgilialoglu *et al.*[36,37] have attributed such differences in reactivity to a polarized, or charge separated, transition state of the type depicted in Figure 1-5. Here it can be seen that in the case of an electropositive metal hydride donor, hydrogen atom transfer to alkoxyl radicals (b) is facilitated by greater stabilization of partial negative charge on oxygen relative to carbon, with a resultant decrease in activation barrier.

(a) $R_3M^{\delta+}$ ----- H ----- $R^{\delta-}$ (b) $R_3M^{\delta+}$ ----- H ----- $OR^{\delta-}$

Figure 1-5. Charge Polarized Transition State for Hydrogen Abstraction from R_3M-H by (a) Alkyl and (b) Alkoxyl radicals.

In the case of thiol donors, the opposite situation ensues. The greater electronegativity of sulfur relative to tin (or other metal atom) gives rise to a reversal in the transition state charge distribution. This arrangement, involving a partially negatively charged sulfur atom, is better suited to the more nucleophilic alkyl radical, where in the alkoxyl case a less- or non-polarized transition state results. Such a mismatch in the latter is partially responsible for the decrease in rate enhancement for hydrogen abstraction from thiols by alkoxyl radicals, relative to their alkyl analogues.

Frontier Molecular Orbital Theory of Atom Abstraction Reactions

FMO theory provides a satisfying rationale for the kinetic characteristics of hydrogen abstraction reactions of free radicals. In general terms, radicals are species containing an unpaired electron in a singly occupied molecular orbital (SOMO), which in the ground state of the radical is its highest occupied orbital. According to the FMO concept, during the course of the reaction this SOMO will interact with both the highest occupied (HOMO) and lowest unoccupied (LUMO) molecular orbitals of the donor molecule. Such interactions between these "frontier molecular orbitals"[24] are not necessarily equal. The extent of SOMO-HOMO and SOMO-LUMO interaction is governed by their energy values, the strongest interaction occurring between orbitals closest in energy.

It is these values, influenced by atom type as well as neighboring substituents, from which the relative descriptors such as "nucleophilic" and "electrophilic" are derived and provide the basis for the previously described concept of "polar factors." Electron donating substituents generally serve to raise both HOMO and LUMO energies, with electron withdrawing groups resulting in lowering. Radicals possessing a low energy SOMO will display electrophilic character, whereas a higher energy SOMO gives rise to a more nucleophilic species. Figure 1-6 depicts the FMO interactions between radical and donor in each of these cases.

During the abstraction process, the primary interaction involves the radical SOMO and the σ and σ^* orbitals of the donor M-H bond. The antibonding σ^* orbitals of the donor are typically quite high in energy, and thus in atom abstraction reactions the SOMO-HOMO interaction dominates.

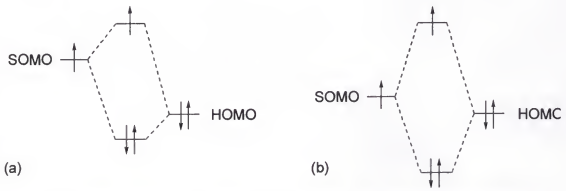

Figure 1-6. FMO Diagram Illustrating the SOMO-HOMO Interaction Between (a) a Nucleophilic Alkyl and (b) an Electrophilic Alkoxyl radical.

Here it is seen that the lower-energy SOMO of the alkoxyl radical (ca. -12 eV, as determined from ionization potential measurements)[25] leads to a reinforced interaction with the donor HOMO (case b). This greater stabilizing interaction results in a lowered activation barrier and hence a more facile transfer reaction, compared to the more nucleophilic alkyl radical, (case a) whose SOMO energies range from -6.9 to -9.8 eV.[25]

Some of the most striking examples of such "polar" factors involve systems where fluorine substitution has taken place at, or adjacent to, the radical center. This is elaborated upon in Chapters 2 and 3, where the effects of fluorination on the structure and reactivity of free radicals are discussed and compelling evidence provided based on kinetic studies of hydrogen transfer to such partially and fully fluorinated alkyl radicals.

Intermolecular Radical Addition Reactions

Over the past twenty years, the intermolecular addition reactions of free radicals (as well as their intramolecular cyclization counterparts) have become an important

addition to the arsenal of C-C bond formation methods available to the synthetic organic chemist. Their mild means of generation from a variety of precursors and tolerance for a wide variety of functional groups provide distinct advantages over ionic processes.

Alkyl radical additions to carbon-carbon double bonds are highly exothermic, as a new σ bond is formed at the expense of a π bond (in the case of methyl radical addition to ethylene (Figure 1-7), ΔH_{rxn}= ca. -22.6 kcal · mol^{-1}).[41,42] In accordance with the Hammond postulate,[43] such additions should proceed via early transition states, with low barriers of activation. This is indeed the case, as supported by a wealth of both experimental[44] and theoretical[41,45-49] data.

$$CH_3^{\bullet} + CH_2{=}CH_2 \longrightarrow CH_3CH_2CH_2^{\bullet}$$

$$E_a = 7.9 \text{ kcal} \cdot \text{mol}^{-1}$$
$$\Delta H_{rxn} = -22.6 \text{ kcal} \cdot \text{mol}^{-1}$$

Figure 1-7. Addition of Methyl Radical to Ethylene, Yielding *n*-Propyl Radical. Experimental Activation Energies and Heats of Reaction are Shown.

FMO Theory of Radical Additions

Quantum mechanical molecular orbital calculations at levels of *ab initio* theory ranging from UHF to UQCISD(T) and varying basis sizes from 3-21G to 6-311G(2df,p) are consistent in their characterization of the transition structure for the above reaction

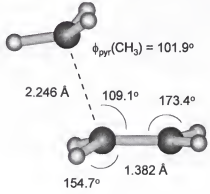

Figure 1-8. UHF/6-31G(d) Transition Structure and Relevant Geometrical Parameters for Addition of Methyl Radical to Ethylene.

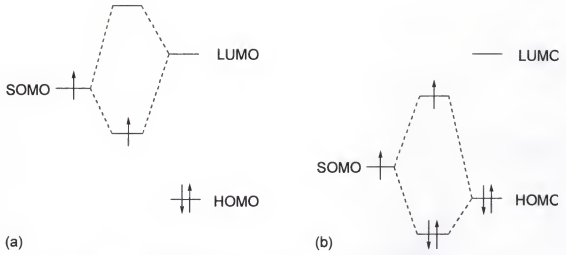

Figure 1-9. FMO Diagram for Addition of (a) Nucleophilic and (b) Electrophilic Radicals to Alkenes.

Table 1-3. Some Relative Rates of Addition of Methyl and *tert*-Butyl Radicals to Alkenes CH_2=CHX.

X	k_{rel} ($CH_3^\bullet$)	k_{rel} ($(CH_3)_3C^\bullet$)
H	1	1
CH_3	0.7	0.74
OCH_2CH_3		0.31
F	0.9	
Cl	4.2	13.2
CN	34[a]	1920

[a] Data for ethyl radical.

(Figure 1-8), which possesses an incipient C-C bond distance of ca. 2.23 - 2.27 Å. The C-C-C attack angle of 109.1° is rationalized in FMO terms based on a primary interaction between the radical SOMO and the LUMO of the alkene. It is in such reactions with high exothermicities and early transition states that FMO interactions are most substantial.[24,50] This postulate enjoys experimental support; for the *t*-butyl radical, a correlation exists between rates of addition to alkenes and the experimentally

determined electron affinities of the latter.[21,51] Such an FMO interaction for nucleophilic radicals is shown in Figure 1-9 (case a) and is influenced by substituents on both radical and olefin, a raising of radical SOMO and/or lowering of alkene MO energies strengthening the SOMO-LUMO interaction and enhancing the rate of addition as seen from the data in Table 1-3.[21,52] Here, the greater nucleophilic character of *t*-butyl relative to methyl is evident from its enhanced rate of addition to olefins bearing electron withdrawing groups.

As previously discussed, electronegative substituents at the radical center which substantially lower its SOMO energy will impart electrophilic character and reinforce the transition state SOMO-HOMO interaction (Figure 1-9, case b). Indeed, it has been shown that rates of addition of dicyanomethyl[53] and perfluorinated[54] radicals correlate with the ionization potentials of the substrate alkenes. The intermediate behavior of "ambiphilic" radicals, such as malonyl and (*tert*-butoxycarbonyl)methyl, has also been documented, these species yielding "U"-shaped correlations between rates of addition and alkene IP and EA values.[55-57]

A more thorough presentation of kinetic results obtained to date for the addition of partially and fully fluorinated radicals to alkenes is given in Chapters 2 and 3.

Steric Effects; Regiochemical Preferences in Addition

Competition studies on both nucleophilic and electrophilic radicals have provided for some generalizations in terms of the regiochemical preference for addition to unsymmetrically substituted olefins.[52] The preferred orientation of radical addition occurs to the unsubstituted end of the double bond, attributed to steric repulsion but also influenced by the effect of substituents on the coefficients of the HOMO and LUMO of the alkene. Such FMO effects can be the decisive factor in polysubstituted olefins if steric effects are in opposition. Strongly spin delocalizing substituents on the alkene reinforce such sterically induced regiochemical preferences and exert slight rate

enhancing effects; however, as such additions occur through early transition states the effect of exothermicity on the kinetics of addition should be minimal.

The concepts introduced in the aforementioned discussion on intermolecular radical additions extend to their intramolecular cyclization analogues, an overview of which will now be presented.

Intramolecular Addition Reactions: Radical Cyclizations

The intramolecular addition reactions of alkenyl radicals enjoy a strong foothold among the available strategies for the construction of cyclic organic molecules. In addition to their synthetic utility, the kinetic, regioelectronic and stereoelectronic characteristics of radical cyclization reactions as a function of substituent continue to fuel an abundance of fundamental physical organic structure-reactivity investigations, more than thirty years after the first report of the archetypal radical ring closure, cyclization of hex-5-en-1-yl radical **1** (Figure 1-10).[58]

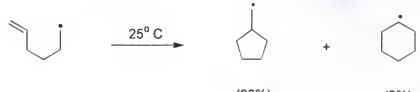

Figure 1-10. Cyclization of Hex-5-en-1-yl Radical **1** to Cyclopentylcarbinyl (**2**) and Cyclohexyl (**3**) Radicals. At 25° C, *5-exo* Closure Dominates 49 : 1.

The most striking aspect of this reaction lies in the preferred regiochemistry of addition. In the case of the parent hydrocarbon, *5-exo*[59] cyclization dominates (E_{act} [*5-exo*] = 6.8 kcal · mol^{-1}, E_{act} [*6-endo*] = 8.5 kcal · mol^{-1})[27,60] yielding the less thermodynamically stable primary cyclopentylcarbinyl radical **2.** This finding has provided the driving force for a number of experimental[61] and theoretical[62-68]

investigations geared toward the understanding of radical cyclization regiochemistry in the hydrocarbon and related substituted systems.

Early explanations,[69] later advanced by semiempirical techniques,[65] attributed this result to a less negative entropy of activation for cyclization to **2**. Although experiment demonstrates this to be true, the difference ($\Delta S^{\ddagger}_{1,5} - \Delta S^{\ddagger}_{1,6} = 2.8$ eu)[60] is insufficient to completely account for the observed regiochemistry; the preferred mode of cyclization resulting primarily from enthalpic ($\Delta H^{\ddagger}_{1,6} - \Delta H^{\ddagger}_{1,5} = 1.7$ kcal mol^{-1}) rather than entropic factors. *Ab initio* computations[66] lend support to this conclusion.

Transition structures for *5-exo* and *6-endo* cyclization of **1** have been located using a variety of theoretical treatments. The UHF/6-31G(d) structures leading to **2** and **3** are shown in Figures 1-11 and 1-12.

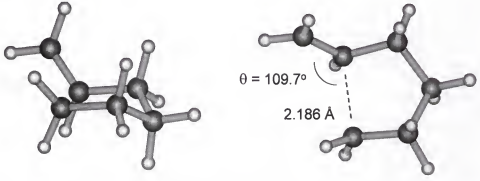

Figure 1-11. Two Views of the UHF/6-31G(d) *"5-exo-chair"* Transition Structure for Cyclization Hex-5-en-1-yl Radical **1** to Cyclopentylcarbinyl Radical **2**.

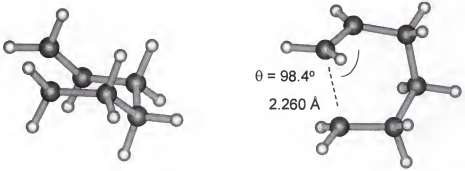

Figure 1-12. Two Views of the UHF/6-31G(d) *"6-endo-chair"* Transition Structure for Cyclization of Hex-5-en-1-yl Radical **1** to Cyclohexyl radical **3**.

Spellmeyer and Houk[66] have also postulated additional "boat-like" transition structures on the basis of molecular mechanics calculations parameterized by *ab initio* results of model systems. Inclusion of these "boat-like" structures as viable competing pathways was found to be necessary for the accurate prediction of regio- and stereoselectivities in cyclizations of alkyl substituted and heteroalkenyl radicals. The existence of such structures is corroborated by higher level *ab initio* treatments performed as part of the present study and are shown in Figures 1-13 and 1-14.

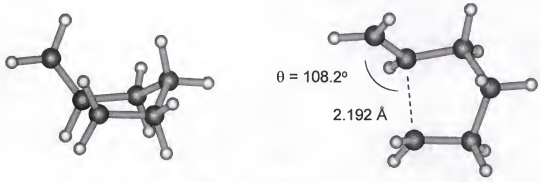

Figure 1-13. Two Views of the UHF/6-31G(d) "*5-exo-boat*" Transition Structure for Cyclization of Hex-5-en-1-yl Radical **1** to Cyclopentylcarbinyl Radical **2**.

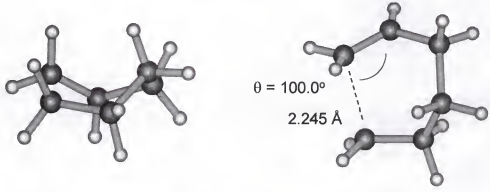

Figure 1-14. Two Views of the UHF/6-31G(d) "*6-endo-twist-boat*" Transition Structure for Cyclization of Hex-5-en-1-yl Radical **1** to Cyclohexyl Radical **3**.

Upon inspection of the forming bond lengths and angles of the *5-exo* structure in Figure 1-11, its similarity to the transition structure for addition of methyl radical to ethylene is readily apparent. The C-C-C angle of attack, 109.7°, is practically identical to

that in Figure 1-8 and fits the requirement for overlap of the radical SOMO with the π^* orbital of the alkene moiety. From Figure 1-12 it is observed that this angle is significantly reduced (98.4°) in the *6-endo* approach. Thus the required disposition of centers for optimal FMO overlap is more readily achieved in the *5-exo* transition structure, leading to the kinetically preferred cyclization product.

Substituent Effects on the Kinetics and Regiochemistry of 5-Hexenyl Cyclizations

Radical **1** cyclizes to cyclopentylmethyl radical **2** with a rate constant (k_{C5}) of 2.3×10^5 s^{-1} at 25 °C.[27] In the parent hydrocarbon, *6-endo* closure competes to a very minor extent (k_{C6} = ca. 4.7×10^3 s^{-1}). However, it will be shown that the rates and regiochemical preferences can be substantially affected by substitution at both the radical center and terminal alkene.

Alkyl Substitution; Steric Effects

Beckwith *et al.* have reported rate constants for a number of alkyl-substituted hexenyl radicals.[70,71] The rates of *5-exo* closure as a function of *gem*-dialkyl substitution on the aliphatic portion of the hexenyl chain is shown in Table 1-4.

It is seen that substitution at the radical center has a nearly negligible effect on the rate of cyclization, due to offsetting polar and steric considerations. Conversely, a significant (> 10-fold) rate enhancement is observed with internal substitution (systems **6**, **8**, and **9**), accelerated by relief of steric compression between alkyl groups during ring formation (the "Thorpe-Ingold", or "*gem*-dimethyl" effect).[72]

Intermediate kinetic behavior would be expected of monosubstituted 5-hexenyl systems. The data in Table 1-5 show this to be the case. In addition, a stereochemical preference for *cis*- or *trans*-dimethylcyclopentanes, depending on the location of the substituent on the chain, is observed. This has been rationalized by Beckwith *et al.*[71]

Table 1-4. *5-exo* Cyclization Rate Constants for *gem*-Disubstituted 5-Hexenyl Radical Derivatives.

Cyclization Reaction	k_{C5}, 10^5 s^{-1} (298 K)
1 **2**	2.3[a]
4 **5**	3.0[b]
6 **7**	36[c]
8 **7**	52[c]
9 **5**	32[c]

[a] Reference 27. [b] Reference 28. [c] Reference 71.

based on the cyclization transition structure depicted in Figure 1-11. Although "early" in terms of the forming C-C bond, the overall orientation of atoms in this structure is quite product-like. According to this rationale, substituents on the aliphatic fragment are likened to those in chair cyclohexane, which then occupy an equatorial position in the chair transition structure. Minor products are assumed to derive from the occupation of

axial positions. The latter has been disputed by Spellmeyer and Houk,[66] whose model indicates that such secondary products originate from an equatorial disposition of substituents in the boat-like transition structure of Figure1-12, rather than from an axial orientation in the chair.

Table 1-5. *Cis-* and *Trans- 5-exo* Cyclization Rate Constants for Monosubstituted 5-Hexenyl Systems. Rate Constants are for 298 K.

Cyclization Reaction			k_{C5} (*cis*), 10^5 s^{-1}	k_{C5} (*trans*), 10^5 s^{-1}
10	*cis*-**11**	*trans*-**11**	1.1[a]	0.42[a]
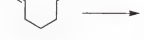 **12**	*cis*-**13**	*trans*-**13**	2.4[b]	4.5[b]
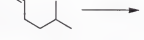 **14**	*cis*-**13**	*trans*-**13**	7.0[b]	2.4[b]
15	*cis*-**11**	*trans*-**11**	0.75[b]	3.6[b]

[a] Reference 73. [b] Reference 71.

In the above examples, *5-exo* products are formed either predominantly (> 97%) or exclusively. Substitution at the vinyl group leads to marked changes in regiochemical ratios as indicated by the data in Table 1-6. Replacement of hydrogen by methyl (**16**) or isopropyl (**19**) at C_5 results in preferential formation 6-membered rings **18** and **21**. Inspection of the data indicates that this shift in regiochemistry is not due to a significant

Table 1-6. Rate Constants at 338 K for *5-exo* and *6-endo* Cyclization for Vinyl-substituted 5-Hexenyl Radicals.

Cyclization Reaction	k_{C5}, 10^5 s^{-1}	k_{C6}, 10^5 s^{-1}
1 **2** **3**	9.4[a]	0.19[a,b]
16 **17** **18**	0.21[b]	0.37[b]
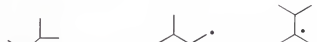 **19** **20** **21**	0.21[b]	0.66[b]
22 **23** **24**	1.0[b]	0.19[b]
25 **26** **27**	22[b]	< 0.1[b]

[a] Calculated from the Arrhenius parameters given in reference 27. [b] Reference 70.

extent to rate enhancement for *6-endo* closure, but rather a substantial (44-fold) retardation of 5-membered ring formation due to a combination of 1,5 steric hindrance and back strain engendered at C_5 upon adaptation of sp^3 character. Substitution at both C_5 and C_6 again favors *5-exo* closure, the rate of which decreased relative to the parent system. Disubstitution at C_6 (**25**) gives rise to a slight (2.3-fold) rate enhancement for *5-exo* closure, sufficiently explained on thermodynamic grounds, which dominates *6-endo*

cyclization by a factor of at least 220. The above data indicates that the kinetic and regiochemical characteristics of alkyl-substituted 5-hexenyl cyclizations may be sufficiently rationalized by steric considerations. The effects of substitution by conjugating, heteroatom-containing groups is outlined below.

FMO Considerations

Studies of 5-hexenyl systems bearing "polar" subsitutents have been investigated by Newcomb.[16,74-77] In line with those of intermolecular radical additions, the kinetics of radical ring closure will be influenced by the impact of substitutents on the SOMO-HOMO and SOMO-LUMO interaction in the cyclization transition state.

Table 1-7. *5-exo* Cyclization Rate Constants For α-Donor- and α-Acceptor-substituted 6,6-Diphenyl-5-hexenyl radicals. Rate Constants are for 298 K.

System	X	Y	k_{C5}, 10^7 s^{-1} (298 K)[a]
28 → **29**	H	H	4
30 → **31**	H	CH_3	2
32 → **33**	CH_3	CH_3	1
34 → **35**	H	OCH_3	4
36 → **37**	H	$CO_2CH_2CH_3$	≈ 3.7
38 → **39**	CH_3	$CO_2CH_2CH_3$	0.04
40 → **41**	CH_3	CN	0.03

[a] Calculated from the Arrhenius parameters provided in reference 76.

As seen from the data in Table 1-7, only a very minor effect is exerted by either α-donor or α-acceptor substituents, relative to parent system **28**. The marked decrease

in rate for **38** and **40** is attributed to an increase in activation energy due to enforced planarity at the radical site induced by the π-delocalizing substituents $CO_2CH_2CH_3$ and CN.[51,78]

Table 1-8. Absolute Rate Constants at 298 K for *5-exo* Cyclization of 5-Hexenyl Systems Bearing Vinylic Donor and Acceptor Substituents.

Cyclization Reaction	k_{C5}, 10^5 s^{-1} (298 K)
1 **2**	2.3[a]
42 **43**	4.2[b]
44 **45**	680[b]
46 **47**	1000[b]

[a] Reference 27. [b] Calculated from the Arrhenius parameters provided in reference 74.

Substitution at the vinyl terminus, especially by strong resonance-withdrawing groups can significantly accelerate the rate of ring closure. Although possessing a radical stabilizing group, methoxy analog **42** enjoys only a very minor increase in rate. The donor substituent raises the energies of the frontier orbitals, increasing the SOMO-HOMO interaction but widening the SOMO-LUMO energy gap, the latter more important

for relatively nucleophilic alkyl radicals (Figure 1-9). Substituents which serve to lower the FMO energies should reinforce the SOMO-LUMO interaction, leading to rate enhancement. The nearly 300-fold increase resulting from cyano substitution (**44**) reflects such an effect. The slight rate increase **46** relative to **45** has been explained on the basis of the suggested slight extra "push-pull," or "captodative" stabilization manifested in donor-acceptor disubstituted systems.[79,80]

The importance of kinetic control was previously mentioned. Care must be taken in assessing the potential for reversibility in such intramolecular additions, which may obscure the effect of steric and/or polar influences on reaction kinetics. This is demonstrated in the *5-exo*:*6-endo* product ratios of highly stabilized systems **48** and **51**.[81,82]

Table 1-9. Product Ratios for 5-Hexenyl Cyclization Reactions Under Full or Partial Thermodyamic Control.

Cyclization Reaction				% *5-exo*	% *6-endo*
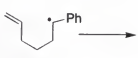		+		< 22	> 78
48	**49**		**50**		
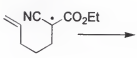		+		16	84
51	**52**		**53**		

Given the data and discussion provided in the above sections, a review of the direct and competitive techniques utilized in the determination of rates of organic radical reactions is now in order.

Methods for Determination of Organic Radical Kinetics

The development of indirect competitive methods, in conjunction with laser flash photolytic generation and time-resolved detection of transient intermediates, has greatly

expanded the dynamic range available for the measurement of radical reactions, especially those at the upper end of the kinetic scale. Such advances have provided for the use of a variety of precursors and the accurate determination of rate constants for reactions approaching the diffusion-controlled limit in solution.[16]

Laser Flash Photolysis; Direct Measurement of Addition Rates

In the time-resolved laser flash photolysis method, described in detail in the literature,[83] radicals are generated from precursors possessing a suitable chromophore by a laser pulse of the appropriate wavelength. Alkyl iodides, diacyl peroxides, and the O-acylthiohydroxamic esters of Barton *et al.*[84] are most commonly utilized in this regard (Figure 1-15).

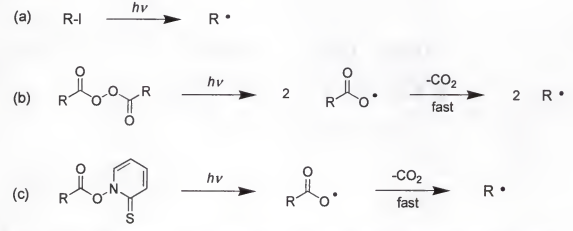

Figure 1-15. Laser Flash Photolytic Generation of Radicals R• from (a) Iodide, (b) Diacyl Peroxide, and (c) O-Acylthiohydroxamic Ester Precursors.

These radicals so generated undergo further reaction, usually bimolecular addition or unimolecular cyclization to a (typically phenyl-substituted) double bond (a styrene in the case of bimolecular additions). The increase in the characteristic absorption of this intermediate benzyl radical ($\lambda_{max} \approx 320$ nm) is then followed in a time-dependent manner by UV-visible spectroscopy (Figure 1-16). For bimolecular additions, this experimental growth curve is fit to the expression in Equation 1-11, yielding absolute

rate of addition k_{add}. With such data in hand, this addition can now serve as a competing basis reaction for the determination of rates of other transformations involving the same or structurally similar radical.

$$k_{obs} = k_0 + k_{add}\,[\text{alkene}] \qquad (1\text{-}11)$$

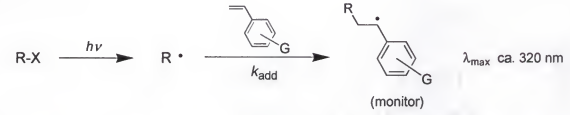

Figure 1-16. LFP Generation of R• and Detection of Transient Benzyl Radical Adduct for Determination of Absolute Rate of Addition k_{add}.

Indirect Methods (Competitive Techniques)

Indirect kinetic methods involve the partitioning of an intermediate between two competing pathways, one with a known rate constant and the other whose rate constant is to be determined. *Post facto* product analyses, typically by chromatographic or spectroscopic means, provide a ratio of rate constants from which the new kinetic value is obtained. Such radical kinetic measurements usually involve competition between two bimolecular reactions or a bimolecular reaction competing with unimolecular rearrangement; examples of both instances are provided in Figures 1-17 and 1-18.

Determination of rates of hydrogen abstraction by this method involves the generation of R• in the presence of two trapping agents; in Figure 1-17, styrene and the hydrogen atom donor. Both traps are typically present in excess to ensure pseudo-first order behavior. Radical R• may undergo addition to styrene (with known rate constant k_{add}) forming the intermediate benzyl radical, itself trapped with excess hydrogen donor, yielding closed shell product with a rate which is kinetically unimportant *provided the addition reaction is irreversible.* Alternatively, R• is trapped directly by hydrogen atom donor with a rate constant k_H, which may be obtained from the pseudo-first order relation

$$\frac{[\text{reduced}]}{[\text{adduct}]} = \frac{[k_H][R\bullet][\text{M-H}]}{[k_{add}][R\bullet][CH_2{=}CHR']} \qquad (1\text{-}12)$$

where [reduced] and [adduct] are the final product concentrations, [M-H] is the concentration of hydrogen atom donor, and [CH_2=CHR'] the concentration of alkene trap. For accurate kinetic determinations, a series of runs is performed where trap concentrations are varied, (again, maintaining at least a five-fold excess) a plot of product ratios versus that of trapping agents yielding the ratio k_H / k_{add}.

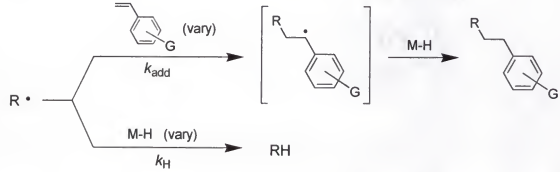

Figure 1-17. Competition Between Bimolecular Addition to an Alkene with Rate Constant k_{add} and Bimolecular Trapping by Hydrogen Atom Donor with Rate Constant k_H.

Determination of rates of cyclization are performed in a similar manner, using hydrogen atom abstraction (with the known value of k_H) as the competitive basis reaction. Unimolecular rearrangement competes with bimolecular trapping with an excess of hydrogen atom donor (Figure 1-18) to yield intermediate cyclic radicals, further trapped to form characterizable products.

The ratio of products of cyclization versus hydrogen abstraction are obtained from the pseudo-first order relation in Equation 1-13, a plot of the ratio of products of hydrogen abstraction to those of cyclization as a function of trapping agent concentration affording ratios k_{C5} / k_H and k_{C6} / k_H.

Finally, the importance of an efficient chain process should be reemphasized. High conversions of precursors, although important for any radical reaction, are crucial in

competitive kinetic experiments. The reliability of data resulting from indirect methods is directly dependent on high "mass balance" values, those of 90% or greater typically being desired.

$$\frac{[\text{ reduced }]}{[\text{ cyclized }]} = \frac{[\,k_H\,]\,[\,R\bullet\,]\,[\,M\text{-}H\,]}{[\,k_{Cn}\,]\,[\,R\bullet\,]} \qquad (1\text{-}13)$$

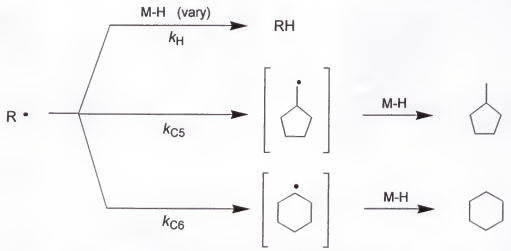

Figure 1-18. Competition Between Bimolecular Hydrogen Atom Abstraction with Rate Constant k_{add} and Unimolecular *5-exo* and *6-endo* Cyclization with Rate Constants k_{C5} and k_{C6}.

Such competitive processes have been employed extensively by the Dolbier research group in the investigation of the rates of addition, hydrogen atom abstraction, and cyclization of a variety of fluorinated open shell systems, providing the first quantitative kinetic data for this class of reactive intermediates.[54,85-91]

Conclusion

The preceeding discussions have attempted to provide the reader with an introduction to the chemistry of organic free radicals. Kinetic data for hydrogen abstraction, addition, and cyclization reactions of hydrocarbon radicals, important benchmarks for comparison of reactivity with other substituted systems, was provided.

Substituent effects, rationalized on the basis of a combination of thermodynamic, steric and FMO considerations, were discussed.

The following chapter provides a review of the effects of fluorine substitution in organic molecules, including fluorinated radicals. Previous research efforts in this area by the Dolbier group are summarized, setting the stage for the presentation of results of the current study.

CHAPTER 2

THE FLUORINE SUBSTITUENT IN ORGANIC SYSTEMS

Introduction

Incorporation of fluorine into organic molecules often imparts dramatic alterations in structure and reactivity. These effects are induced by three major characteristics inherent to the fluorine atom: extreme electronegativity, non-bonded electron pairs, and relatively small size.

Fluorine possesses the highest electronegativity of all the elements, with a value of 4.10 on the Pauling scale, compared to oxygen (3.50), chlorine (2.83), bromine (2.74), carbon (2.50), and hydrogen (2.20).[92] As a substituent in organic systems, this results in strong inductive withdrawal of electron density through the σ molecular framework and highly polarized bonds with substantial ionic character.

Three non-bonding pairs of electrons in 2p orbitals similar in size to those of other second-row elements provide for optimal overlap, and therefore an offsetting back donation of electron density into the molecule to which it is bonded.

The accepted van der Waals radius of fluorine, 1.47 Å, suggests minimal steric impact in comparison with other halogens (chlorine, 1.73 Å; bromine, 1.84 Å; iodine, 2.01 Å; carbon, 1.70 Å; oxygen, 1.52 Å; hydrogen, 1.20 Å).[93] This has allowed for the complete replacement of hydrogen by fluorine in organic systems, a feat not possible to such an extent with any other element.

The following sections, based on a number of excellent reviews,[94-97] provide an introduction to the fascinating behavior exhibited by fluorinated stable molecules and reactive intermediates due to a combination of the above effects.

Structure, Bonding, and Reactivity in Saturated Systems

The data provided in Tables 2-1 and 2-2[95,97] reveal a trend unique to fluorine within the halogenated methanes. An incremental shortening of C-F interatomic distances, with a resultant increase in bond dissociation energies, is observed as the series is traversed. No such trend exists for any other member of the halomethane family; on the contrary, it is seen from the data in Table 2-2 that such C-X BDE values instead *decrease* with increasing halogen content. Strengthening of C-H bonds is also observed within the fluoromethanes (CH_3F, 101.3 kcal · mol^{-1}; CH_2F_2, 103.2 kcal · mol^{-1}; CF_3H, 106.7 kcal · mol^{-1}).[95]

Table 2-1. Carbon-Halogen Interatomic Distances (Ångstroms) of Halomethanes

X	CH_3X	CH_2X_2	CHX_3	CX_4
F	1.385	1.357	1.332	1.319
Cl	1.781	1.772	1.758	1.767
Br	1.939	1.934	1.930	1.942

Table 2-2. Carbon-Halogen Bond Dissociation Energies (D^0, kcal · mol^{-1}) of Halomethanes

X	CH_3X	CH_2X_2	CHX_3	CX_4
F	108.3	119.5	127.5	130.5
Cl	82.9	81.0	77.7	72.9
Br	69.6	64	62	56.2
I	57.2	51.3	45.7	-

Data for geminally fluorinated ethanes parallel that of the methane series, demonstrating a progressive strengthening and shortening of both C-C and C-F bonds with increasing fluorination (Table 2-3). Conversely, vicinal fluorination gives rise to the opposite effect on C-C bonds, a steady lengthening and weakening being observed.

A variety of hypotheses have been put forth to explain the observed trends. One rationalization, invoked by Pauling[98] and based on valence bond theory, involves "double bond, no bond" resonance of the type depicted in Figure 2-1.

Table 2-3. Interatomic Distances and Dissociation Energies of Fluoroethanes

Ethane	r (C-C), Å	D^0 (C-C), kcal · mol^{-1}	r (C-F), Å	D^0 (C-F), kcal · mol^{-1}
CH_3-CH_3	1.532	90.4	-	-
CH_3-CH_2F	1.502	91.2	1.398	107.9
CH_3-CHF_2	1.498	95.6	1.343	Unknown
CH_3-CF_3	1.494	101.2	1.335	124.8
CH_2F-CF_3	1.501	94.6	Unknown	109.4 (CH_2F)
CF_3-CF_3	1.545	98.7	Unknown	126.8

As the degree of geminal fluorination is increased, the number of such resonance forms involving doubly bonded fluorine increases (0, 2, 6, and 12 in the case of CH_3F, CH_2F_2, CH_3F, and CF_4, respectively). This is supported by *ab initio* calculations at the RHF/4-31G and 4-31G(d) levels,[99-101] which illustrate back donation of electron density from fluorine into the C-F σ^* orbitals. It is further observed that the overlap population between the 2p orbitals of carbon and those of fluorine increases continually with successive fluorination; in contrast, such carbon-chlorine overlap populations decrease steadily from CH_3Cl to CCl_4.

Figure 2-1. "Double Bond, No Bond" Resonance in Geminally Fluorinated Alkanes.

Alternative explanations based on hybridization schemes have also been advanced. It is postulated that for electronegative elements bound to carbon, rehybridization occurs causing an increase in the amount of p character directed toward

the substituent. Thus, in CH_3F, the C-F bond possesses greater p character, with greater s character in the C-H bonds. This rationale accounts not only for incremental C-F bond strengthening, but also for the observed changes in geometry within the fluoromethane series. Accumulation of p character in C-F bonds should lead to a decrease in FCF bond angle, accompanied by HCH widening. This is consistent with experimental observation ($\angle$FCF in CF_4, 109.5°; CHF_3, 108.7°; CH_2F_2, 108.3°;[102,103] for CH_2F_2, $\angle$HCH = 113.7°).[103]

Finally, a more recent argument has been advanced by Wiberg,[104] on the basis of Coulombic interactions between carbon and fluorine substituents. From charge-fitting treatments based on calculated electrostatic potentials, a linear increase in positive charge on carbon is observed, while the degree of negative charge on each of the fluorine substituents remains quite constant. Thus, incremental fluorine substitution strengthens not only new, but also previous, C-F bonds. This finding will be further discussed in Chapter 3, as such ESP-derived charges calculated for larger fluorinated systems as part of the present study were found to provide a cogent explanation for the remarkable and contrasting effects of fluorination on the strengths of both C-C and α and β C-H bonds.

Structure, Bonding, and Reactivity in Unsaturated Systems

The most reliable structural and π-BDE data for the fluoroethylenes is provided in Table 2-4.[95,97] Vinylic fluorine substitution results in shorter C=C bonds than in the parent hydrocarbon, and shorter C-F bonds than fluoroalkanes bearing the same number of geminal or vicinal fluorine substituents. *Ab initio* investigations by Radom[99] and others[105-107] attribute the C-F bond contraction to delocalization of fluorine 2p electrons into the C-C π bond (depicted in resonance terms in Figure 2-2). Computed atomic charges are consistent with this conclusion.

Table 2-4. Interatomic Distances, Angles, and π Bond Dissociation Energies of Fluoroethenes.

	CH_2=CH_2	CH_2=CHF	CH_2=CF_2	CHF=CF_2	CF_2=CF_2
r (C=C), Å	1.339	1.333	1.316	1.309	1.311
r (C-F), Å	-	1.348	1.324	1.336	1.319
∠HCH, deg.	117.8	114.7	119.3	-	-
∠HCF, deg.	-	111.3	-	114.0	-
∠FCF, deg.	-	-	109.7	109.1	112.6
π D^o, kcal · mol^{-1}	63 - 64	Unknown	62.8	Unknown	52.3

The marked decrease in FCF bond angles has been rationalized by Bernett[108] and Kollman[109] on the basis of hybridization arguments; Epiotis has advanced an alternative explanation involving nonbonded attraction between fluorine atoms.[110,111]

Figure 2-2. Fluorine 2p Electron Delocalization in Unsaturated Systems.

Photoelectron[112] and electron attachment[113] spectral data for the fluoroethylene series are provided in Table 2-5. A significant lowering (over a range of 3.1 eV) of the σ MO energies is observed, with only a slight (ca. 0.3 eV) variation in the π MOs. Stabilization of the σ MOs is ascribed to extensive delocalization over the fluorine substituents; such an interaction within the π system is diminished and counteracted by strong C-F antibonding overlap.[112] A steady increase in electron attachment energies with successive fluorination can also be seen, attributed to destabilization of π^* resulting from an antibonding interaction with the fluorine 2p AOs.[113]

Heats of hydrogenation provided in Table 2-6[95] illustrate the reactivities of fluorinated alkenes. In general, transformation of a polyfluorinated olefin into a saturated

Table 2-5. Vertical Ionization Potentials (I.P.) and Electron Attachment Energies (EA) for the Fluoroethenes.

Ethene	π I.P., eV	σ I.P., eV	E.A., eV
CH_2=CH_2	10.6	12.85	1.78
CH_2=CHF	10.58	13.79	1.91
CH_2=CF_2	10.72	14.79	1.84
cis-CHF=CHF	10.43	13.97	2.18
trans-CHF=CHF	10.38	13.90	2.39
CF_2=CHF	10.53	14.64	2.45
CF_2=CF_2	10.52	15.95	3.00

derivative is more exothermic than for the parent hydrocarbon. This arises from a combination of the destabilizing effect of polyfluorination on double bonds and the thermodynamic preference for *gem*-difluoro substitution at saturated carbon. The deviation of CH_2=CHF in Table 2-6 is explained by the preference of a single fluorine substituent to reside at the vinylic position (Figure 2-3).[114]

Table 2-6. Heats of Hydrogenation of the Fluoroethenes.

Ethene	ΔH^o (H_2), kcal · mol^{-1}
CH_2=CH_2	-32.6
CH_2=CHF	-29.7
CH_2=CF_2	-38.8
CF_2=CF_2	-45.7

Fluorine Non-Bonded Interactions in Reactive Intermediates

The π-donor ability of the fluorine substituent is reflected in its activating and *ortho*, *para*-directing character in electrophilic aromatic substitution reactions,[115] consistent with ^{13}C NMR measurements of fluorobenzene, where shielding of these positions is observed.[116]

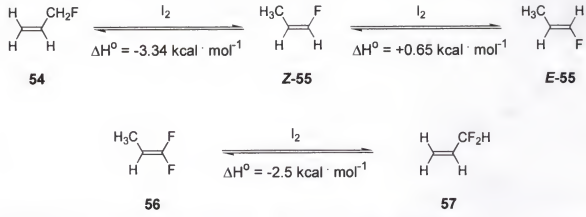

Figure 2-3. Thermodynamic Equilibria in Mono- and Difluoropropenes.

Delocalization of fluorine's nonbonded electrons into the vacant 2p orbital on carbon more than compensates for its inductive withdrawal in α-fluoro carbocations, resulting in net stabilization. In the gas phase, carbocation stability increases along the series $^{+}CH_3 < {}^{+}CF_3 < {}^{+}CH_2F < {}^{+}CHF_2$ and $^{+}CH_2CH_3 << {}^{+}CF_2CH_3 \cong {}^{+}CHFCH_3$.[117,118] The $^{+}CF_3$ cation has been observed in the gas phase, with many others having been successfully generated in solution.[119-121] In constrast, fluorination at the β position and beyond destabilizes carbocations due to inductive effects; simple alkyl β-fluoro carbocations not benefiting from additional stabilizing factors have yet to be detected.

Electron pair repulsion in α-fluoro carbanions results in a strong preference for pyramidal geometries, *ab initio* calculations[122-124] predicting an FCF angle of ca. 99.5° and an inversion barrier of 119 kcal · mol^{-1} for $^{-}CF_3$. Although fluorination does increase C-H bond acidities in such pyramidal systems,[125] a destabilizing effect is observed in cases such as the 9-fluorofluorenyl anion (Figure 2-4, X = F) where coplanarity is forced between the 2p orbitals on fluorine and the remainder of the π system.[126] Fluorine substitution in the β position stabilizes carbanions through a combination of inductive and hyperconjugative effects, (Figure 2-5) the latter supported by X-ray crystallographic data of perfluoroalkyl anion salts as well as through calculation.[122,127,128]

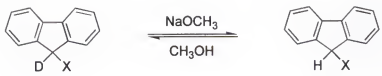

58 **59**

X	$k_{exc\ (rel)}$
D	1
F	0.125
Cl	400
Br	700

Figure 2-4. Fluorine Destabilization in Planar 9-Halofluorenyl Anions.

Figure 2-5. Negative Hyperconjugation in β-Fluorocarbanions.

Fluorine Steric Effects

The minimal spatial requirements of fluorine, the smallest non-hydrogenic substituent, would imply a very minor steric impact on reaction kinetics and thermochemistry. In most cases this is true; however, examples of steric inhibition in reactions of fluoro-substituted systems do exist, typically in conformational and other dynamic processes occuring via highly congested transition states. This is illustrated in Figure 2-6;[129,130] the *meta* ring flip in **61** (X = F) exhibiting the largest known rate retardation induced by a single fluorine substituent.

The disparate behavior observed in the Cope rearrangements of ***d,l-*** and ***meso-*** **62** (Figure 2-7)[131] provides a particularly striking example of a fluorine steric effect. Transformation of ***d,l-*****62** to **63** proceeds via a typical chair-like transition structure, where in ***meso-*****62** a "boat-like" structure is required for C_1 - C_6 bond formation. The higher $\Delta H^{\ddagger}$

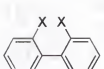

X = H, $\Delta G^{\ddagger}$ < 6 kcal · mol^{-1} (340 K)
X = F, $\Delta G^{\ddagger}$ = 11.1 kcal · mol^{-1} (340 K)

60

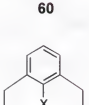

$k_H / k_F = 10^{11}$ (298 K)

61

Figure 2-6. Inhibition of Conformational Dynamics by Fluorine Substitution.

and *positive* $\Delta S^{\ddagger}$ implies a dissociative, rather than concerted, transition state for rearrangement of ***meso*-62**. This is induced by severe electrostatic repulsion between the high charge densities of the terminal fluorine substituents, separated by less than the sum of their van der Waals radii in the Cope transition state.[132]

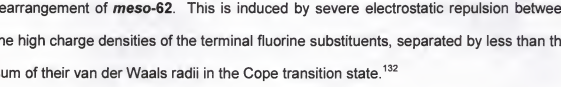

***d,l*-62** $\Delta H^{\ddagger}$ = 22.4 kcal · mol^{-1} **63**
$\Delta S^{\ddagger}$ = -17.5 eu

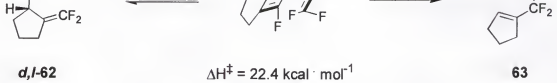

***meso*-62** $\Delta H^{\ddagger}$ = 49.5 kcal · mol^{-1} **63**
$\Delta S^{\ddagger}$ = +8.1 eu

Figure 2-7. Chair- versus Boat-Constrained Cope Rearrangement Reactions of Terminally Fluorinated Dienes ***d,l*-** and ***meso*-62**.

Steric effects are enhanced by perfluoroalkylation and branching. Cyclohexane *A* values[133] and modified Taft steric parameters[134] demonstrate that CF_3 is at least as large as isopropyl; evidence exists[135] to suggest that perfluoroisopropyl and *tert*-butyl are comparable in size. The most remarkable example of the above affects is the existence of perfluorinated radical **64**, (Figure 2-8) found to be persistent by ESR even in the presence of molecular oxygen.[136] The astounding kinetic stability of **64** derives from steric sheltering of the unpaired electron by the neighboring perfluoroalkyl groups.

64

Figure 2-8. Scherer's Persistent Perfluoroalkyl Radical.

The Fluorine Substituent in Free Radicals

Early application of organofluorine radical chemistry was comprised of the chain-mediated addition of polyhalomethanes and ethanes to olefins, first by Haszeldine[137] and soon thereafter by Tarrant.[138,139] Subsequent relative rate studies by Stefani *et al.*[140] followed by those of Tedder[141,142] clearly demonstrate the contrasting behavior of fluorinated and non-fluorinated radicals in their bimolecular additions to alkenes.

The fluorine substituent has a substantial effect on the structure of organic radicals as well as dramatic, but comprehensible, alterations in hydrogen abstraction and addition reactivity in comparison to hydrocarbon systems, resulting primarily from fluorine's potent σ-withdrawing character.

Structural Aspects

In contrast to the planar, π-type methyl radical, α-fluorination results in increasingly pyramidal, σ-type radicals, as indicated by electron paramagnetic

resonance measurements[143] and *ab initio* theoretical studies.[144-147] Calculations by Pasto at the UHF/4-31G level indicate barriers to inversion of 0.5, 6.8, and 25.1 kcal · mol^{-1} for $^{\bullet}CH_2F$, $^{\bullet}CHF_2$, and $^{\bullet}CF_3$, respectively.[147] Geometries of the fluoromethyl radicals computed at the UHF/6-31G(d) level are provided in Figure 2-9.

Figure 2-9. UHF/6-31G(d) Pyramidalization Angles of $^{\bullet}CH_3$, $^{\bullet}CH_2F$, $^{\bullet}CHF_2$, and $^{\bullet}CF_3$.

Inversion barriers in the series appear somewhat sensitive to the level of theory employed and substantially increase with the inclusion of polarization functions. SCF calculations by Dykstra[145] employing a polarized double-ζ basis result in an inversion barrier of 33 kcal · mol^{-1} for $^{\bullet}CF_3$; inclusion of electron correlation (QCISD(T)/ 6-31G(d)//UHF/6-31G(d), present work) affords a value of 29.4 kcal · mol^{-1}. Such successive deviation from planarity is due to a combination of effects; relief of Iπ repulsion between the singly-occupied orbital on carbon and the fluorine 2p electrons is further reinforced by overlap between the carbon 2p and C-F antibonding orbitals. This strong tendency for pyramidalization has been shown to be responsible for the low π bond energy in tetrafluoroethylene (Tables 2-4 and 2-6).[148]

The structures of fluorinated C_2 radicals have been theoretically probed by Paddon-Row and Chen *et al.*[149-152] Alkyl substitution induces slight pyramidalization as observed in the ethyl radical, (Figure 2-10) due to hyperconjugation between the SOMO and the staggered β C-H bond.[153] Fluorination at the radical center exerts an effect similar to that observed in the methyl series, while the structures of alkyl radicals are found to be relatively insensitive to β-fluorination.

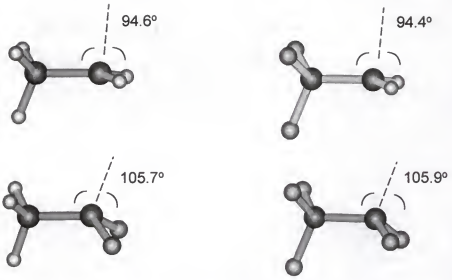

Figure 2-10. UHF/6-31G(d) Pyramidalization Angles for Ethyl Radicals $CH_3CH_2^{\bullet}$, $CF_3CH_2^{\bullet}$, $CH_3CF_2^{\bullet}$, and $CF_3CF_2^{\bullet}$.

Radical Stability

FMO theory dictates that for radicals bearing electronegative substituents with lone pairs (F, OH, NH_2, SH) an inductive, destabilizing influence exists, countered by stabilization resulting from delocalization of the unpaired electron.[154] Thus, in the σ sense, fluoroalkyl radicals are destabilized. Furthermore, the opposing π-stabilizing effect of the fluorine lone pairs decreases with pyramidalization of the radical site, due to diminished overlap with the 2p AO on carbon.

The progressive decrease in stability of alkyl radicals with α- or β-fluorination has been illustrated by Pasto,[80,147] in the form of calculated radical stabilization energies (RSE) based on isodesmic reactions (Table 2-7). The aforementioned increase in C-H bond dissociation energies along the fluoromethane series lends experimental support.

Although some degree of β C-F hyperconjugative interaction is observed in 2-fluoro substituted radicals,[152] such a contribution to overall radical stability is minor and inductive destabilizing influences dominate, as indicated by experimental and theoretical C-H BDEs for the 2-fluoroethanes (Table 2-8).

Table 2-7. Isodesmic Equation and Radical Stabilization Energies (RSE, kcal · mol^{-1}, 4-31G) for α- and β-Substituted Systems. Positive Values Denote Radical Stabilization.

$$X_n{}^{\bullet}CH_{3-n} + CH_4 \rightarrow X_nCH_{4-n} + {}^{\bullet}CH_3 \qquad (2\text{-}1)$$

X	RSE	X	RSE
F	+1.64	CH_3	+3.27
F_2	+0.56	OH	+5.73
F_3	-4.21	OCH_3	+5.30
CH_2F	+1.46	CN	+5.34
CHF_2	+0.16	NH_2	+10.26
CF_3	-1.34	$^{+}NH_3$	-4.07
		SH	+5.66
		$^{+}SH_2$	-3.17

Table 2-8. Experimental and Theoretical C-H Bond Dissociation Energies (kcal · mol^{-1}) of 2-Fluoroethanes.

CH_3CH_2-H	CH_2FCH_2-H	CF_2HCH_2-H	CF_3CH_2-H
101.1[a,b]	103.6[f]		106.7[a,f]
97.7[c]	99.6[c]	101.3[c]	102.0[c]
100.0[d]			104.3[d]
102.0[e]	104.1[e]	105.9[e]	107.1[e]

[a] Experimental Value; Reference 155. [b] Experimental Value, Reference 156.
[c] MP2/6-311G(d,p)//MP2/6-31G(d,p); Reference 157. [d] B3LYP/6-31G(d); Reference 91 and Present Study. [e] MP2/6-311+G(3df,2p)//MP2/6-31G(d); Reference 158.
[f] Experimental Value; Reference 159.

Organofluorine Radical Reactivity

As a result of the σ-withdrawing character of the fluorine substituent and interaction of the SOMO with C-F σ* orbitals, fluoroalkyl radicals should possess lowered SOMO energies and therefore exhibit enhanced SOMO-HOMO interactions in comparison with reactions of their hydrocarbon counterparts. Experimental ionization

potential and electron affinity data, although sparse, has been compiled in a recent review by Dolbier[90] and demonstrates the greater absolute electronegativity of the fluoroalkyl radicals. Calculated quantities, inferred from Koopmans' theorem[160] or based on radical-ion energy differences, follow the expected trend although quantitative agreement is often lacking.[161,162] The combination of such FMO, geometric, and enthalpy factors in hydrogen atom abstraction, intermolecular addition, and cyclization reactions of fluoroalkyl radicals is now discussed.

Hydrogen Atom Abstraction Reactions

A review by Tedder[163] has underlined the importance of polar and enthalpic factors in radical abstraction reactions. Activation parameters for abstraction by methyl and trifluoromethyl radicals from a series of hydrogen donors are provided in Table 2-9.

Table 2-9. Arrhenius Parameters for Hydrogen Atom Abstraction by Methyl and Trifluoromethyl Radicals.

	$CH_3^{\bullet}$		$CF_3^{\bullet}$	
H-Donor	E_a[a]	log A	E_a[a]	log A
CH_3-H	14.2	8.8	11.3	8.9
CH_3CH_2-H	11.8	8.8	6.9	8.4
$(CH_3)_2CH$-H	10.1	8.8	6.5	8.1
$(CH_3)_3C$-H	8.0	8.3	4.9	7.7
H-Cl	2.5[b]		5.0[c]	

[a] In kcal · mol^{-1}. [b] ΔH°_{rxn} = -1 kcal · mol^{-1}. [c] ΔH°_{rxn} = -3 kcal · mol^{-1}.

In the first four examples, the decrease in activation barrier for both $CH_3^{\bullet}$ and $CF_3^{\bullet}$ abstractions from alkanes are in line with the greater stability of the product radical; in each case, the barrier to abstraction by $CF_3^{\bullet}$ is substantially lowered. In contrast,

abstraction of hydrogen atom from HCl by $CF_3^\bullet$ is much less facile, occuring with a barrier twice that of $CH_3^\bullet$ in spite of its slightly greater exothermicity.

In collaboration with Lusztyk and Ingold at NRCC, LFP-determined rates of perfluoroalkyl radical addition to a number of alkenes have been determined by the Dolbier group.[54,85,88,91] This has afforded, via competitive kinetic techniques, absolute rate constants for hydrogen abstraction by the perfluoro-*n*-heptyl radical from a series of donors, summarized in Table 2-10.[54,86,87,89] For comparison, abstraction rate constants for hydrocarbon *n*-alkyl radicals were provided in Table 1-1.

Table 2-10. Absolute Rate Constants for Hydrogen Atom Abstraction for Perfluoro-*n*-heptyl Radicals. Rate Constants are at 303 K.

	Et_3SiH	$(TMS)_2Si(CH_3)H$	nBu_3GeH	$(TMS)_3SiH$	nBu_3SnH	PhSH
$k_H(n\text{-}C_7F_{15}^\bullet)$, $10^8\ M^{-1}\ s^{-1}$	0.75	16	15	51	203	0.28

For the first five donors in the series, a substantial rate enhancement is observed over hydrocarbon radicals, ranging from 75-fold in the case of nBu_3SnH to nearly 900-fold in the case of Et_3SiH, after slight temperature correction to 303 K. Although hydrogen transfer to perfluoroalkyl radicals is more exothermic (see the previous discussion on C-H BDEs) this is insufficent to account for a nearly three order of magnitude difference in rate constants. Furthermore, thiophenol, an excellent donor to hydrocarbon radicals, is found to suffer a greater than 400-fold *decrease* in transfer rate to perfluoroalkyls.

These characteristics are explained by the ability of the radical-donor pair to accommodate charge transfer interactions in the hydrogen transfer transition state, as previously discussed in Chapter 1. The relatively electropositive donor agents (stannanes, germanes, and silanes) lead to a more favorable polarity matchup with the electronegative perfluoroalkyl radical than with the hydrocarbon. Conversely, transfer from the more electronegative thiophenol results in a non-polarized or polarity-

mismatched transition state. The existence of such polar effects were confirmed by a correlation between rates of hydrogen transfer to perfluoro-*n*-heptyl radicals by a series of substituted thiophenols, versus their Hammett σ+ constants (Figure 2-11).[87] The resulting ρ value of -0.56, when compared to that obtained in the case of *tert*-butoxyl (-0.30)[164] again reflects the high electrophilicity of perfluoroalkyl radicals.

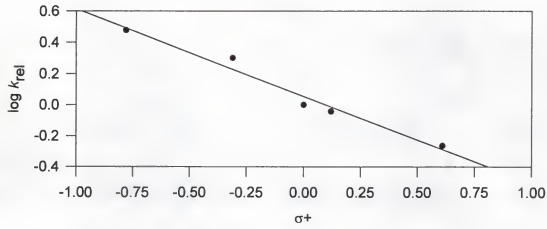

Figure 2-11. Hammett Plot for Hydrogen Abstraction from *para*-Substituted Thiophenols by Perfluoro-*n*-heptyl Radical.

Intermolecular Addition Reactions

Relative rates of addition of small fluorocarbon radicals to fluorinated and non-fluorinated olefins have been extensively investigated by Tedder and Walton, culminating in a critial review in 1980.[52] Table 2-11 illustrates the relative reactivity of

Table 2-11. Relative Rates of Addition of the Fluoromethyl Radicals to Ethene and Tetrafluoroethene.

Radical	k_{add} (C_2F_4) / k_{add} (C_2H_4) (437 K)
$^{\bullet}CH_3$	9.5
$^{\bullet}CH_2F$	3.4
$^{\bullet}CHF_2$	1.1
$^{\bullet}CF_3$	0.1

the fluoromethyl radicals towards ethylene and tetrafluoroethylene. Additional studies, utilizing a number of unsymmetrical methyl- and trifluoromethyl-substituted olefins, solidified the ascription of relative rates and regiochemical preferences to a combination of polar and steric influences.

Absolute rates of addition of perfluoroalkyl radicals to alkenes have been determined by laser flash photolysis, a subset of the data acquired to date presented in Table 2-12.[90] The dramatic rate acceleration enjoyed by the perfluoroalkyl radicals versus hydrocarbon *n*-alkyls is readily apparent, ranging from factors of 300 to 30,000 in the case of the heptafluoropropyl radical addition to electron-rich alkenes. The rate of addition to pentafluorostyrene, in constrast, is increased by only a factor of 42.

Table 2-12. Absolute Rate Constants for Addition of Perfluoroalkyl Radicals to Alkenes.

	k_{add}, 10^6 M^{-1} s^{-1} (298 K)					
Alkene	$^{\bullet}C_3F_7$	$^{\bullet}C_7F_{15}$	$^{\bullet}C_8F_{17}$	$^{\bullet}C_2F_5$	$^{\bullet}CF_3$	$RCH_2^{\bullet}$
Styrene	43	46	46	79	53	0.12
α-Methylstyrene	78	89		94	87	0.059
β-Methylstyrene	3.8	3.7		7.0	17	
Pentafluorostyrene	13			23	26	0.31
4-Methylstyrene			61			
4-Methoxystyrene			65			
4-Chlorostyrene			36			
4-(CF_3)Styrene			35			
1-Hexene	6.2	7.9		16		0.0002

Such enhancements may potentially be attributed to a combination of factors. Relative reaction enthalpies should play a role, as a stronger C-C bond (from CH_3-CH_3 versus CF_3-CH_3 BDE data in Table 2-3, ca. 11 kcal · mol^{-1}) is formed upon perfluoroalkyl

addition. However, only slight increases (factors of 5-7) in addition rates of the perfluoroalkyls to styrene versus 1-hexene are observed, despite the greater exothermicity (ca. 16 kcal · mol^{-1}) of the former. This demonstrates the relatively minor importance of reaction enthalpy, in accord with the early transition states expected for radical addition.

The pyramidal, σ-character of the fluoroalkyl radicals should afford a kinetic advantage (further discussed in Chapter 3) over the planar hydrocarbon, the LFP-measured rate of addition of 1,1-difluoropentyl radical to styrene, 2.7 x 10^6 M^{-1} s^{-1},[88] giving rise to a 22-fold enhancement relative to *n*-alkyls.

The primary factor responsible for such striking increases in reactivity is believed to be charge transfer influences (Figure 2-12) similar to those postulated for hydrogen atom transfer reactions. The lowered SOMO energies of the perfluoroalkyl radicals and resulting enhanced SOMO-HOMO interactions with alkenes in the addition transition state leads to substantial rate enhancement. Supporting evidence, in the form of a Hammett relation involving *para*-substituted styrenes and correlations between addition rates and alkene ionization potentials, has been offered.[54] *Ab initio* computations concur with the experimental findings and are discussed in Chapter 3.

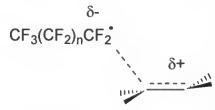

Figure 2-12. Polarized Transition State for Addition of Perfluoroalkyl Radicals to Alkenes.

Intramolecular Cyclization Reactions

Cyclopolymerization of fluorinated monomers has long been known as a means for the generation of macromolecular materials with unique physical properties.[165-168]

However, despite the widespread popularity of the unimolecular 5-hexenyl radical cyclization for the generation of five-membered rings, synthesis of fluorinated cyclic products utilizing radical methodology has received limited attention.[90] This is somewhat surprising, in light of the current interest and demonstrated importance of fluorinated analogues and mimics of pharmaceutical and agricultural agents.[169]

Until recently, no quantitative kinetic data existed for cyclization reactions of fluorinated radicals. With the competitively-determined rate constants of hydrogen abstraction by perfluoroalkyl radicals serving as basis reactions, rates of cyclization of a number of fluorinated 5-hexenyl systems have now been determined,[86,89,170] examples of which are provided in Figure 2-13.

Most obvious of the data is the remarkable rate acceleration in the *5-exo* cyclizations of **65** and **68**, occurring with 163- and 41-fold increases relative to the parent hydrocarbon **1** and ascribed to charge-transfer effects analogous to those occurring in bimolecular additions. Consequently, with no such polarity matchup in **71** (which involves cyclization of an electrophilic radical onto an electron-deficient double bond) only a minor increase in rate is observed. The *5-exo* cyclization rates of **71** and **74**, in line with those other hexenyl systems bearing fluorinated double bonds,[170] demonstrate the lack of kinetic impact of vinylic substitution.

Especially surprising is the degree to which **65** and **68** undergo *6-endo* closure, the former with a 1040-fold, and the latter a 700-fold acceleration relative to **1**. This is further discussed in Chapter 4, in which the reactivities of a series of lightly-fluorinated 5-hexenyl systems are investigated.

In the preceeding discussions of hydrogen abstraction, addition, and cyclization reactivity, the observed kinetic behavior was found to be due to a combination of geometric and polar effects induced by polyfluorination. Related studies of partially fluorinated alkyl radicals, addressed in the next two chapters, will aid in separating the effects of fluorination at the α and β positions and beyond, providing insight into the

extent to which the effects of perfluorination on the reactivity of organic radicals are the sum of their parts.

Table 2-13. Some Absolute Rate Constants for *5-exo* and *6-endo* Cyclization of Fluorinated 5-Hexenyl Radicals. Rate Constants are for 303 K.

Cyclization Reaction	k_{C5}, 10^5 s^{-1}	k_{C6}, 10^5 s^{-1}
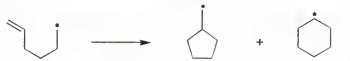 **1** **2** **3**	2.7	0.05
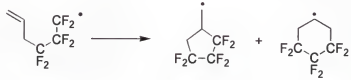 **65** **66** **67**	440	52
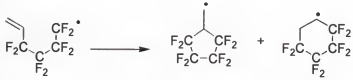 **68** **69** **70**	110	35
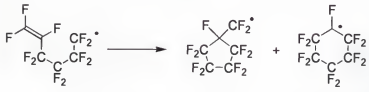 **71** **72** **73**	4.9	N/A
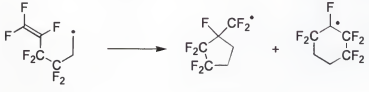 **74** **75** **76**	4.3	N/A

Conclusion

An introduction to the general structural and reactivity characteristics imparted by fluorine substitution in organic systems has been provided. Such substitution can either be stabilizing or destabilizing, depending on the nature of the ground state molecule, intermediate, or reaction in question.

A summary of the first absolute kinetic data obtained for reactions of fluorinated radicals has been presented. Results of these studies, involving per- or otherwise highly fluorinated systems, demonstrate the combined influence of polarity, structural, and enthalpic factors. The following studies of the addition, hydrogen abstraction, and cyclization kinetics of partially fluorinated alkyl radicals will serve to dissect the relative magnitudes of these influences on organic radical reactivity.

CHAPTER 3

THE REACTIVITY OF PARTIALLY FLUORINATED RADICALS IN INTERMOLECULAR ADDITION AND HYDROGEN ABSTRACTION REACTIONS

Introduction

Initial studies of the addition rates of some partially-fluorinated radicals to alkenes[88] demonstrated observable rate enhancements relative to *n*-alkyls, though not nearly as great as those of perfluoroalkyl systems. Such reactivity derives from the combination of structural and polar characteristics induced by fluorine substitution.

The current study extends the amount of absolute rate data assembled for the addition of partially fluorinated radicals to olefins. In addition, through competitive kinetic techniques, absolute rate constants for hydrogen abstraction from tri-*n*-butyltin hydride (nBu_3SnH) have been determined. Such kinetic data is necessary for the determination of absolute rates of cyclization of partially fluorinated 5-hexenyl radicals, discussed in Chapter 4, and allows for the partitioning of the gross reactivity characteristics of perfluoralkyl radicals into the separate influences of α, β, and γ fluorination. This is accomplished by use of the following systems: $RCH_2CH_2CF_2^{\bullet}$ (α,α-difluoro), $RCH_2CF_2CH_2^{\bullet}$ (β,β-difluoro), $RCH_2CF_2CF_2^{\bullet}$ ($\alpha,\alpha,\beta,\beta$-tetrafluoro), $CF_3CF_2^{\bullet}$ ($\alpha,\alpha,\beta,\beta,\beta$-pentafluoro), and $R_fCH_2CH_2^{\bullet}$ (γ-perfluoro).

The existence of charge transfer stabilization in the transition states for fluorinated radical addition to alkenes is corroborated by *ab initio* calculations, and the thermodynamics of C-H and C-C bonding and radical stablization in hydrofluorocarbons rationalized on the basis of Coulombic interactions.

Precursor Syntheses and Competitive Kinetic Studies

In each of the competitive kinetic runs, hydrofluorocarbon radicals were generated from bromide or iodide precursors by photoassisted C-X bond homolysis. These radicals subsequently underwent competitive trapping with known, varying concentrations of styrene or nBu_3SnH, adjusted to ensure pseudo-first-order kinetic behavior and to allow for accurately measurable amounts of trapping products, as depicted in Figure 1-17 and in greater detail below.

1,1-Difluorohex-1-yl Radical (**77**)

The synthesis of bromide precursor **80** was achieved in two steps (Figure 3-1) in a straightforward manner. Copper(I)-mediated addition of dibromodifluoromethane to 1-pentene (**78**), based on a modification by Gonzalez *et al.*[171] of a procedure by Burton and Kehoe[172] afforded 1,3-dibromo-1,1-difluorohexane **79** in typical yield. Regioselective displacement of the internal bromine was accomplished via sodium borohydride reduction in DMSO, providing precursor **80** contaminated with a small amount of overreduction product **81**. Pure samples of each were obtained by preparative GC separation, the former utilized in the competition run and the latter for spectral comparison with kinetic NMR data.

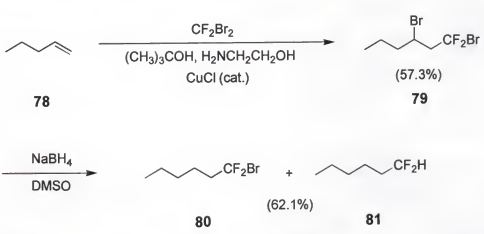

Figure 3-1. Preparation of 1-Bromo-1,1-difluorohexane **80** and 1,1-Difluorohexane **81**.

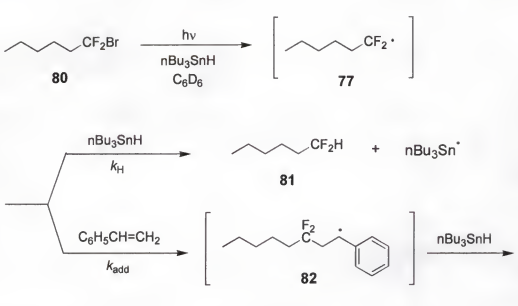

Figure 3-2. k_H / k_{add} Competitive Kinetic Scheme for 1,1-Difluorohex-1-yl Radical **77**.

Photolysis of **80** as a C_6D_6 solution in the presence of an excess of nBu_3SnH and styrene (Figure 3-2) afforded intermediate radical **77**. Subsequent entrapment by these agents (both irreversible processes) yielded **81** and **82**, respectively; the latter further trapped by nBu_3SnH to yield 3,3-difluoro-1-phenyloctane **83**. Throughout the course of the reaction, $nBu_3Sn^{\bullet}$ radicals are generated to propagate the chain process via abstraction of halogen from precursor **80**.

Product ratios for varied concentrations of trapping agents were determined by ^{19}F NMR analysis according to the pseudo-first-order relation in Equation 3-1,

$$\frac{[\,\mathbf{81}\,]}{[\,\mathbf{83}\,]} = \frac{[\,k_H\,]\,[\,\mathbf{77}\,]\,[\,nBu_3SnH\,]}{[\,k_{add}\,]\,[\,\mathbf{77}\,]\,[\,C_6H_5CH{=}CH_2\,]} \qquad (3\text{-}1)$$

a plot of product ratios obtained for each data point versus that of trapping agents affording the ratio k_H / k_{add}. The stability of trapped products under the reaction conditions and lack of appreciable side reactions were demonstrated by the high

conversion of precursor **80** to **81** and **83** versus an internal standard of α,α,α,-trifluorotoluene, (ϕ -63.24) indicating in turn the high efficiency of the chain process and reliability of the kinetic results. A partial ^{19}F NMR spectrum of the first of six data points is provided in Figure 3-3, a doublet of triplets (-CF_2H, ϕ -116.0) observed for **81** versus an overlapping triplet of triplets at ϕ -99.1 (-CF_2-) for **83**. Full kinetic data and yields are given in Table 3-1 below, the plot of which located in Figure 3-4. The slope of the line (3.39 ± 0.02) in conjunction with the known absolute rate constant for addition of

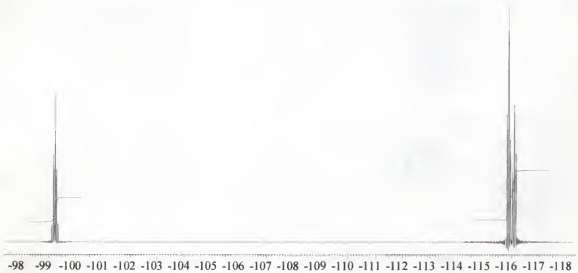

Figure 3-3. Partial ^{19}F NMR Spectrum of Data Point 1 for k_H / k_{add} Competition of 1,1-Difluorohex-1-yl Radical **77**.

Table 3-1. Competitive Kinetic Data for k_H / k_{add} Competition of 1,1-Difluorohex-1-yl Radical **77**.

[**80**]	[$C_6H_5CH=CH_2$]	[nBu_3SnH] / [$C_6H_5CH=CH_2$]	[**81**] / [**83**]	% Yield
0.094	2.01	0.719	2.30	95
0.094	1.81	0.847	2.73	95
0.094	1.61	1.01	3.26	96
0.094	1.41	1.21	3.93	97
0.094	1.21	1.49	4.88	96
0.094	1.01	1.87	6.21	95

1,1-difluoropent-1-yl radical to styrene, 2.7 (± 0.5) x 10^6 M^{-1} s^{-1}, resulted in an absolute rate constant k_H of 9.1 (± 1.7) x 10^6 M^{-1} s^{-1}. It should be noted that the accuracy of such derived k_H values can be no better than those reported in the LFP determinations of k_{add}, the error estimates in the former reflecting both the least-squares fit of the line and propagated error of the latter. Synthesis of styrene adduct **83** was performed by classic means for characterization and spectral comparison (Figure 3-5).

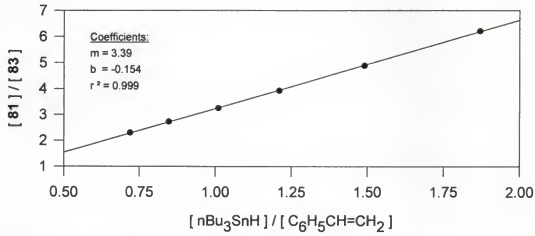

Figure 3-4. Plot of the Data in Columns 3 and 4 of Table 3-1.

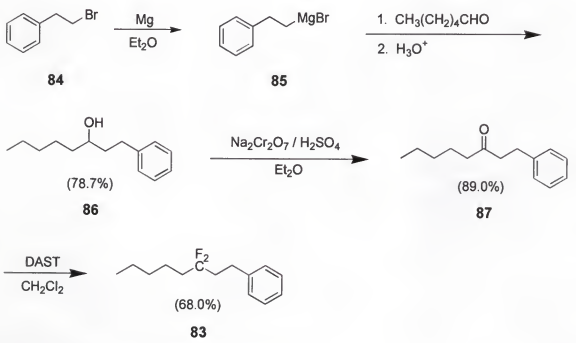

Figure 3-5. Preparation of Styrene Adduct **83**.

2,2-Difluorohex-1-yl Radical (**88**)

In accordance with literature precedent,[173] α-bromination of 2-hexanone in the presence of urea in acetic acid selectively afforded 1-bromo isomer **90** in 72.2% yield. Subsequent treatment with diethylaminosulfurtrifluoride (DAST) provided bromo precursor **91**, originally purified by preparative GC for use in the kinetic study. However, a sluggish chain reaction (further hindered by the strong UV absorption of the excess styrene present in the kinetic samples) led to the preparation of iodo precursor **92** (Figure 3-6) via Finkelstein transformation at elevated temperature.

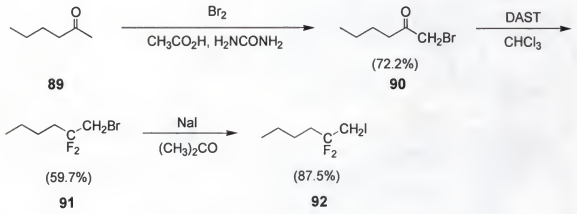

Figure 3-6. Preparation of 1-Iodo-2,2-Difluorohexane, (**92**) Precursor to 2,2-Difluorohex-1-yl Radical **88**.

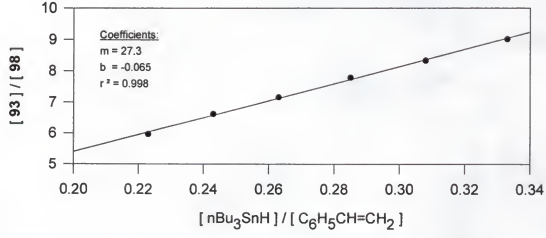

Figure 3-7. Plot for k_H / k_{add} Competition of 2,2-Difluorohex-1-yl Radical **88**.

The competition plot for k_H / k_{add} determination is found in Figure 3-7; raw data for this and all remaining experiments in this chapter may be found in Chapter 5. With the absolute rate constant for addition of 2,2-difluoropent-1-yl radical to styrene known from LFP experiments, a k_H value of 1.4 (± 0.5) x 10^7 M^{-1} s^{-1} was determined. Authentic samples of **93** and **98** were prepared for spectral comparison and characterization as illustrated below in Figure 3-8.

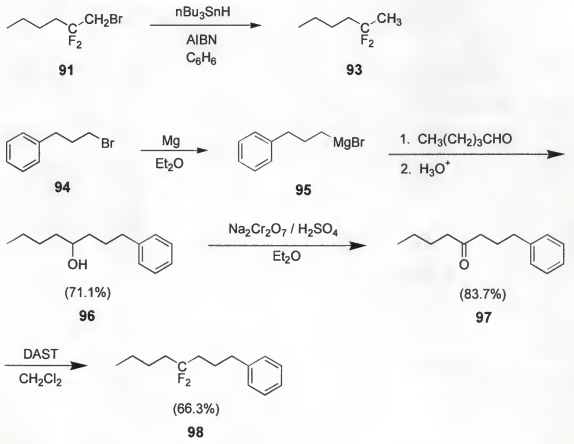

Figure 3-8. Preparation of Hydrogen Abstraction Product **93** and Styrene Adduct **98**.

1,1,2,2-Tetrafluorobut-1-yl (**99**) and 1,1,2,2-Tetrafluorohex-1-yl (**100**) Radicals

At the time of this study, no absolute rate constants for addition of a 1,1,2,2-tetrafluorinated radical to alkenes had been determined. Thus, in order to obtain a k_H value for such a system, a precursor suitable for absolute k_{add} measurements was first required. Bromide precursors, although in most cases sufficient for competition

experiments, are ineffective under the LFP operating conditions used in our k_{add} determinations (308 nm excimer laser pulses) due to their relatively short wavelength chromophore and small extinction coefficient (for **102**, ε_{max} = 37.3 M^{-1} cm^{-1}, λ_{max} = 218 nm, cyclohexane solvent). The instability of O-acylthiohydroxamic esters of the perfluoroalkanoic acids has been noted by Barton.[174] With neither these nor diacyl peroxide precursors lending themselves to isolation and / or shipment to the NRCC in Canada, the synthesis of a suitable iodide precursor was undertaken.

1-Bromo-1,1,2,2-tetrafluorohexane (**102**, Figure 3-9) was prepared in one step from 6-bromo-5,5,6,6-tetrafluorohex-1-ene (supplied by Halocarbons, Inc.) and its transformation to the corresponding iodide or carboxylic acid (the latter of which could be converted to the iodide via Hunsdieker methodology) attempted under a variety of conditions (Figure 3-10).

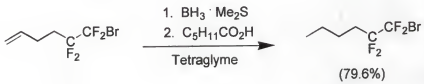

101 **102**

Figure 3-9. Preparation of 1-Bromo-1,1,2,2-tetrafluorohexane (**102**).

Although the conversion of perfluoroalkyl iodides to their lighter analogues is known in the literature,[175,176] downward transhalogenation of perfluoroaliphatic halides is exceedingly difficult. Indeed, all attempts at conversion of **102** to the corresponding iodide were met with failure. Perfluoroalkyl Grignard reagents, generated either directly (and in low yield) or via transmetallation by an alkylmagnesium halide, utilize iodide starting materials.[177,178] Investigations of perfluoroalkylzinc halides by Miller[179] resulted in a similar conclusion; perfluoro-*n*-propyl iodide may be converted to the organozinc reagent in ca. 60-80% yield (as determined by aqueous hydrolysis or capture with halogen electrophiles) after a brief induction period. On the contrary, reaction of heptafluoro-*n*-propyl bromide with zinc in 1,2-dimethoxyethane afforded no product after

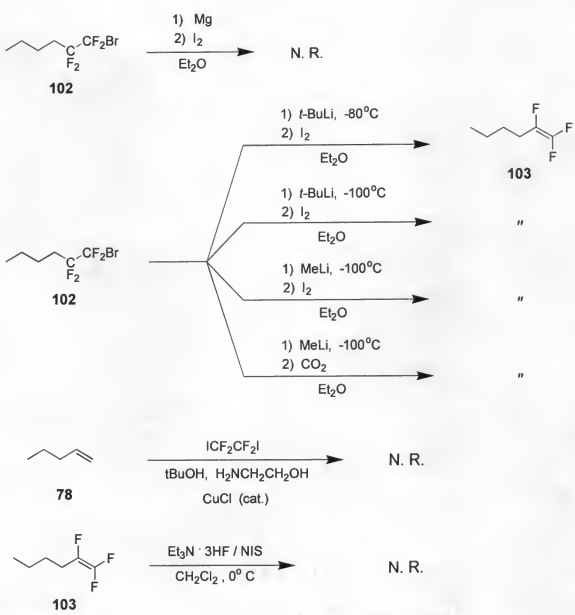

Figure 3-10. Attempted Preparation of Iodo Analogue of **102**.

73 hours at 90° C; a 60% yield of the zinc derivative was obtained (inferred via hydrolysis) after a period of 1.5 months. Attempted lithiation of **102** at low temperature resulted in the formation of β-fluoride elimination product 1,1,2-trifluoro-1-hexene, (**103**) as identified by its ^{19}F NMR spectrum. Additionally, neither Cu(I)-induced addition of 1,2-diiodotetrafluoroethane to 1-pentene nor iodofluorination of **103** utilizing the triethylamine trihydrofluoride / N-halosuccinimide methodology of Alvernhe *et al.*[180] were successful.

Synthesis of a C_4 iodide was achieved through modification of a DuPont literature procedure,[181] whereby 1,4-diiodo-1,1,2,2-tetrafluorobutane was produced in 40.1% yield via direct thermal addition of 1,2-diiodotetrafluoroethane to ethylene (Figure 3-11). DBU-induced elimination of hydrogen iodide in ether followed by diimide hydrogenation with hydrazine-hydrogen peroxide in methanol afforded tetrafluoroiodo precursor **107** in 2.8% overall yield after preparative GC purification, which was sent to the NRCC for absolute k_{add} measurements.

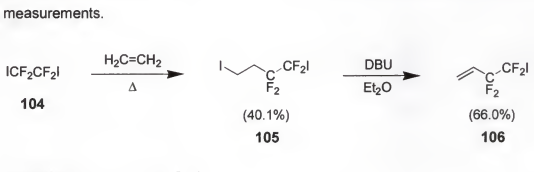

Figure 3-11. Preparation of 1,1,2,2-Tetrafluoro-1-iodobutane (**107**).

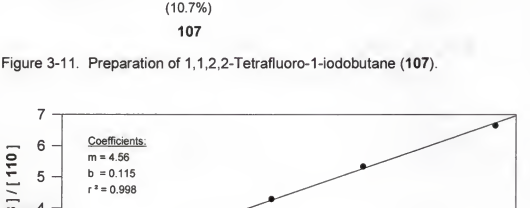

Figure 3-12. Plot for k_H / k_{add} Competition of 1,1,2,2-Tetrafluorohex-1-yl Radical **100**.

Bromide **102** was utilized in the k_H / k_{add} competition, the kinetic plot for which given in Figure 3-12. An authentic sample of styrene addition product **110** was prepared

by slow syringe pump addition of nBu_3SnH to a heated, irradiated solution of **102** and styrene in benzene (Figure 3-13).

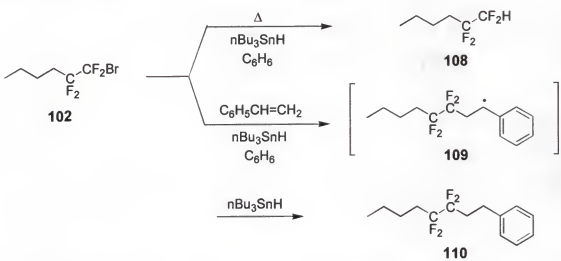

Figure 3-13. Preparation of Hydrogen Abstraction Product **108** and Styrene Adduct **110**.

2-[Perfluorohexyl]eth-1-yl Radical (**111**)

2-[Perfluorohexyl]-1-iodoethane **112** was provided as a gift from Prof. Neil Brace. The k_H / k_{add} competition plot is found in Figure 3-14; hydrogen abstraction product 1-[perfluorohexyl]ethane (**113**) and styrene adduct 1-[perfluorohexyl]-4-phenylbutane (**117**) were prepared as shown in Figure 3-15.

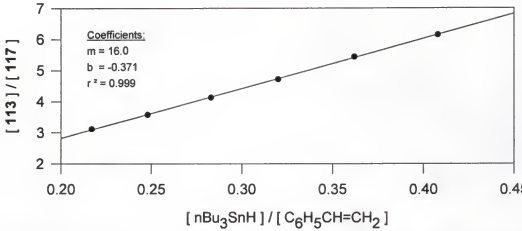

Figure 3-14. Plot for k_H / k_{add} Competition of 2-[Perfluorohexyl]eth-1-yl Radical **111**.

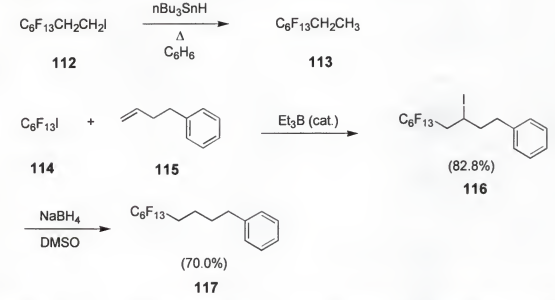

Figure 3-15. Preparation of Hydrogen Atom Abstraction Product **113** and Styrene Adduct **117**.

Pentafluoroethyl Radical (**118**)

Iodopentafluoroethane (**119**) was obtained from PCR, Inc. Due to the high volatility of both this precursor (bp 12-13° C) and hydrogen atom abstraction product pentafluoroethane (**120**, bp -48.5° C) **119** was handled as a solution in degassed C_6D_6. The k_H / k_{add} competition experiment (Figure 3-16) was performed in tubes which were quickly flame-sealed upon injection of an aliquot of the chilled precursor stock solution.

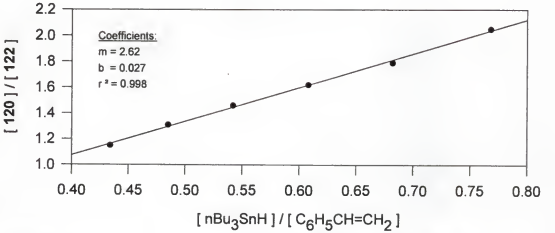

Figure 3-16. Plot for k_H / k_{add} Competition of Pentafluoroethyl Radical **118**.

Samples of **120** and **122** were prepared under free radical conditions for characterization purposes as shown in Figure 3-17.

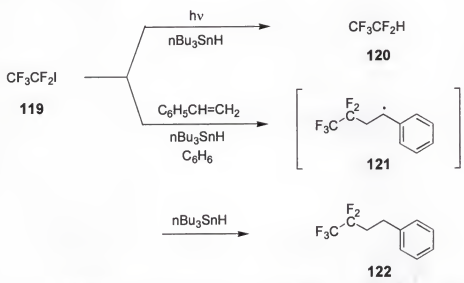

Figure 3-17. Preparation of Hydrogen Atom Abstraction Product **120** and Styrene Adduct **122**.

Discussion

Absolute rate constants for addition and hydrogen atom abstraction for systems studied in this chapter are provided in Table 3-2. For comparison, data for hydrocarbon (*n*-pentyl) and perfluoroalkyl (perfluoro-*n*-heptyl) radicals are included.

It is seen from the data that the reactivity trends for partially fluorinated radical additions to styrene are generally adhered to in hydrogen abstractions. However, the actual rate constants for the latter are observed to differ (on the average, by a factor of 11) from those for addition, and span a narrower range. The decrease in abstraction rate ratios as a function of substitution is due to the proximity (within an order of magnitude) to diffusion control for the more reactive radicals **100**, **118**, and **127**.

C-H and C-C bond dissociation energies of the fluoroalkanes should reflect the relative thermochemistry of hydrogen atom abstraction and addition to alkenes by their respective radicals. However, very few experimentally determined BDE values for such

Table 3-2. Absolute Rate Constants for Hydrogen Abstraction from Tributyltin Hydride and Addition to Styrene by Partially Fluorinated Radicals. Rate Constants are for 298 K.

Radical	k_{add} (M^{-1} s^{-1})	$k_{add\ (rel)}$	k_H (M^{-1} s^{-1})	$k_{H\ (rel)}$
$RCH_2CH_2^\bullet$ (**123**) [a]	1.2 x 10^5 [b]	1	2.4 x 10^6 [c]	1
$RCH_2CF_2^\bullet$ (**124**, **77**) [d]	2.7 (± 0.5) x 10^6 [e]	22.5	9.1 (± 1.7) x 10^6 [f]	3.8
$RCF_2CH_2^\bullet$ (**125**, **88**) [g]	5.2 (± 1.8) x 10^5 [e]	4.3	1.4 (± 0.5) x 10^7 [f]	5.8
$RCF_2CF_2^\bullet$ (**99**, **100**) [h]	2.0 (± 0.1) x 10^7 [f]	167	9.2 (± 0.8) x 10^7 [f]	38
$R_fCH_2CH_2^\bullet$ (**126**, **111**) [i]	1.3 (± 0.2) x 10^5 [e]	1.1	2.1 (± 0.3) x 10^6 [f]	0.9
$CF_3CF_2^\bullet$ (**118**)	7.9 (± 1.0) x 10^7 [f]	658	3.2 (± 0.3) x 10^8 [f]	133
$C_7F_{15}^\bullet$ (**127**)	4.6 (± 0.6) x 10^7 [j]	383	2.0 (± 0.3) x 10^8 [j]	83

[a] R = C_3H_7. [b] Reference 182, After Modification for Temperature and Other Factors in Table III of Reference 183. [c] Reference 27. [d] For k_{add} Experiment, R = C_3H_7 (**124**); for k_H Experiment, R = C_4H_9 (**77**). [e] Reference 88. [f] Reference 91 and Present Study. [g] For k_{add} Experiment, R = C_3H_7 (**125**); for k_H Experiment, R = C_4H_9 (**88**). [h] For k_{add} Experiment, R = C_2H_5 (**99**); for k_H Experiment, R = C_4H_9 (**100**). [i] For k_{add} Experiment, R_f = C_4F_9 (**126**); for k_H Experiment, R_f = C_6F_{13} (**111**). [j] Reference 54.

systems have been reported. Theoretical studies by Boyd[157,184] at the MP2 level have provided reasonably accurate C-H and C-C BDEs for C_2 hydrofluorocarbons. A more recent investigation based on isodesmic reactions by Marshall and Schwartz,[158] published after the completion of the present study, has yielded C-H BDEs of appreciably high quality for some linear (C_2) and branched (up to C_4) polyfluoroalkanes. Out of interest in determining additional C-H and C-C BDEs for larger (through C_4) fluorinated *n*-alkyls, the geometries of a series of partially fluorinated ethanes, propanes, and butanes, along with their respective radicals generated from terminal C-H or C-CH_3 bond cleavage, were optimized at the hybrid density functional level. This DFT method was chosen due to its implicit consideration of electron correlation at only slightly greater

computational expense than that of Hartree-Fock theory. Utilizing the three-parameter exchange functional of Becke[185] and the correlation functional of Lee, Yang, and Parr[186] with the 6-31G(d) basis, bond dissociation energies obtained in this "direct" fashion were found to be, in the cases where such values are known, within 1-3 kcal · mol^{-1} of those determined experimentally and in comparable or better agreement with experiment than the MP2/6-311G(d,p) values obtained by Boyd for C_2 systems. Tabulated experimental (where known) and calculated C-H and C-C BDE values are provided below in Tables 3-3 and 3-4, respectively.

Table 3-3. Theoretical and Experimental C-H Bond Dissociation Energies.

C-H Bond	Calculated BDE, kcal · mol^{-1} [a]	Experiment
CH_3CH_2-H	100.0 [b] 97.7 [c] 102.0 [d]	101.1 ± 1 [e]
CH_3CF_2-H	97.4 [b] 97.0 [c]	99.5 ± 2.5 [f]
CF_3CH_2-H	104.3 [b] 102.0 [c] 107.1 [d]	106.7 ± 1 [f]
CF_3CF_2-H	99.5 [b] 99.7 [c] 104.6 [d]	102.7 ± 0.5 [f]
$CH_3CH_2CH_2$-H	100.3 [b]	100.4 ± 0.6 [e]
$CH_3CH_2CF_2$-H	97.7 [b]	
$CH_3CF_2CH_2$-H	103.1 [b]	
$CH_3CF_2CF_2$-H	100.1 [b]	
$CF_3CH_2CH_2$-H	101.4 [b]	
$CF_3CF_2CH_2$-H	103.8 [b]	

[a] Reported as D_0 (298.15 K). [b] B3LYP/6-31G(d); Reference 91 and Present Study. [c] MP2/6-311G(d,p)//MP2/6-31G(d,p); Reference 157. [d] MP2/6-311+G(3df,2p)//MP2/6-31G(d); Reference 158. [e] Reference 187. [f] Reference 95.

Table 3-4. Experimental and Theoretical C-C Bond Dissociation Energies.

C-C Bond	Calculated BDE, kcal · mol^{-1} [a]	Experiment
CH_3-CH_3	89.4 [b] 90.6 [c]	90.4 ± 0.2 [d]
CF_3-CH_3	99.6 [b] 103.3 [c]	101.2 ± 1.1 [d]
CH_3CH_2-CH_3	86.3 [b]	
CH_3CF_2-CH_3	91.4 [b]	
CF_3CH_2-CH_3	91.4 [b]	
CF_3CF_2-CH_3	95.5 [b]	
$CH_3CH_2CH_2$-CH_3	86.7 [b]	
$CH_3CH_2CF_2$-CH_3	91.6 [b]	
$CH_3CF_2CH_2$-CH_3	89.9 [b]	
$CH_3CF_2CF_2$-CH_3	95.4 [b]	
$CF_3CH_2CH_2$-CH_3	87.8 [b]	

[a] Reported as D_0 (298.15 K). [b] B3LYP/6-31G(d); Reference 91 and Present Study.
[c] MP2/6-311G(d,p)//MP2/6-31G(d,p); Reference 157. [d] Reference 95.

Inspection of the data reveals interesting trends within both the C-H and C-C BDE series. From Table 3-3, it is observed that α-fluorination results in a weakening of C-H bonds, on the order of 1-3 kcal · mol^{-1}, as predicted by the various levels of theory and supported by experiment in the case of ethane versus 1,1-difluoroethane. Conversely, β-fluoro substitution results in a 3-5 kcal · mol^{-1} *increase* in terminal C-H BDEs. Furthermore, strengthening of C-C bonds (Table 3-4) is observed for all systems examined, whether substituted at the α, β, or even (albeit diminished) γ position. An explanation for this behavior, consistent with the given BDE and other thermochemical data, is provided later in the chapter.

With the relative thermodynamics of C-H and C-C bond formation investigated, attention is turned to polarity effects. As mentioned previously, rate constants for

addition of the perfluoroalkyl radicals to subtituted styrenes (Table 2-12) are observed to increase with decreasing ionization potential (styrene, IP 8.43 eV; α-methylstyrene, IP 8.19 eV; pentafluorostyrene, IP 9.20 eV).[188] In contrast, 1,1-difluoropentyl radical (**124**) was found to add with rates equal, within experimental error, for all three olefins.[88] From this observation, along with derived absolute electronegativities for the radicals $CH_3^{\bullet}$ (4.96), $CH_2F^{\bullet}$ (4.73), $CHF_2^{\bullet}$ (4.91), and $CF_3^{\bullet}$ (5.74) it was concluded that α-fluoro substitution alone does not impart electrophilicity to an alkyl radical, and may instead give rise to nucleophilic behavior.[88]

A series of theoretical studies by Wong *et al.*[48,49,189,190] have assessed the degree of charge transfer interaction in the transition states for methyl, hydroxymethyl, cyanomethyl and *tert*-butyl radical additions to a series of monosubstituted olefins. Based in part on the computation of partial charges, it was concluded that the addition of methyl radical was governed primarily by enthalpic effects, with no evidence for nucleophilic character arising from either Mulliken or Bader-based charge-fitting schemes. Hydroxymethyl and *tert*-butyl were found to be nucleophilic, with cyanomethyl exhibiting substantial electrophilicity.

In order to determine such tendencies for the fluorinated radicals under investigation, transition structures for the addition of hydrocarbon and fluoro-substituted ethyl radicals to ethylene and C_1 of propene have been located at the UHF/6-31G(d) level. Partial atomic charges were then computed, based on fits to the electrostatic potential at points selected according the Merz-Kollman-Singh scheme.[191,192]

Previous studies by Houk *et al.* utilizing the 3-21G basis found that addition of ethyl radical to ethylene occurs preferentially via a gauche conformation, with an incipient C-C-C-C dihedral angle of ca. 60°.[46] Such gauche and anti structures computed at the UHF/6-31(d) level are depicted in Figure 3-18, the former ca. 0.1 kcal · mol^{-1} lower in energy than that of (b). Inclusion of electron correlation at the spin-

projected PMP2/6-311G(d,p)//UHF/6-31G(d) level increases this energy difference to ca. 0.3 kcal · mol^{-1}.

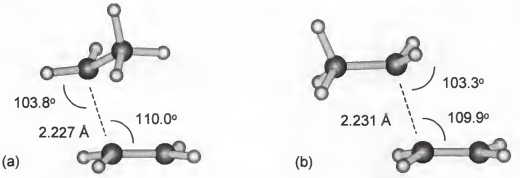

Figure 3-18. UHF/6-31G(d) (a) Gauche and (b) Anti Transition Structures for Addition of Ethyl Radical to Ethylene. Relevant Geometrical Parameters are Shown.

Consistent with UHF/3-21G results, the preferred mode of addition of the ethyl and radical to C_1 of propene involves a gauche arrangement of the radical with the alkene C=C π bond and a transoid orientation of the methyl group of the radical with respect to that of the olefinic C_2 carbon (Figure 3-19). This 'gauche-transoid' structure lies ca. 0.1 and 0.4 kcal · mol^{-1} below the 'anti' and 'gauche-cisoid' conformers, respectively, at the UHF/6-31(d) level after zero-point energy correction. Inclusion of correlation effects (PMP2/6-311G(d,p)//UHF/6-31G(d)) yields energy differences of 0.3 and 0.4 kcal · mol^{-1}. These orientation preferences extend to the fluoroethyl series, as seen in Tables 3-5 and 3-6.

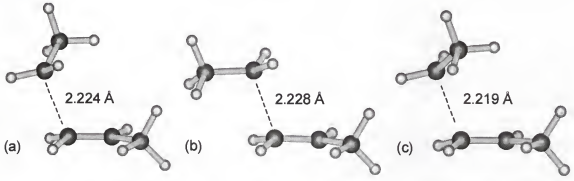

Figure 3-19. UHF/6-31G(d) (a) 'Gauche-transoid', (b) 'Anti', and (c) 'Gauche-cisoid' Transition Structures for Addition of Ethyl Radical to C_1 of Propene.

Table 3-5. Geometric Parameters and Total and Relative Energies of Transition Structures for Addition of Fluorinated Methyl and Ethyl Radicals to Ethylene.

Radical	r (C-C) (Å)	r (C=C) (Å)	∠ C-C-C (Deg.)	ϕ_{pyr} [c] (Deg.)	E_{tot} [d] (au)	ZPE (au)	E_{rel} [e]
$CH_3^\bullet$	2.246	1.382	109.1	101.9	-117.575692 (-118.045817)	0.089165	-
$CF_3^\bullet$	2.300	1.372	106.6	108.6	-414.156036 (-415.285304)	0.067955	-
$CH_3CH_2^\bullet$ [a]	2.227	1.384	110.0	103.8	-156.612999 (-157.243689)	0.120578	0.0 (0.0)
$CH_3CH_2^\bullet$ [b]	2.231	1.383	109.9	103.3	-156.612807 (-157.243039)	0.120455	0.05 (0.34)
$CH_3CF_2^\bullet$ [a]	2.235	1.378	110.0	108.6	-354.333278 (-355.404529)	0.105597	0.0 (0.0)
$CH_3CF_2^\bullet$ [b]	2.245	1.378	106.3	108.2	-354.332326 (-355.403222)	0.105470	0.53 (0.75)
$CF_3CH_2^\bullet$ [a]	2.258	1.380	109.0	104.1	-453.202939 (-454.490483)	0.097486	0.0 (0.0)
$CF_3CH_2^\bullet$ [b]	2.258	1.380	107.4	103.5	-453.203135 (-454.490294)	0.097452	-0.14 (0.10)
$CF_3CF_2^\bullet$ [a]	2.275	1.375	108.2	108.6	-650.904439 (-652.632413)	0.081977	0.0 (0.0)
$CF_3CF_2^\bullet$ [b]	2.280	1.375	104.7	108.1	-650.904343 (-652.632131)	0.081948	0.04 (0.16)

[a] Gauche. [b] Anti. [c] Degree of Radical Pyramidalization. [d] UHF/6-31G(d) Values; PMP2/6-311G(d,p)//UHF/6-31G(d) Values in Parentheses. [e] Relative Conformer Energy Differences, kcal · mol^{-1}. UHF/6-31G(d); PMP2/6-311G(d,p)//UHF/6-31G(d) Values in Parentheses.

Inspection of the data reveals the similarity in both angle of attack and forming C-C bond length, regardless of either the nature of the radical or conformation of the transition structure. Incipient bond lengths range from ca. 2.22 to 2.30 Å, generally slightly longer for additions of the fluorinated members of the series. These somewhat earlier transition states are also reflected in the shorter olefinic C=C bonds, 1.382 Å in the case of methyl radical addition to ethylene versus 1.372 Å for trifluoromethyl, in turn

Table 3-6. Geometric Parameters and Total and Relative Energies of Transition Structures for Addition of Fluorinated Methyl and Ethyl Radicals to C_1 of Propene.

Radical	r (C-C) (Å)	r (C=C) (Å)	∠ C-C-C (Deg.)	ϕ_{pyr} [d] (Deg.)	E_{tot} [e] (au)	ZPE (au)	E_{rel} [f]
$CH_3^\bullet$	2.243	1.383	109.3	102.0	-156.614381 (-157.244918)	0.119634	-
$CF_3^\bullet$	2.297	1.372	106.4	108.9	-453.195586 (-454.485598)	0.098359	-
$CH_3CH_2^\bullet$ [a]	2.224	1.385	110.2	103.9	-195.651571 (-196.442757)	0.150984	0.0 (0.0)
$CH_3CH_2^\bullet$ [b]	2.219	1.385	111.3	104.2	-195.651075 (-196.442411)	0.151060	0.35 (0.26)
$CH_3CH_2^\bullet$ [c]	2.228	1.384	110.1	103.3	-195.651399 (-196.442053)	0.150878	0.05 (0.38)
$CH_3CF_2^\bullet$ [a]	2.233	1.379	109.5	108.7	-393.372286 (-394.604285)	0.135951	0.0 (0.0)
$CH_3CF_2^\bullet$ [b]	2.228	1.380	110.7	108.9	-393.371834 (-394.603661)	0.135994	0.31 (0.42)
$CH_3CF_2^\bullet$ [c]	2.242	1.379	106.0	108.5	-393.371641 (-394.603448)	0.135892	0.37 (0.49)
$CF_3CH_2^\bullet$ [a]	2.254	1.381	109.3	104.2	-492.242374 (-493.691081)	0.127933	0.0 (0.0)
$CF_3CH_2^\bullet$ [b]	2.248	1.381	110.9	104.6	-492.242279 (-493.691288)	0.128087	0.15 (-0.04)
$CF_3CH_2^\bullet$ [c]	2.257	1.381	107.7	103.6	-492.242269 (-493.690171)	0.127869	0.03 (0.54)
$CF_3CF_2^\bullet$ [a]	2.274	1.375	108.0	108.7	-689.944220 (-691.833274)	0.112383	0.0 (0.0)
$CF_3CF_2^\bullet$ [b]	2.266	1.375	110.1	108.9	-689.944106 (-691.833236)	0.112473	0.12 (0.07)
$CF_3CF_2^\bullet$ [c]	2.279	1.375	104.6	108.3	-689.944068 (-691.832854)	0.112356	0.08 (0.25)

[a] Gauche-transoid. [b] Gauche-cisoid. [c] Anti. [d] Degree of Radical Pyramidalization.
[e] UHF/6-31G(d) Values; PMP2/6-311G(d,p)//UHF/6-31G(d) Values in Parentheses.
[f] Relative Conformer Energy Differences, kcal · mol^{-1}. UHF/ 6-31G(d); PMP2/ 6-311G(d,p)//UHF/6-31G(d) Values in Parentheses.

in accord with the greater exothermicity for the latter (ΔE_{rxn} = -22.35 kcal · mol^{-1} versus -34.52 kcal · mol^{-1}, respectively, at the [QCISD(T)/6-311G(d,p)]'//UHF/6-31(d) level, and C-C BDE data in Table 3-4).

Gauche-transoid addition of ethyl radical to C_1 of propene occurs via a transition structure with a forming C-C interatomic distance of 2.224 Å and and a C=C bond length of 1.385 Å, in comparison with 2.274 Å and 1.375 Å for addition of pentafluoroethyl along the same trajectory. Attack angles appear slightly smaller for additions of the fluorinated radicals, most notably in the case of $CH_3^{\bullet}$ versus $CF_3^{\bullet}$ and consistent with a reinforced SOMO-HOMO interaction for the latter. However, such differences are barely significant, and in the ethyl series appear to be influenced more by the conformation of the transition structure than the nature of the attacking radical, in line with the previously observed insensitivity of transition state geometry to additions of both nucleophilic and electrophilic radicals.[47,48]

Of note is the degree of pyramidalization at the radical site in the addition transition structure, ranging from 102-105° for radicals of the $RCH_2^{\bullet}$ type and 108-109° for α-fluorinated species. Considering the pyramidal nature of the ground states of the latter as well (Figures 2-9 and 2-10) it follows that α-fluoroalkyl radicals enjoy a kinetic advantage over their hydrocarbon analogues in that little or no additional bending is necessary to accommodate the addition transition structure. The energetic cost of pyramidalization of the methyl and *tert*-butyl radicals to the same extent as required for their addition to ethylene has been computed at 1.5 and 1.6 kcal · mol^{-1}, respectively, at the RMP2/6-31G(d)//UHF/6-31G(d) level.[49]

Calculated degrees of charge transfer (CT) between radical and olefin moieties of the addition transition structures are provided in Table 3-7. Where applicable, lowest energy conformations (gauche in the case of ethyl radical additions to ethylene, gauche-

transoid for additions to C_1 of propene) were used in the determination of the electrostatic potential-derived charges.

Table 3-7. Calculated Charge Transfer Data (Electrons) for Transition Structures of Hydrocarbon and Fluorinated Methyl and Ethyl Radical Addition to Ethylene and C_1 of Propene.

Radical	Ethylene [a]	Propene [b]
$CH_3^\bullet$	-0.019	-0.004
$CF_3^\bullet$	-0.013	-0.006
$CH_3CH_2^\bullet$	+0.036	+0.052
$CH_3CF_2^\bullet$	+0.030	+0.052
$CF_3CH_2^\bullet$	-0.047	-0.037
$CF_3CF_2^\bullet$	-0.045	-0.034

Note: Derived from UHF/6-31G(d) Electrostatic Potentials. Negative Values Denote Electron Transfer from Alkene to Radical. [a] Gauche Transition Structure. [b] Gauche-transoid Transition Structure.

Consistent with previous investigation, addition of $CH_3^\bullet$ to ethylene involves only a slight degree of charge transfer (-0.019 e) from olefin to radical (Mulliken and Bader analyses yield values of -0.017 and -0.011, respectively)[48] and even less so for addition to propene. Somewhat surprisingly, $CF_3^\bullet$ addition is also predicted to occur without appreciable polarization.

Along the ethyl series, such interactions appear more clearly defined. Ethyl radical addition to both ethylene and propene involves a shift of electron density from the radical to the alkene (0.036 and 0.052 e, respectively) well in accord with the expected nucleophilicity of the alkyl radicals. $CH_3CF_2^\bullet$ is predicted to be nucleophilic as well, exhibiting transition state polar characteristics very similar to those of its hydrocarbon counterpart and consistent with the experimentally deduced non-electrophilicity of the α-fluoro radicals.

A striking reversal in these trends occurs upon fluorination at the β carbon atom, regardless of the nature of the radical site itself. Here it is seen that both $CF_3CH_2^{\bullet}$ and $CF_3CF_2^{\bullet}$ exhibit substantial electrophilicty, with ca. 0.04 - 0.05 units of electron density transferred from the alkene to the radical center. To place such values into some degree of perspective, addition of the strongly electrophilic cyanomethyl radical to C_2 of electron-rich vinylamine is predicted to occur with a transfer of ca. 0.11 electrons from CH_2=$CHNH_2$ to $^{\bullet}CH_2CN$.[48]

It is especially noteworthy that the degree of CT in the case of $CF_3CH_2^{\bullet}$ and $CF_3CF_2^{\bullet}$ addition is practically unaffected by fluorination at the α carbon (-0.047 versus -0.045 and -0.037 versus -0.034, respectively). This, along with the demonstrated lack of kinetic impact of fluorine substitution at the γ position (Table 3-2) leads to the conclusion that the electrophilic character of the perfluoroalkyl radicals derives exclusively from substitution at the 2-position.

With geometric, enthalpic, and polar considerations for hydrofluorocarbon radicals having been addressed, the influences of each of these effects on determined k_{add} and k_H values are now discussed.

α,α-Difluoroalkyl Radicals (**77**, **124**)

The 1,1-difluoroalkyl radicals, as mentioned previously, benefit from pyramidalization at their radical site, leading to a more facile adoption of the transition structure for addition or hydrogen atom abstraction. However, such an advantage is counteracted by the experimentally and theoretically demonstrated lack of electrophilicity for such species. Moreover, the terminal C-H bond weakening effect of *gem*-difluoro substitution (2 - 3 kcal · mol^{-1}, Table 3-3) leads to a slight thermodynamic disadvantage for hydrogen abstraction by the corresponding radical relative to the hydrocarbon. Thus, the 3.8-fold rate enhancement enjoyed by **77** may be completely ascribed to the σ-type,

pyramidal nature of its ground state, attenuated by enthalpic and polarity factors working in opposition. In contrast, the strengthening effect of *gem*-difluorination on C-C bonds compliments that of pyramidal geometry, leading to a more substantial (22.5-fold) rate enhancement for the addition of **124** to styrene versus hydrocarbon **123**.

β,β-Difluoroalkyl Radicals (**88**, **125**)

The rate enhancements for addition (4.3) and hydrogen abstraction (5.8) observed for 2,2-difluoroalk-1-yl radicals are due to a complimentary combination of polar and enthalpic effects. The terminal C-H bond in 2,2-difluoropropane is predicted to be 2.8 kcal · mol^{-1} stronger than that of propane itself; similarly, *gem*-difluorination at C_2 of butane leads to a 3.2 kcal · mol^{-1} strengthening of its C_3-C_4 bond. In spite of these favorable considerations, the near-planar ground state geometry of **88** results in a modest net rate acceleration for hydrogen abstraction from nBu_3SnH. This also functions to oppose the CT and enthalpic advantages present in the addition reaction of **125**, giving rise to only a slight rate increase relative to *n*-alkyls and certainly diminished in comparison with that enjoyed by **124**.

γ-Fluorinated Radicals (**111**, **126**)

Due to the near-planar geometric character of 3-fluoroalk-1-yls and the lack of effect (ca. 1 kcal · mol^{-1}) on terminal C-H and C-C BDE values, fluorination beyond two carbon atoms removed from the radical site exhibits a negligible effect on the rates of both addition and hydrogen transfer. The reactivities of **111** and **126** are found to be, within experimental error, identical to those of the corresponding hydrocarbon.

α,α,β,β-Tetrafluoroalkyl Radicals (**99**,**100**) and Pentafluoroethyl Radical (**118**)

Radicals substituted at the α and β positions benefit from both pyramidal geometries and electrophilic character. Since the degree of pyramidalization of 1,1-

difluoroalkyl radicals remains constant regardless of substitution at the β- and further positions, geometrically induced influences on the reactivities of such polyfluorinated radicals are expected to be uniform. Consequently, rate enhancements for radicals of the type $RCH_2CF_2CF_2^{\bullet}$, $R_fCF_2CF_2CF_2^{\bullet}$, and $CF_3CF_2^{\bullet}$ versus $RCH_2CH_2CF_2^{\bullet}$ (for k_H: 38, 83, and 133 versus 3.8; for k_{add}: 167, 383 and 658 versus 22.5; all relative to *n*-alkyls) derive from either an increasing degree of transition state charge transfer stabilization, increasingly greater exothermicity of reaction, or a combination of both. The relevant C-H BDE data in Table 3-3 yields no direct correlation between reaction rate and enthalpy for the polyfluorinated radical series, with values of 97.7, 100.1, and 99.5 kcal · mol^{-1} corresponding to hydrogen abstraction by radicals **77**, **100**, and **118**. Similarly, terminal C-C BDEs of 91.6, 95.4, and 95.5 kcal · mol^{-1}, equated with the additions of **124**, **99**, and **118**, illustrate that although β-fluoro substitution should lead to rate enhancement on thermochemical grounds, such an effect does not account for the incremental acceleration across the series.

With the degree of radical electrophilicity related to its substitution at the 2-position and the potential for additional β C-F σ* delocalization made possible by the "extra" fluorine substituent in $CF_3CF_2^{\bullet}$ relative to $RCH_2CF_2CF_2^{\bullet}$ and $R_fCF_2CF_2CF_2^{\bullet}$, it follows that the increasing resonance and inductive withdrawal ability of these groups relative to $RCH_2CH_2CF_2^{\bullet}$ sufficiently explain both the enhanced reactivity of these radicals as a whole, as well as the observed trend.

Fluorine Substituent Effects on Bond Dissociation Energies; Coulombic Interactions

As previously discussed, substitution by fluorine in hydrocarbons gives rise to nearly additive and sometimes opposite effects on C-H and C-C homolytic bond dissociation energies. For example, the aforementioned 1-3 kcal · mol^{-1} weakening effect of α,α-difluoro substitution and the 3-5 kcal · mol^{-1} strengthening of terminal C-H

bonds by β-fluorination lead to near cancellation in the case of pentafluoroethane and 1,1,2,2-tetrafluoropropane, yielding BDE values very near those of the parent hydrocarbon (Table 3-3.) Furthermore, the 4.9 kcal · mol^{-1} strengthening brought about by substitution at the breaking C-C bond is reinforced by an additional 3-5 kcal · mol^{-1} upon further fluorine incorporation at the β position, leading to net increases of nearly 10 kcal · mol^{-1} over the parent in the C_2-C_3 homolysis of 1,1,1,2,2-pentafluoropropane and cleavage of the terminal C-C bond of 2,2,3,3-tetrafluorobutane.

The opposite effects of α,α-difluoro substitution on C-H and C-C bond dissociation energies bear special mention. Experimental BDE values in the fluoromethanes are in accord with the general RSE expectations of Pasto (Table 2-7) in that although substitution at a radical center by a single fluorine is stabilizing, its further incorporation leads to a successive decrease in RSE, resulting in net destabilization for $CF_3^{\bullet}$. This is consistent with the incremental strengthening of C-F bonds along the fluoromethane series, leading to a C-H BDE in CF_3H which is 1.9 kcal · mol^{-1} stronger than that of methane itself (methane BDE, 104.8 kcal · mol^{-1}; see discussion below Table 2-2) and the comparatively weaker C-H bonds in CH_3F and CH_2F_2.

The considerable stability of the 2,2-difluoroalkanes relative to their 1,1-difluoro isomers, demonstrated by the isodesmic reaction in Equation 3-2 (calculated from B3LYP/6-31G(d) total energies and zero-point corrections) provides the underlying reason for why the stability trends observed above do not extend to C-C bonds.

$$CH_3CF_2CH_3 + CH_3CH_3 \rightleftharpoons CH_3CF_2H + CH_3CH_2CH_3 \qquad (3\text{-}2)$$

$$\Delta E_{rxn} = +\,7.8 \text{ kcal} \cdot mol^{-1}$$

In Chapter 2, the Wiberg rationale of electrostatic attraction for the incremental strengthening and shortening of C-F bonds in the fluoromethanes was introduced. Similarly, it is found that such a Coulombic-based argument sufficiently explains the observed effects of fluorine substitution on C-H and C-C bond dissociation energies.

Atomic charges for select hydrofluorocarbons based on the B3LYP/6-31G(d) electrostatic potential (Merz-Kollman radii) are provided in Table 3-8.

The dipolar nature of the C-C bond in 1,1,1-trifluoroethane and its resultant increase in BDE relative to ethane and hexafluoroethane (Table 2-3) was first postulated by Rodgers.[156] Such stabilization due to increased C-C bond ionicity is seen in Equations 3-3 (derived from experimental heats of formation[188]) and 3-4 (from B3LYP/6-31G(d) total and zero-point energies).

Table 3-8. Atomic Charges in Hydrofluorocarbons, Based on B3LYP/6-31G(d) Density.

Hydrofluorocarbon	χF	χC_α	χC_β	χH_α	χH_β
$C_\alpha H_3C_\alpha H_3$ Ethane		-0.055		+0.018	
$C_\alpha H_2F_2$ Difluoromethane	-0.200	+0.320		+0.041	
$C_\beta H_3C_\alpha F_2H$ 1,1-Difluoroethane	-0.228	+0.467	-0.386	+0.020	+0.110 (2H) +0.135 (1H)
$C_\beta H_3C_\alpha F_2C_\beta H_3$ 2,2-Difluoropropane	-0.245	+0.631	-0.477		+0.133 (4H) +0.140 (2H)

$$CF_3CF_3 + CH_3CH_3 \rightleftharpoons 2\ CH_3CF_3 \qquad (3\text{-}3)$$

$$\Delta E_{rxn} = -16.9\ kcal \cdot mol^{-1}$$

$$CH_3CH_2CH_2CH_3 + CH_3CF_2CF_2CH_3 \rightleftharpoons 2\ CH_3CF_2CH_2CH_3 \qquad (3\text{-}4)$$

$$\Delta E_{rxn} = -5.0\ kcal \cdot mol^{-1}$$

The significant electrostatic attraction between adjacent carbon atoms in both CH_3CF_2H and $CH_3CF_2CH_3$ is readily apparent from the data in Table 3-8, providing an explanation for the strengthening of these bonds relative to their hydrocarbon or perfluorocarbon analogues. In addition, C-H repulsion in difluoromethane and 1,1-difluoroethane is predicted, in accord with the observed weakening of these bonds compared to those of methane and ethane. Conversely, the strong attraction between

the β carbon and hydrogen atoms of CH_3CF_2H (χC, -0.386; χH_{avg}, +0.118) and $CH_3CF_2CH_3$ (χC, -0.477; χH_{avg}, +0.135) is consistent with their greater theoretical and experimental BDEs.

Conclusion

Based on time-resolved k_{add} measurements, absolute rate constants for hydrogen abstraction from tri-*n*-butyltin hydride have been determined for a series partially fluorinated radicals. The reactivities of such radicals towards nBu_3SnH follow those of addition to alkenes. The enhanced reactivity of α,α-difluoroalkyl radicals in hydrogen abstraction reactions derives exclusively from their pyramidal geometry. β-Fluorination leads to a favorable combination of polar and thermodynamic factors in both addition and hydrogen transfer reactions, giving rise to the exceptional reactivity of $CF_3CF_2^{\bullet}$ and the perfluoroalkyl radicals as a whole. In Chapter 4, the k_H values so obtained are utilized in the determination of absolute rates of cyclization for partially fluorinated 5-hexenyl radicals.

A self-consistent rationale for the impact of fluorine substitution on C-H and C-C bond dissociation energies based on electrostatic considerations was offered, providing new understanding of the thermochemistry of bonding and radical stabilization in hydrofluorocarbons.

CHAPTER 4

THE REACTIVITY OF PARTIALLY FLUORINATED RADICALS IN INTRAMOLECULAR CYCLIZATION REACTIONS

Introduction

The intramolecular addition reactions of 5-hexen-1-yl radicals continue to attract the attention of synthetic and physical organic chemists alike. Such cyclizations to (predominantly) *5-exo* products have been utilized as probes for the detection of radical intermediates and as basis reactions for the competitive determination of absolute kinetic data for a number of free radical transformations.[16] Rationalization of the rates, and especially the regio- and stereochemistry, of intramolecular radical additions on the basis of force field[63,64,66,67] and molecular orbital[62,65,66,68] techniques has proven to be one of the greatest successes of theory in the prediction of organic reactivity. Due in no small part to such structure-reactivity studies, application of free radical methodology to the singular and tandem construction of 5-membered rings has been equally exploited, providing for the assembly of functionalized organic systems under mild conditions, often accomplished with a high degree of stereocontrol.[11-15]

Determination of absolute rates of cyclization of per- and other highly fluorinated 5-hexenyl systems[86,69,170] have aided in solidifying the understanding of the effect of fluorine substitution on the reactivity of organic radicals, though at the same time generating a number of new questions, particularly with regard to cyclization regiochemistry.

In order to examine the potentially more subtle influences of partial fluorination on 5-hexenyl radical reactivity, and to obtain a set of data through which the effect of

incremental *gem*-difluoro substitution along the aliphatic portion of the 5-hexenyl chain may be assessed, absolute rates of *5-exo* and *6-endo* cyclization for some partially fluorinated 5-hexenyl radicals have been determined based on competitive kinetic technique and the absolute rates of hydrogen abstraction obtained in Chapter 3.

Precursor Syntheses and Competitive Kinetic Studies

As in the bimolecular addition versus hydrogen abstraction competition studies, bromide precursors were utilized in the generation of partially fluorinated 5-hexenyl radicals. Photolysis by UV irradiation (Rayonet photoreactor) in the presence of known, varying concentrations of hydrogen atom donor, carefully adjusted to ensure pseudo-first order kinetic behavior and to allow for accurately measurable amounts of cyclization and hydrogen abstraction products, provided the kinetic ratio k_H / k_{Cn}. Absolute rate constants for *5-exo* and (where applicable) *6-endo* cyclization were then determined from the known value of hydrogen abstraction rate constant k_H, illustrated in Figure 1-18 and in greater detail below.

1,1-Difluorohex-5-en-1-yl Radical (**128**)

Synthesis of bromide **135** was achieved in six steps in ca. 14.5% overall yield, starting from commercially available 3-buten-1-ol (**129**, Figure 4-1). Curiously, direct addition of dibromodifluoromethane to **129** could not be induced, even through extended reaction time at elevated temperatures. Although the presence of the alcohol functionality in the alkene starting material would not have been expected to exhibit a detrimental effect (in light of the hydroxylic nature of the ethanolamine / *tert*-butanol cosolvent medium) protection of the hydroxyl moiety as its *tert*-butyldimethylsilyl ether **130** (TBDMSCl, imidazole in dimethylformamide) followed by dibromodifluoromethane addition indeed afforded 1,3-dibromo-1,1-difluoro adduct **131** in good yield. Highly selective displacement of the internal bromine yielded bromodifluoromethyl derivative

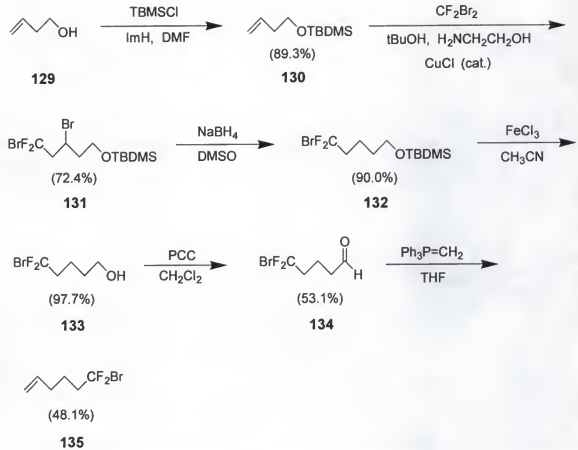

Figure 4-1. Preparation of 6-Bromo-6,6-difluorohex-1-ene, Precursor to 1,1-Difluorohex-5-en-1-yl Radical **128**.

132 with virtually no overreduction product, as monitored via ^{19}F NMR through high conversion of starting material. Lewis acid deprotection via the method of Cort[193] and subsequent pyridinium chlorochromate oxidation provided aldehyde **134**, further subjected to Wittig olefination to yield precursor **135**.

Generation of **128** was achieved via irradiation of a solution of **135** in C_6D_6 in the presence of excess nBu_3SnH (Figure 4-2) and an internal standard of α,α,α-trifluorotoluene. Direct capture of **128** by hydrogen atom donor afforded reduction product 6,6-difluorohex-1-ene **136**, whereas intermediate **137**, subsequently trapped by nBu_3SnH to yield spectroscopically observable cyclization product **138**, was generated via irreversible, unimolecular rearrangement with rate constant k_{C5} (no *6-endo* cyclization was observed, within NMR detection limits, (ca. 4%) for **128**). During the course of the

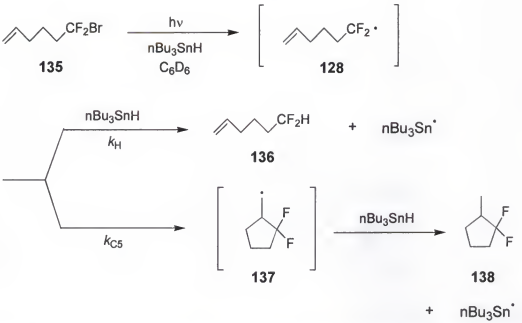

Figure 4-2. k_H / k_C Competitive Kinetic Scheme for 1,1-Difluorohex-5-en-1-yl Radical **128**.

reaction, tributylstannyl radicals generated by transfer of hydrogen atom from nBu_3SnH to **128** and **137** served to propagate the chain process via bromine abstraction from **135**.

Product ratios for varied concentrations of nBu_3SnH were determined by ^{19}F NMR analysis according to the pseudo-first-order relation in Equation 4-1,

$$\frac{[\,\mathbf{136}\,]}{[\,\mathbf{138}\,]} = \frac{[\,k_H\,]\,[\,\mathbf{128}\,]\,[\,nBu_3SnH\,]}{[\,k_{C5}\,]\,[\,\mathbf{128}\,]} \qquad (4\text{-}1)$$

a plot of which obtained for each data point versus nBu_3SnH concentration providing the ratio k_H / k_{C5}. Exceptionally clean spectra and high mass balances were obtained for each kinetic point, indicating the efficiency of the radical chain process and reliability of the obtained rate constant ratios. A partial ^{19}F spectrum of the first of six data points is provided in Figure 4-3, a doublet of triplets ($-CF_2H$, ϕ -116.2) observed for **136** versus overlapping doublets of doublets of triplets at ϕ -100.3 and -107.8 for the diastereotopic $-CF_2-$ resonances of **138**. Kinetic data and product yields are given in Table 4-1, a plot of which found in Figure 4-4. The slope of the line (2.57 ± 0.05) in conjunction with the

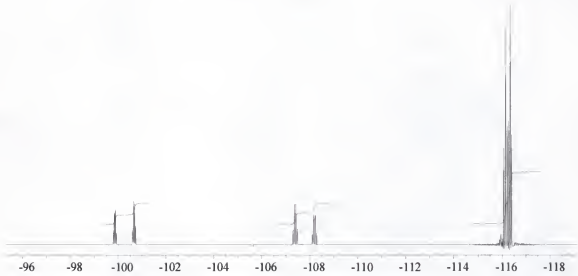

Figure 4-3. Partial ^{19}F NMR Spectrum of Data Point 1 for k_H / k_C Competition of 1,1-Difluorohex-5-en-1-yl Radical **128**.

Table 4-1. Competitive Kinetic Data for k_H / k_C Competition of 1,1-Difluorohex-5-en-1-yl Radical **77**.

[**135**]	[nBu_3SnH]	[**136**] / [**138**]	% Yield
0.054	0.673	1.53	88
0.054	0.807	1.91	100
0.054	0.942	2.28	89
0.054	1.08	2.57	94
0.054	1.21	2.93	95
0.054	1.35	3.29	92

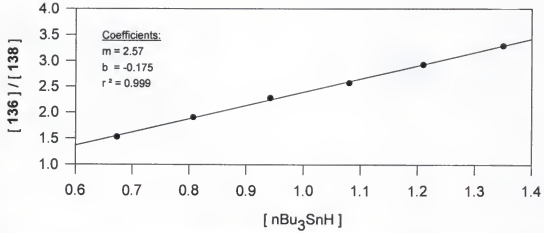

Figure 4-4. Plot of the Data in Columns 2 and 3 of Table 4-1.

known absolute rate constant for hydrogen atom abstraction from nBu_3SnH by 1,1-difluorohex-1-yl radical **77**, 9.1 (± 1.7) x 10^8 M^{-1} s^{-1}, resulted in a k_{C5} value of 3.5 (± 0.59) x 10^6 s^{-1} for *5-exo* closure of **128**, with errors in k_C reflecting both the least-squares fit of the line and propagated error in k_H. Syntheses of hydrogen atom transfer and cyclization products **136** and **138** were performed as shown in Figure 4-5.

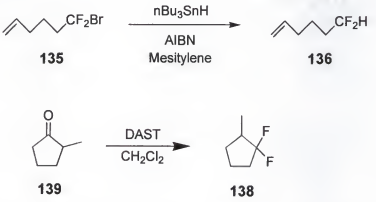

Figure 4-5. Preparation of Hydrogen Abstraction and *5-Exo* Cyclization Products **136** and **138**.

2,2-Difluorohex-5-en-1-yl Radical (**140**)

Bromide **144** was obtained in a three-step synthesis starting from 1,2-epoxy-5-hexene (Figure 4-6). Regiospecific ring opening by a Corey[194] procedure afforded bromohydrin **142**, converted to the corresponding α-haloketone via Jones oxidation. Treatment of **143** with DAST in dichloromethane afforded precursor **144** in 40.9% overall yield, purified by preparative GC for competitive kinetic study.

In contrast to the virtually regiospecific *5-exo* closure of **128**, a broad singlet resonance at ϕ -95.8, comprising approximately 9% of cyclized products, was observed in the ^{19}F NMR spectra for the k_H / k_C competition of **140**. This is attributed to competing *6-endo* cyclization to **148** (Figure 4-7), the presence of which was confirmed by spectral comparison with that of an authentic sample of **149**.

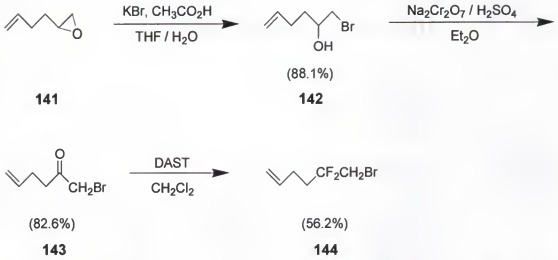

Figure 4-6. Preparation of 6-Bromo-5,5-difluorohex-1-ene, Precursor to 2,2-Difluorohex-5-en-1-yl Radical **140**.

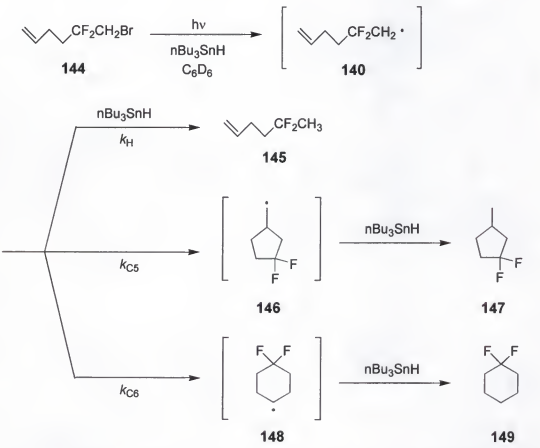

Figure 4-7. k_H / k_C Competitive Kinetic Scheme for 2,2-Difluorohex-5-en-1-yl Radical **140**.

Cyclizations of β,β-difluoroalkyl radicals have appeared in the synthetic literature,[195] utilized in the generation of alkoxy-substituted *gem*-difluorocyclopentane, cyclohexane, and tetrahydropyran derivatives, though reported to undergo addition in an *exo*-specific manner. However, the regiochemical behavior exhibited in the cyclization of **140** provided experimental verification of that previously predicted on the basis of *ab initio* calculations, performed as part of the present study and elaborated upon in the Discussion section of the chapter. Competition plots for k_H / k_{C5} and k_H / k_{C6} are found in Figures 4-8 and 4-9, respectively. Preparation of hydrogen abstraction and *5-exo* and *6-endo* cyclization products was performed as shown in Figure 4-10.

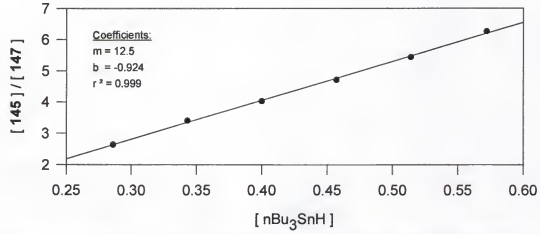

Figure 4-8. Plot of k_H / k_{C5} Competition of 2,2-Difluorohex-5-en-1-yl Radical **140**.

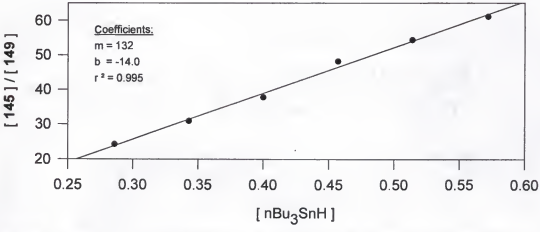

Figure 4-9. Plot of k_H / k_{C6} Competition of 2,2-Difluorohex-5-en-1-yl Radical **140**.

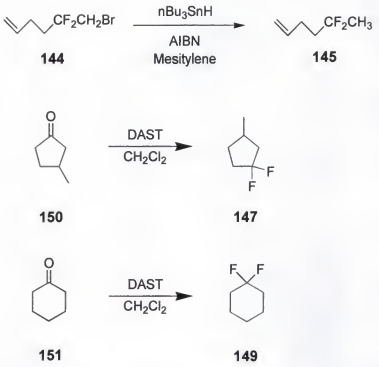

Figure 4-10. Preparation of Hydrogen Abstraction and *5-Exo* and *6-Endo* Cyclization Products **145**, **147**, and **149**.

1,1,2,2-Tetrafluorohex-5-en-1-yl Radical (**152**)

Bromide **101** (Halocarbons, Inc.) served as the precursor to α,α,β,β-tetrafluorinated radical **152**. However, attempts at determination of accurate k_H / k_C ratios using nBu_3SnH as a trapping agent met with failure, leading primarily to reduction product **153**, with only minor amounts of **155** and **177** evident in the ^{19}F NMR baseline which could not be integrated accurately over a span of hydrogen atom donor concentrations (Figure 4-11). In principle, lowering the concentration of both radical precursor (typically in the 0.05 - 0.1 M range) and trapping agent (while still maintaining pseudo-first order conditions) should effectively decrease the amount of reduction product and allow for a greater degree of cyclization to be observed. However, too great of a decrease in precursor concentration leads to decreased NMR signal to noise ratios, the necessity of longer acquisition times per sample, and increased potential for the introduction of systematic error.

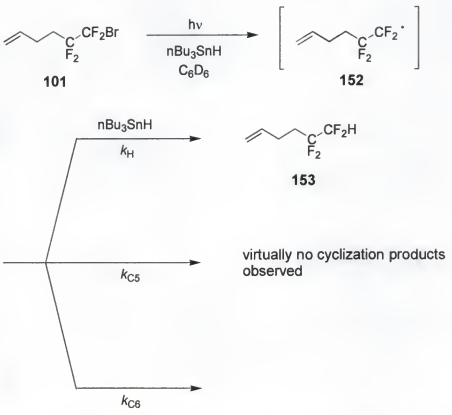

Figure 4-11. Attempted k_H / k_C Competition of 1,1,2,2-Tetrafluorohex-5-en-1-yl Radical **152** with nBu_3SnH as Trapping Agent.

As it was evident that any cyclization reaction of **152** occurred with a rate constant too low to be competitive with transfer of hydrogen from nBu_3SnH, attention was turned to alternative trapping agents. With the rate of hydrogen atom transfer to perfluoroalkyl radicals by a number of reducing agents having been accurately determined (Table 2-10), it was decided to investigate the suitability of tris(trimethylsilyl)silane ($(TMS)_3SiH$) as a competitive trapping agent for the calibration of cyclization rate constants for **152**, due to its approximately four-fold decrease in hydrogen transfer rate to perfluoroalkyls relative to nBu_3SnH. For such a competition to be of kinetic value, however, it was necessary to determine rate constant k_H for tetrafluoroalkyl radical **100** with $(TMS)_3SiH$, using its known rate of addition to styrene as a competing basis reaction. The plot for the k_H ($(TMS)_3SiH$) / k_{add} (styrene) competition of **100** is provided in Figure 4-12.

With the k_H ($(TMS)_3SiH$) value of 1.8 (± 0.1) x 10^7 M^{-1} s^{-1} for **100** in hand (which, along with its k_H (nBu_3SnH) of 9.2 (± 0.8) x 10^7 M^{-1} s^{-1}, (Table 3-2) may be compared with 5.1 x 10^7 M^{-1} s^{-1} and 2.0 x 10^8 M^{-1} s^{-1}, respectively, for perfluoro-*n*-alkyl radicals; Table 2-10) rate constants k_{C5} and k_{C6} for **152** were then determined (Figures 4-13 and 4-14.) Use of this slower hydrogen transfer agent allowed for sufficient competitive (including significant *6-endo*) cyclization such that accurate k_H / k_{Cn} ratios could be obtained. Isolation of products **153**, **155**, and **157** was achieved by slow syringe pump addition of nBu_3SnH to a heated, irradiated solution of **101** in mesitylene (Figure 4-15).

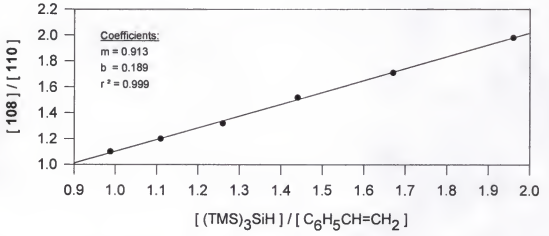

Figure 4-12. Plot for k_H ($(TMS)_3SiH$) / k_{add} (Styrene) Competition of 1,1,2,2-Tetrafluorohex-1-yl Radical **100**.

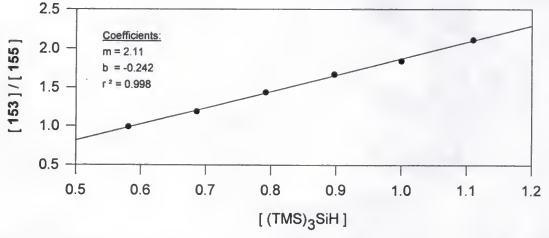

Figure 4-13. Plot of k_H / k_{C5} Competition of 1,1,2,2-Tetrafluorohex-5-en-1-yl Radical **152**.

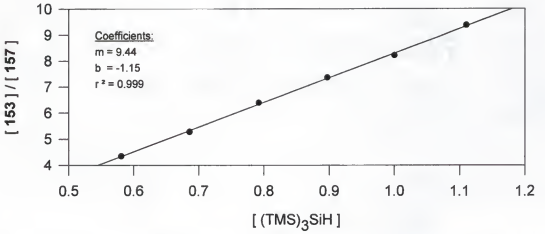

Figure 4-14. Plot of k_H / k_{C6} Competition of 1,1,2,2-Tetrafluorohex-5-en-1-yl Radical **152**.

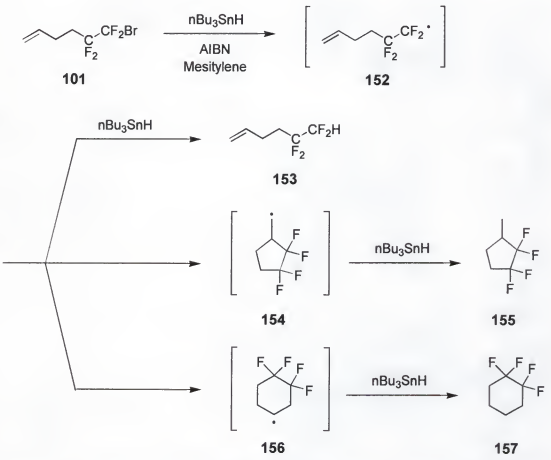

Figure 4-15. Preparation of Hydrogen Abstraction and *5-Exo* and *6-Endo* Cyclization Products **153**, **155**, and **157**.

Discussion

Absolute rate constants of cyclization for radicals **128**, **140**, and **152** are given in Table 4-2. For comparison, such k_{C5} and (where applicable) k_{C6} values for parent hydrocarbon **1** and fluorinated radicals **65** and **68** are also provided, the latter two systems along with those of the current study found to give rise to the greatest impact on cyclization kinetics and regiochemistry. Recent studies of 5-hexenyl systems bearing vinylic fluorine substituents have demonstrated that the effect of such substitution is relatively minor, with no *6-endo* products observed within the detection limits imposed by NMR analysis and $k_{C5\ (rel)}$ values with respect to **1** ranging from ca. 0.09 to 2.3.[170]

Cyclization Kinetics

Rates of intramolecular addition of partially-fluorinated radicals to alkenes should be governed by the same combination of steric, polar, and thermodynamic factors which influence the reactivity of their intermolecular counterparts. As seen by comparison of the data in Tables 3-2 and 4-2, the reactivity characteristics of the above radicals in unimolecular cyclization reactions, particularly *5-exo* closure, generally reflect those observed in bimolecular additions. This is logical in light of the similarity of their transition structures, elaborated upon in Chapters 1 and 3.[66]

The pyramidal nature of α,α-difluoroalkyl radicals, combined with the more favorable thermodynamics of C-C bond formation involving fluorinated carbon (see related discussions in Chapters 2 and 3, along with cyclization transition structures and energies of reaction below) provide sufficient explanation for the 13-fold increase in rate of *5-exo* ring closure of **128** relative to **1**. The factor of 22.5 observed for addition of **77** versus **124** to styrene is consistent with the observed cyclization rate ratios.

The increase in k_{C5} of 4.1 enjoyed by **140** parallels that of bimolecular addition of **125** to styrene, (4.3) due to its increased electrophilicty over both hydrocarbon **1** and

Table 4-2. Absolute Rate Constants for *5-Exo* and *6-Endo* Cyclization of Partially Fluorinated 5-Hexenyl Radicals. Rate Constants are for 303 K; Relative k_{Cn} Values in Parentheses.

Cyclization Reaction	k_{C5}, 10^5 s^{-1}	k_{C6}, 10^5 s^{-1}
1 **2** **3**	2.7 [a] (1)	0.05 [a] (1)
128 **137** **158**	35 (± 5.9) [b] (13.0)	N/A [b,c]
140 **146** **148**	11 (± 3.8) [b] (4.1)	1.1 (± 0.34) [b] (22)
152 **154** **156**	87 (± 4.1) [b] (32.2)	19 (± 1.1) [b] (380)
65 **66** **67**	440 (± 46) [d] (163)	52 (±6.4) [d] (1040)
68 **69** **70**	110 (±1.7) [d] (40.7)	35 (± 4.4) [d] (700)

[a] Reference 16. [b] Current Study. [c] *6-Endo* Cyclization Not Observed Within ^{19}F NMR Detection Limits (Approximately 4%). [d] Reference 170.

α,α-difluorocarbon **128** and greater exothermicity of addition relative to *n*-alkyls, though tempered by the effectively planar, π-nature of its radical center.

α,α,β,β-Tetrafluorinated radical **152**, as in the case of bimolecular additions, benefits from favorable thermodynamics of addition as well as its electrophilicty and σ-character, leading to the 32-fold increase in k_{C5} compared to parent **1**. It should be noted that such unimolecular cyclizations possess an inherent entropic advantage over their bimolecular analogues, generally proceeding with log A values ca. 2 units larger than those for the latter[16] and resulting in a leveling of rate ratios relative to intermolecular additions.

Upon additional fluorination of the aliphatic moiety of the 5-hexenyl chain (**65**, **68**) such radicals undertake perfluoroalkyl character, leading to further increase in reactivity akin to that observed for $C_7F_{15}^{\bullet}$ (**127**, $k_{add\ (rel)}$ = 383) versus $CH_3CH_2CF_2CF_2^{\bullet}$ (**99**, $k_{add\ (rel)}$ = 167, relative to *n*-alkyl) in bimolecular additions to styrene. Geminal difluorination at the allylic position (**68**) serves to diminish the transition state SOMO-HOMO interaction, and hence k_{C5} and k_{C6}, relative to **65**.

Cyclization Regiochemistry

The significant degree to which **152**, **65**, **68**, and even **140** undergo *6-endo* cyclization is particularly striking, with six-membered ring formation in **140** occuring with a rate nearly half, and **65** and **68** more than an order of magnitude greater than, that of *5-exo* closure for hydrocarbon **1**. In comparison, 5-hexenyl systems bearing alkyl substituents along the aliphatic fragment exhibit regiochemical profiles similar to that of the unsubstituted parent.[70,71]

The question of potential reversibility in the above cyclizations has been addressed, in light of the greater relative thermodynamic stability of secondary cyclohexyl radicals. Upon independent generation of *5-exo* adduct radical **69** from precursor 1-(iodomethyl)-2,2,3,3,4,4,5,5-octafluorocyclopentane in the presence of

hydrogen atom donor triethylsilane in C_6D_6, the only product observed after complete consumption of starting material was that resulting from direct capture of **69** by Et_3SiH.[170] The lack of *6-endo* or ring-opened products originating from **69**, coupled with the *ab initio* predictions based on relative energies of cyclization transition structures described below, demonstrates that the regiochemical characteristics of fluorinated 5-hexenyl radical cyclizations are indeed kinetic in nature.

Of further note is that system **68**, which undergoes the greatest percentage (24.1%) of *6-endo* closure (that is, exhibiting the least selectivity) is not the most reactive. Hexafluoro system **65**, though forming **67** with a rate constant 1.5 times that of analogous closure of **68** to **70**, does so only to an extent of 10.6% of total cyclized products.

A combined *ab initio* / molecular mechanics approach has allowed for accurate regiochemical predictions for a number of alkyl and heteroalkyl intramolecular radical additions.[66] In order to examine the effect of the degree and location of fluorine substitution on transition structure geometry and energetics, as well as on activation barriers and reaction enthalpy, the "chair-like" and "boat-like" *5-exo* and *6-endo* cyclization transition structures for the parent hydrocarbon and various fluorinated 5-hexenyl systems, along with their respective open-chain radicals and products of 5- and 6-membered ring closure, have been investigated with *ab initio* techniques.

In accordance with a UMINDO/3 investgation of Bischof,[62] the lowest energy conformation of 5-hexenyl radical **1** was found to be an all-*trans* methylene chain in a gauche orientation with the internal vinyl hydrogen (Figure 4-16.) Alignment of the singly occupied orbital of **1** with the adjacent C-H bond was found to be slightly preferred (ca. 0.1 kcal · mol^{-1}) over similar C-C alignment at the UHF/6-31G(d) + ZPE level.

From the calculated structures and energies of cyclization products (cyclopentylmethyl and cyclohexyl radicals) it was possible to compute energies of reaction for hydrocarbon **1** and its fluorinated analogues. Total energies of reactant and

product radicals and exothermicities of *5*-exo and *6-endo* cyclization for **1**, **128**, **152**, and **65** are provided below in Table 4-3.

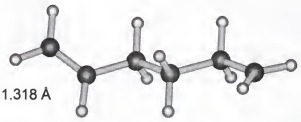

Figure 4-16. Lowest Energy Conformation of 5-Hexen-1-yl Radical **1**; SOMO (On Right) Aligned with Adjacent C-H Bond. UHF/6-31G(d) Optimized Geometry.

As expected from C-C BDE data, (Table 3-4) intermolecular additions of the fluorinated species are, as a whole, more exothermic than for parent **1**. However, no direct correlation exists between either absolute rates of *5*-exo and *6*-endo addition or relative percentage of 6-membered ring formation and its corresponding reaction exothermicity. Although a steady increase in both k_{C5} and k_{C6} is observed along the series (**1** → **128** → **152** → **65**), both cyclizations of **65** are predicted to be less exothermic than those of **152**. Furthermore, relative enthalpies ($\Delta E_{rxn(1,5)}$ - $\Delta E_{rxn(1,6)}$) are found to rise with the degree of fluorination, favoring *6-endo* closure in consistent manner for both levels of theory employed. This is at variance with the lesser extent of *6-endo* closure in **65** compared to **152**.

Total, zero-point, and relative energies along with pertinent geometrical parameters for the UHF/6-31G(d) cyclization transition structures of **1**, (depicted in Figures 1-11 - 1-14) **128**, **140**, **152**, and **65** are reported in Table 4-4. Although the calculated energy differences between "chair" and "boat" forms of either *5-exo* or *6-endo* transition structures are quite consistent among the theoretical methods, energies of the "*6-endo-chair*" and "*6-endo-twist-boat*" structures relative to the "*5-exo-chair*" and "*5-exo-boat*" appear to be overestimated at the PMP2/6-311G(d,p)//UHF/6-31G(d) level compared to both UHF and QCISD(T) results. Bearing this in mind, relative transition

Table 4-3. Total and Zero-Point Energies and Energies of Reaction for *5-Exo* and *6-Endo* Cyclizations of Hydrocarbon and Partially Fluorinated 5-Hexenyl Radicals.

Radical	E_{tot} [a]	ZPE [b]	ΔE_{rxn} (*5-Exo*) [c]	ΔE_{rxn} (*6-Endo*) [c]	$\Delta\Delta E_{rxn}$ [d]
1	-233.543768 (-234.461575) [-234.391386]	0.161154	-13.20 (-18.58) [-15.90]	-19.45 (-23.44) [-21.22]	6.25 (4.86) [5.32]
2	-233.567930 (-234.494315) [-234.419913]	0.164664			
3	-233.579940 (-234.504105) [-234.431547]	0.166947			
128	-431.260147 (-432.620036)	0.148540	-19.91 (-23.09)	-27.50 (-29.51)	7.59 (6.42)
137	-431.291745 (-432.656712)	0.148402			
158	-431.305809 (-432.668897)	0.150592			
152	-628.970751 (-630.769253)	0.132048	-20.29 (-23.38)	-29.15 (-31.30)	8.86 (7.92)
154	-629.003100 (-630.806518)	0.132061			
156	-629.018995 (-630.820937)	0.134061			
65	-826.678248 (-828.915986)	0.115172	-18.68 (-21.77)	-28.22 (-30.36)	9.54 (8.59)
66	-826.708181 (-828.950843)	0.115350			
67	-826.724889 (-828.966024)	0.117035			

[a] In Hartrees. UHF/6-31G(d); PMP2/6-311G(d,p)//UHF/6-31G(d) Values in Parentheses, QCISD(T)/6-31G(d)//UHF/6-31G(d) Values in Brackets. [b] In Hartrees, from UHF/6-31G(d) Vibrational Frequencies. [c] In kcal $\cdot$ mol^{-1}; UHF/6-31G(d); PMP2/6-311G(d,p)//UHF/6-31G(d) Values in Parentheses, [QCISD(T)/6-311G(d,p)]´//UHF/6-31(d) Values in Brackets. [d] ($\Delta E_{rxn(1,5)}$ - $\Delta E_{rxn(1,6)}$) in kcal $\cdot$ mol^{-1}; UHF/6-31G(d); PMP2/6-311G(d,p)//UHF/6-31G(d) Values in Parentheses, [QCISD(T)/6-311G(d,p)]´//UHF/6-31(d) Values in Brackets.

Table 4-4. UHF/6-31G(d) Geometric Parameters and Energies of Transition Structures for Hydrocarbon and Fluorocarbon 5-Hexenyl Cyclizations.

Radical	r (C-C) (Å)	r (C=C) (Å)	∠ C-C-C (Deg.)	E_{tot} [e] (au)	ZPE (au)	ΔS (eu)	E_{rel} [f]
1 [a]	2.186	1.393	109.7	-233.525546 (-234.455098) [-234.379299]	0.161472	78.11	0
1 [b]	2.192	1.394	108.2	-233.522908 (-234.452664) [-234.376772]	0.161317	78.91	1.57 (1.44) [1.38]
1 [c]	2.260	1.384	98.4	-233.521897 (-234.450180) [-234.375531]	0.161801	76.91	2.24 (3.27) [2.47]
1 [d]	2.245	1.386	100.0	-233.517681 (-234.446462) [-234.371537]	0.161736	77.77	5.08 (5.56) [4.81]
128 [a]	2.192	1.387	108.9	-431.244513 (-432.614627)	0.146381	86.27	0
128 [b]	2.199	1.388	107.0	-431.241713 (-432.611948)	0.146261	86.97	1.69 (1.61)
128 [c]	2.259	1.383	96.8	-431.241187 (-432.609955)	0.146926	85.37	2.39 (3.24)
128 [d]	2.240	1.385	99.9	-431.237289 (-432.606471)	0.146800	85.89	4.76 (5.35)
140 [a]	2.190	1.391	109.2	-431.248280 (-432.615856)	0.145212	85.54	0
140 [b]	2.193	1.393	107.4	-431.245575 (-432.613199)	0.145080	86.64	1.62 (1.59)
140 [c]	2.272	1.382	98.0	-431.247082 (-432.613844)	0.145752	83.98	1.05 (1.57)
140 [d]	2.257	1.384	99.6	-431.241993 (-432.608898)	0.145540	84.99	4.13 (4.55)
152 [a]	2.193	1.386	108.6	-628.954014 (-630.762361)	0.129951	93.47	0
152 [b]	2.195	1.387	106.5	-628.951440 (-630.759854)	0.129840	94.44	1.55 (1.51)
152 [c]	2.269	1.381	96.3	-628.953289 (-630.760695)	0.130521	92.33	0.77 (1.36)

Table 4-4-- continued

Radical	r (C-C) (Å)	r (C=C) (Å)	∠ C-C-C (Deg.)	E_{tot} [e] (au)	ZPE (au)	ΔS (eu)	E_{rel} [f]
152 [d]	2.249	1.383	100.0	-628.947730 (-630.754984)	0.130365	78.91	4.17 (4.86)
65 [a]	2.195	1.387	107.9	-826.661679 (-828.909230)	0.113158	76.91	0
65 [b]	2.199	1.389	106.3	-826.659545 (-828.907252)	0.113017	77.77	1.26 (1.16)
65 [c]	2.271	1.381	96.8	-826.660359 (-828.906567)	0.113677	86.27	1.12 (1.96)
65 [d]	2.252	1.383	99.3	-826.656303 (-828.902416)	0.113613	86.97	3.62 (4.53)

[a] *5-Exo-chair.* [b] *5-Exo-boat.* [c] *6-Endo-chair.* [d] *6-Endo-twist-boat.* [e] UHF/6-31G(d); PMP2/6-311G(d,p)//UHF/6-31G(d) Values in Parentheses, QCISD(T)/6-31G(d)//UHF/6-31G(d) Values in Brackets. [f] In kcal · mol^{-1}; UHF/6-31G(d); PMP2/6-311G(d,p)// UHF/6-31G(d) Values in Parentheses, [QCISD(T)/6-311G(d,p)]˜//UHF/6-31(d) Values in Brackets.

state free energies were obtained for each structure based on the UHF/6-31G(d) energies and entropies, and regiochemical ratios determined based on a Boltzmann distribution including all four transition structures.

In a similar manner, the above structures along with those of 1,1,2,2,3,3,4,4-octafluoro radical **68**, perfluorinated system **71**, and partially fluorinated **74** were also investigated with the UHF/4-31G model, this smaller basis set implemented due to the size of the latter three systems. Relative free energies for all systems investigated are provided in Table 4-5, with resultant predicted and experimental *5-exo* : *6-endo* ratios for each cyclization given in Table 4-6.

Agreement between the computed and observed values is quite remarkable, even with the relatively small 4-31G basis, the largest deviation from experiment approximately eight percent. From these results, in can be inferred that the regioselectivities for a variety of radical cyclizations (hydrocarbon, fluorocarbon, or otherwise) can be predicted with a reasonably high degree of confidence at minimal

Table 4-5. Relative Free Energies of Hydrocarbon and Fluorocarbon Transition Structures (kcal · mol^{-1}) at 303 K.

Radical	*5-Exo-chair*	*5-Exo-boat*	*6-Endo-chair*	*6-Endo-twist-boat*
1	0.0 (0.0)	1.22 (1.33)	3.10 (2.84)	5.33 (5.19)
128	0.0 (0.0)	1.44 (1.48)	2.91 (2.67)	4.94 (4.88)
140	0.0 (0.0)	1.23 (1.29)	1.35 (1.53)	4.28 (4.30)
152	0.0 (0.0)	1.26 (1.26)	1.07 (1.12)	4.57 (4.37)
65	0.0 (0.0)	1.15 (1.22)	1.68 (1.45)	4.02 (3.96)
68	0.0 (0.0)	0.72	0.83	4.01
71	0.0 (0.0)	0.61	2.95	6.66
74	0.0 (0.0)	1.14	2.10	6.57

Note: UHF/4-31G; UHF/6-31G(d) Values in Parentheses.

computational expense and without the introduction of experimentally-based parameters. This is due in part to the fact that the degree of spin contamination in each of these structures, though rather high (with <S^2> values ranging in magnitude from approximately 1.0 to 1.1) is fairly consistent. This is not true, however, of the ground state starting structures, which adversely affects computed activation barriers as discussed below.

The experimental activation barriers for *5-exo* and *6-endo* closure of **1** are 6.8 and 8.5 kcal · mol^{-1}, respectively.[63,64] Calculated energies of activation for the parent hydrocarbon and number of fluorinated analogues are found in Table 4-7.

It can be seen from the results of **1** that absolute barriers for radical cyclization reactions are extremely difficult to model theoretically. Even with the inclusion of

Table 4-6. Computed and Experimental Regiochemical Ratios at 303 K for Hydrocarbon and Fluorocarbon 5-Hexenyl Radical Cyclizations.

Radical	5-Exo : 6-Endo Ratio [a]	
	Predicted	Observed
1	100 : 0 (99.3 : 0.7)	98 : 2
128	100 : 0 (98.9 : 1.1)	> 96 : < 4
140	91.3 : 8.7 (93.3 : 6.7)	90.9 : 9.1
152	86.9 : 13.1 (87.8 : 12.2)	82.1 : 17.9
65	94.8 : 5.2 (92.6 : 7.4)	89.4 : 10.6
68	83.8 : 16.2	75.9 : 24.1
71	99.5 : 0.5	> 96 : < 4
74	97.4 : 2.6	> 96 : < 4

[a] UHF/4-31G; UHF/6-31G(d) Values in Parentheses.

electron correlation, accuracy leaves quite a bit to be desired. These results are in accord with the those of Wong and Radom,[41] whose systematic investigation of intermolecular additions of small model radicals to olefins has demonstrated that high levels of theory are required to accurately reproduce (and predict) activation barriers for radical reactions. This is due in part to the differing degree of spin contamination in the starting radicals and transition structures as mentioned previously, the former possessing "acceptable" <S^2> values in the range of 0.76 - 0.79, versus that of 0.75 for a "pure" doublet radical. Such differential spin contamination has a disastrous effect on activation barriers computed using perturbation theory. For example, UMP2/6-311G(d,p)//UHF/6-31G(d) yields values of 13.5 and 17.3 kcal · mol^{-1}, respectively, for **1**; calculations at the UMP4SDQ/6-311G(d,p) level on UHF/6-31G(d) geometries fare only slightly better with values of 12.1 and 15.3, only a modest improvement over UMP2/

Table 4-7. Calculated Activation Barriers for *5-Exo* and *6-Endo* Cyclizations of Hydrocarbon and Fluorocarbon 5-Hexen-1-yl Radicals.

Radical	UHF/4-31G	UHF/6-31G(d)	PMP2/6-311G(d,p)//UHF/6-31G(d)
1	*5-exo* : 10.67 *6-endo* : 13.38	*5-exo* : 11.61 *6-endo* : 14.09	*5-exo* : 4.24 *6-endo* : 7.51
128	*5-exo* : 6.10 *6-endo* : 8.75	*5-exo* : 8.60 *6-endo* : 10.99	*5-exo* : 2.18 *6-endo* : 5.42
140	*5-exo* : 6.16 *6-endo* : 6.89	*5-exo* : 9.33 *6-endo* : 10.10	*5-exo* : 3.15 *6-endo* : 4.51
152	*5-exo* : 6.56 *6-endo* : 7.93	*5-exo* : 9.27 *6-endo* : 10.39	*5-exo* : 3.11 *6-endo* : 5.07
65	*5-exo* : 8.86 *6-endo* : 9.41		

Note: In kcal · mol^{-1}. Includes 0.8929 ZPE Correction.

6-311G(d,p) and still worse than the Hartree-Fock results. The slow convergence of the UMPn series in systems suffering from severe spin contamination has been noted by Nobes *et al.*[196]

The spin-projected PMP2/6-311G(d,p) values, though faring somewhat better in the case of **1**, do not reproduce the correct trends for either *5-exo* or *6-endo* reactivity along the fluorinated series. Methods of high accuracy such as coupled cluster (CC) and quadratic configuration interaction (QCI) have also been shown to be robust against spin contamination[197,198] but at significant (and, for larger systems, prohibitive) expense. Results of QCISD(T) barrier calculations for **1** and **128** are provided in Table 4-8, the former requiring 7-10 and the latter 28-35 hours of CPU time and approximately 2-4 GB of disk space on the Cray C90 at the San Diego Supercomputer Center for *each* calculation of the energies of starting species and transition structures. As expected, however, the agreement between theory and experiment for **1** is much improved at this level, especially with partial inclusion of basis extension effects by evaluation at the PMP2/6-311G(d,p) level.

Table 4-8. Activation Barriers for *5-Exo* and *6-Endo* Cyclization of **1** and **128** at the QCISD(T) Level.

Radical	QCISD(T)/6-31G(d)	[QCISD(T)/6-311G(d,p)]′ [a]
1	*5-exo* : 7.76 *6-endo* : 10.31	*5-exo* : 7.30 *6-endo* : 9.77
128	*5-exo* : 4.98 *6-endo* : 7.21	*5-exo* : 5.21 *6-endo* : 7.75

Note: UHF/6-31G(d) Geometries, kcal · mol^{-1}. Includes 0.8929 ZPE Correction.
[a] E[QCISD(T)/6-311G(d,p)]′ ≈ E[QCISD(T)/6-311G(d,p)] = E[QCISD(T)/6-31G(d)] + E(PMP2/6-311G(d,p)) - E(PMP2/6-31G(d)).

With such wide variations in variations in regiochemistry observed in the cyclizations of **1**, it is difficult to provide a rationale which satisfactorily accounts for all of the data. This is especially so given the insensitivity of cyclization transition structure geometry to substitution (Table 4-4 demonstrates the similarity in geometric trends to those of intermolecular additions). However, the predictive value of the *ab initio* results is encouraging, allowing for the potential design of precursors with desired regiochemical behavior in cyclization and cyclopolymerization reactions.

Conclusion

Based on absolute rate constants of hydrogen abstraction from tributylstannane and *tris*(trimethylsilyl)silane by partially fluorinated alkyl radicals, absolute rate constants for *5-exo* and *6-endo* intramolecular addition reactions of partially fluorinated 5-hexen-1-yl radicals have been obtained through competitive kinetic methods. Regardless of either the degree or location of fluorine substitution on the 5-hexenyl chain, closure proceeds predominantly in an *exo* fashion, although in some cases substantial competing *6-endo* cyclization is observed.

The kinetics of cyclization are found to follow those observed in the bimolecular addition of partially fluorinated radicals to alkenes. The pyramidal nature of α,α-difluoroalkyl radicals in combination with increased electrophilic character as function of

incremental fluorine substitution are responsible for their enhanced reactivity over hydrocarbon analogues.

Consistent with high level computational studies on model radical addition reactions, it is found that absolute activation barriers for intramolecular addition reactions of 5-hexenyl radicals prove extremely difficult to model theoretically. Predictions of cyclization regiochemistry based on relative *ab initio* transition state free energies may be made with a reliable degree of accuracy.

CHAPTER 5

EXPERIMENTAL

General Methods- Experimental

NMR nuclear magnetic resonance (NMR) spectra (300 MHz, 75 MHz and 282 MHz for ^{1}H, ^{13}C, and ^{19}F respectively) are reported in parts per million ppm downfield (δ) versus tetramethylsilane (TMS) for ^{1}H and ^{13}C, and in ppm upfield (ϕ) versus $CFCl_3$ for ^{19}F. All NMR spectra were recorded on Varian VXR-300 or Gemini-300 spectrometers.

Preparative gas chromatographic (GC) separations were carried out with a 20 foot x 0.25 inch copper column packed with 20% SE-30 on Chromosorb P and performed on a Varian Aerograph A-90 gas chromatograph equipped with a thermal conductivity detector.

High resolution mass spectra were obtained on a Finnegan MAT-95 spectrometer.

Ultraviolet (UV) spectra were obtained on a Perkin-Elmer Lambda 9 UV/VIS/NIR spectrophotometer.

All reagents, unless otherwise specified, were purchased from Aldrich, Fisher, PCR, or Acros, and used as received. Styrene (Fisher) was freed from inhibitor by passage through a column of neutral alumina. Dichloromethane was distilled from calcium hydride and used immediately. Diethyl ether and tetrahydrofuran (THF) were distilled from sodium benzophenone ketyl and used immediately. Benzene was distilled from lithium aluminum hydride and stored over 4 Å molecular sieves. Chloroform, dimethylsulfoxide, and tetraglyme were commercial anhydrous grade. All reactions were performed under an inert atmosphere of argon.

General Methods- Theoretical

All *ab initio* calculations were performed with the *Gaussian92* and *Gaussian94* program systems[199] on Cray Y-MP 4/32 or Cray C90 supercomputers, an IBM RS/6000 SP2 cluster, or Intel-based PCs. Geometry optimizations were performed using standard gradient techniques. All stationary points were characterized by harmonic frequency analysis, minima and transition structures giving rise to zero or exactly one negative eigenvalue, respectively, in the second derivative matrix. All post-Hartree-Fock calculations were performed with core orbitals frozen. Hartree-Fock frequencies and resultant zero-point energies have been scaled by a factor of 0.8929.

Density functional theory calculations were performed with the *Gaussian94* program on an IBM RS/6000 SP2 cluster or Intel-based PCs, implementing the (75,302)p pruned integration grid. Zero-point energy corrections were scaled by 0.9806 as suggested by Scott and Radom and by Bauschlicher and Partridge.[200,201] For bond dissociation energy calculations, a thermal correction of $4RT$ (for C-C BDEs) or $2.5RT$ (for C-H BDEs) has been applied as recommended by Hehre *et al.*[202] Where applicable, reported BDEs correspond to those resulting from the lowest electronic energy conformer of the closed-shell species and / or radical.

Synthetic Procedures

Preparation of 1,3-Dibromo-1,1-difluorohexane (**79**)

A Carius tube of approximately 200 mL capacity equipped with a small magnetic stir bar was charged with 0.14 g (1.42×10^{-3} mol) cuprous chloride, 4.36 g (7.12×10^{-2} mol) ethanolamine, 12 mL *tert*-butanol, 10.0 g (1.42×10^{-1} mol) 1-pentene, and 59.84 g (2.85×10^{-1} mol) dibromodifluoromethane. The tube was flushed with nitrogen and flame-sealed; upon swirling, a deep blue coloration was observed. The tube was immersed halfway into a silicon oil bath preheated at 85° C and allowed to stir for 48 hours, during which time the coloration turned from deep blue to olive green to brown.

(Caution: this procedure should be performed behind a safety shield). The tube was cooled in an ice bath, opened, and the contents transferred to a 250-mL Erlenmeyer flask (at this point, unreacted dibromodifluoromethane may be recovered by distillation) and the tube rinsed with three 50 mL portions of hexanes. All organic material (which consisted of a cloudy yellow-green supernatant and a brown resin) was filtered through 50 mL of silica gel, which was rinsed with two additional 50 mL portions of hexanes. The resulting colorless filtrate was concentrated by rotary evaporation and subject to reduced pressure fractional distillation through a 15 cm Vigreux column. A total of 22.79 g (57.3%) **79** was obtained as a colorless liquid, bp 80-85° C / 25 mm Hg.

1,3-Dibromo-1,1-difluorohexane (**79**): ^{1}H NMR: δ 0.96 (3H, t, $^{3}J_{HH}$ = 7.42 Hz), 1.50 (2H, m), 1.86 (2H, m), 3.01 (2H, m), 4.24 (1H, m); ^{13}C NMR: δ 13.2, 20.4, 40.5, 46.6, 52.7 (t, $^{2}J_{CF}$ = 21.8 Hz), 120.6 (t, $^{1}J_{CF}$ = 306.9 Hz); ^{19}F NMR: ϕ -43.2 (m); HRMS for $C_6H_{10}F_2Br_2$: calc. 277.9117, calc. (M-Br) 198.9934, found 198.9983; CHN for $C_6H_{10}F_2Br_2$: calc. 25.74% C, 3.60% H, found 25.53% C, 3.43% H.

Preparation of 1-Bromo-1,1-difluorohexane (**80**) and 1,1-Difluorohexane (**81**)

A 250 mL three-necked round-bottomed flask equipped with an ice-water condenser, argon inlet, and magnetic stir bar was charged with 20.0 g (7.14 x 10^{-2} mol) 1,3-dibromo-1,1-difluorohexane (**79**) dissolved in 100 mL anhydrous dimethylsulfoxide. A total of 10.8 g (2.85 x 10^{-1} mol) of sodium borohydride was then added in small portions with vigorous stirring over the course of 1 hour, during which time the flask became warm and a semisolid gel was observed to form. After the addition was complete, the bath temperature was raised to 70° C over the course of 1 hour and heating continued for an additional 6 hours (^{19}F NMR analysis of a small aliquot of the reaction mixture at this time showed complete consumption of starting material.) The flask was cooled to room temperature, the contents transferred to a 1 L Erlenmeyer flask, and the reaction quenched with chips of ice. The resulting mixture was *carefully*

acidified with concentrated aqueous HCl, 100 mL ether was added, and the aqueous / DMSO layer extracted with three 50 mL portions of ether. The combined ether layers were washed with three 25 mL portions of water, dried over $MgSO_4$, and subject to ambient pressure fractional distillation through a 15 cm Vigreux column. After concentration in this way, 8.91 g (62.1%) **80** (contaminated with a small amount of **81**) was obtained as a colorless liquid, bp 125-128° C. Preparative GC separation afforded analytically pure samples of each.

1-Bromo-1,1-difluorohexane (**80**): ^{1}H NMR: δ 0.92 (3H, t, $^3J_{HH}$ = 7.5 Hz), 1.35 (4H, m), 1.62 (2H, m), 2.33 (2H, m); ^{13}C NMR: δ 13.8, 22.3, 23.6, 30.6, 44.3 (t, $^2J_{CF}$ = 21.1 Hz), 123.3 (t, $^1J_{CF}$ = 303.5 Hz); ^{19}F NMR: ϕ -43.9 (t, $^3J_{FH}$ = 14.7 Hz); HRMS for $C_6H_{11}F_2Br$: calc. 200.0012, calc. (M-Br) 121.0829, found 121.0832; CHN for $C_6H_{11}F_2Br$: calc. 35.84% C, 5.51% H, found 35.47% C, 5.54% H.

1,1-Difluorohexane (**81**): ^{1}H NMR: δ 0.91 (3H, t, $^3J_{HH}$ = 6.9 Hz), 1.34 (4H, m), 1.45 (2H, m), 1.80 (2H, m), 5.79 (1H, tt, $^3J_{HH}$ = 4.5 Hz, $^2J_{HF}$ = 57 Hz); ^{13}C NMR: δ 13.8, 21.8 (t, $^3J_{CF}$ = 5.5 Hz), 22.4, 31.2, 34.1 (t, $^2J_{CF}$ = 20.6 Hz), 117.5 (t, $^1J_{CF}$ = 237.4 Hz); ^{19}F NMR: ϕ -116.3 (dt, $^3J_{FH}$ = 17.1 Hz, $^2J_{FH}$ = 56.2 Hz); HRMS for $C_6H_{12}F_2$: calc. 122.0907, calc. (M-H) 121.0829, found 121.0825.

Preparation of 1-Phenyloctan-3-ol (**86**)

Into a flame-dried 300 mL three-necked round-bottomed flask equipped with a 125 mL pressure-equalizing addition funnel, condenser with argon inlet, and magnetic stir bar was dispensed 3.94 g (1.62×10^{-1} mol) Mg turnings and a small crystal of iodine. (2-Bromoethyl)benzene (10.0 g, 5.40×10^{-2} mol) was dissolved in 100 mL of anhydrous ether and added to the funnel. After addition of a small amount of solution and initiation of the reaction, addition was continued at a rate that maintained gentle reflux, after which time the mixure was refluxed for an additional 2 hours. The flask was then cooled to room temperature and 5.41 g (5.40×10^{-2} mol) of hexanal was dissolved in 50 mL

anhydrous ether, added to the addition funnel and dispensed dropwise at a rate that maintained gentle reflux. The mixture was refluxed for an additional 2 hours, cooled to room temperature, and quenched with a mixture of 100 g of ice and 50 mL concentrated aqueous HCl. The layers were separated, the aqueous layer extracted with three 50 mL portions of ether, and the combined organic extracts washed twice with 20 mL 5% aqueous $NaHCO_3$ and once with 20 mL of water. The organic layer was dried over $MgSO_4$, the solvent rotary evaporated, and the resulting liquid subjected to reduced pressure fractional distillation through a 15 cm Vigreux column. 8.75 g (78.7%) **86** was obtained as a colorless liquid, bp 148-151° C / 0.1 mm Hg.

1-Phenyloctan-3-ol (**86**): ^1H NMR: δ 0.94 (3H, t, $^3J_{HH}$ = 5.7 Hz), 1.34 (4H, m), 1.51 (4H, m), 1.81 (2H, m), 2.76 (2H, m), 3.67 (1H, m), 7.28 (5H, m); ^{13}C NMR: δ 14.0, 22.6, 25.2, 31.8, 32.0, 37.5, 39.0, 71.4, 125.7, 128.3, 128.4, 142.2; HRMS for $C_{14}H_{22}O$: calc. 206.1671, found 206.1672.

Preparation of 1-Phenyloctan-3-one (**87**)

Into a 100 mL round-bottomed flask was placed 3.8 g (1.84 x 10^{-2} mol) of 1-phenyloctan-3-ol (**86**) dissolved in 10 mL ether. Jones' reagent (8.5 mL, previously prepared with of 5.0 g $Na_2Cr_2O_7$ and 3.65 mL concentrated H_2SO_4 diluted with water to a total volume of 25 mL) was added dropwise to the alcohol solution with stirring, and allowed to react for 4 hours at room temperature. The dark green reaction mixture was diluted with 20 mL ether and 20 mL water. The aqueous layer was extracted with three 20 mL portions of ether, and the combined organic extracts washed twice with 20 mL saturated $NaHCO_3$, once with 20 mL brine, and dried over $MgSO_4$. Rotary evaporation of the solvent followed by reduced pressure fractional distillation through a 10 cm Vigreux column afforded 3.34 g (89.0%) **87**, bp 108-111° C / 0.35 mm Hg.

1-Phenyloctan-3-one (**87**): ^1H NMR: δ 0.87 (3H, t, $^3J_{HH}$ = 6.9 Hz), 1.26 (4H, m), 1.55 (2H, overlapping tt, $^3J_{HH}$ = 7.5 Hz), 2.37 (2H, t, $^3J_{HH}$ = 7.2 Hz), 2.72 (2H, m), 2.89

(2H, m), 7.23 (5H, m); ^{13}C NMR: δ 13.9, 22.4, 23.5, 29.8, 31.4, 43.0, 44.2, 126.0, 128.3, 128.4, 141.2, 210.3; HRMS for $C_{14}H_{20}O$: calc. 204.1514, found 204.1532; CHN for $C_{14}H_{20}O$: calc. 82.30% C, 9.87% H, found 82.53% C, 10.14% H.

Preparation of 3,3-Difluoro-1-phenyloctane (**83**)

Into a 100 mL three-necked round-bottomed flask equipped with stir bar, rubber septum, and condenser with argon inlet was placed 2.0 g (9.80 x 10^{-3} mol) of 1-phenyloctan-3-one (**87**) dissolved in 15 mL anhydrous CH_2Cl_2. Into the reaction mixture was slowly injected 1.74 g (1.08 x 10^{-2} mol) diethylaminosulfurtrifluoride (DAST) with stirring, during which time the flask became slightly warm. The mixture was heated at reflux for 72 hours, over which time a dark amber coloration was observed. After cooling, the reaction mixture was carefully decanted onto 50 mL of ice water and diluted with 10 mL CH_2Cl_2. The organic layer was separated and the aqueous layer extracted with three 20 mL portions of CH_2Cl_2. The combined organic extracts were washed once with 10 mL of 10% aqueous $NaHCO_3$ and once with 10 mL water, dried over $MgSO_4$, and the solvent rotary evaporated. Fractional reduced pressure distillation of the resulting liquid afforded 1.66 g (68.0%) **83**, bp 100-105° C / 0.2 mm Hg.

3,3-Difluoro-1-phenyloctane (**83**): ^1H NMR: δ 0.92 (3H, t, $^3J_{HH}$ = 6.3 Hz), 1.33 (4H, m), 1.48 (2H, m), 1.87 (2H, m), 2.13 (2H, m), 2.82 (2H, m), 7.27 (5H, m); ^{13}C NMR: δ 13.9, 22.0, 22.4, 28.5, 31.5, 36.5 (t, $^2J_{CF}$ = 25.1 Hz), 38.2 (t, $^2J_{CF}$ = 25.5 Hz), 124.8 (t, $^1J_{CF}$ = 239.4 Hz), 126.1, 128.3, 128.5, 140.8); ^{19}F NMR: ϕ -99.1 (overlapping tt, $^3J_{FH}$ = 17.1 Hz); HRMS for $C_{14}H_{20}F_2$: calc. 226.1533, found 226.1529; CHN for $C_{14}H_{20}F_2$: calc. 74.30% C, 8.91% H, found 74.14% C, 9.15% H.

Preparation of 1-Bromohexan-2-one (**90**)

Into a 250 mL three-necked round-bottomed flask equipped with an argon inlet, magnetic stir bar, and 100 mL pressure-equalizing addition funnel was placed 10.0 g (9.98 x 10^{-2} mol) of 2-hexanone, 40 mL glacial acetic acid, and 9.75 g (1.62 x 10^{-1} mol)

urea. The flask was cooled to 0° C and 17.15 g (1.07×10^{-1} mol) of bromine was introduced dropwise into the reaction mixture over the course of 1 hour. After the addition was complete, the cooling bath was removed and the reaction mixture allowed to warm to room temperature and stirred overnight. The contents were then transferred to a separatory funnel, diluted with 200 mL water, and extracted with four 50 mL portions of CH_2Cl_2. The combined organic extracts were washed with three 20 mL portions of 10% aqueous $NaHCO_3$, dried over $MgSO_4$, and the solvent rotary evaporated. Fractional reduced pressure distillation through a 15 cm Vigreux column yielded 12.91 g (72.2%) **90**, contaminated with ca. 6% (by ^1H NMR) of the 3-bromo isomer, bp 85-88° C / 15 mm Hg. Column chromatography (silica gel, 20% ethyl acetate in hexanes) of a small sample yielded pure **90**, which was used in characterization.

1-Bromohexan-2-one (**90**): ^1H NMR: δ 0.91 (3H, t, $^3J_{HH}$ = 7.5 Hz), 1.33 (2H, overlapping tt, $^3J_{HH}$ = 7.5 Hz), 1.60 (2H, overlapping tt, $^3J_{HH}$ = 7.5 Hz), 2.64 (2H, t, $^3J_{HH}$ = 7.2 Hz), 3.88 (2H, s); ^{13}C NMR: δ 13.7, 22.1, 25.9, 34.3, 39.5, 202.2; HRMS for $C_6H_{11}BrO$: calc. 177.9993, found 177.9934; CHN for $C_6H_{11}BrO$: calc. 40.25% C, 6.19% H, found 40.10% C, 6.19% H. *(Caution: α-bromoketones are powerful lachrymators).*

Preparation of 1-Bromo-2,2-difluorohexane (**91**)

A 100 mL three-necked round-bottomed flask equipped with magnetic stir bar, condenser with argon inlet, and rubber septum was charged with 5.0 g (2.79×10^{-2} mol) 1-bromohexan-2-one (**90**) dissolved in 20 mL anhydrous $CHCl_3$. DAST (9.15 g, 5.68×10^{-2} mol) was slowly injected into the reaction mixture, which was then heated at 50° C for 48 hours. The flask was cooled and the contents carefully dispensed into 50 mL of ice water. The layers were separated, the aqueous layer extracted with three 5 mL portions of CH_2Cl_2, and the combined organic extracts washed twice with 10 mL portions of 10% aqueous $NaHCO_3$ and once with 10 mL of water. Drying over $MgSO_4$, evaporation of the halogenated solvents by ambient-pressure distillation through a 10

cm Vigreux column, and fractional, ambient pressure distillation afforded 3.35 g (59.7%) **91** as a colorless liquid, bp 120-122° C.

1-Bromo-2,2-difluorohexane (**91**): ^{1}H NMR: δ 0.94 (3H, t, $^3J_{HH}$ = 7.2 Hz), 1.42 (4H, m), 2.02 (2H, m), 3.51 (2H, t, $^3J_{HF}$ = 13.2 Hz); ^{13}C NMR: 13.7, 22.3, 24.1, 31.4 (t, $^2J_{CF}$ = 34.1 Hz), 34.2 (t, $^2J_{CF}$ = 24.0 Hz), 121.5 (t, $^1J_{CF}$ = 240.9 Hz); ^{19}F NMR: ϕ -99.2 (m); HRMS for $C_6H_{11}F_2Br$: calc. 200.0012, calc. (M-H) 198.9934, found 198.9974; CHN for $C_6H_{11}F_2Br$: calc. 35.84% C, 5.51% H, found 36.00% C, 5.48% H.

Preparation of 1-Iodo-2,2-difluorohexane (**92**)

1-Bromo-2,2-difluorohexane (**91**) (2.0 g, 9.95 x 10^{-3} mol) was placed into a thick-walled Carius tube of approximately 150 mL capacity, along with a small magnetic stir bar. 100 mL of a hot saturated solution of sodium iodide in acetone was added to the tube, which was then cooled in a dry ice-isopropanol slush and flame-sealed. After warming to room temperature, the tube was immersed halfway in an oil bath atop a magnetic stirrer. The mixture was stirred at 85-90° C for 96 hours (a safety shield is recommended) at which time the tube was cooled, opened, and the contents transferred to a 250 mL round-bottomed flask. Most of the solvent was removed by rotary evaporation, and the remaining residue taken up in a mixture of 50 mL of water and 50 mL of ether. The layers were separated, the aqueous layer extracted with three 50 mL portions of ether, and the combined organic extracts washed with 20 mL of water. Drying over $MgSO_4$, rotary evaporation of the solvent, and fractional reduced-pressure distillation afforded 2.16 g (87.5%) of very pure **92**, bp 101-102° C / 68 mm Hg.

1-Iodo-2,2-difluorohexane (**92**): ^{1}H NMR: δ 0.93 (3H, t, $^3J_{HH}$ = 7.2 Hz); 1.41 (4H, m), 2.06 (2H, m), 3.40 (2H, t, $^3J_{HF}$ = 14.4 Hz); ^{13}C NMR: δ 3.95 (t, $^2J_{CF}$ = 31.5 Hz), 13.7, 22.3, 24.4, 35.0 (t, $^2J_{CF}$ = 24.5 Hz), 121.1 (t, $^1J_{CF}$ = 240.8 Hz); ^{19}F NMR: ϕ -94.9 (overlapping tt, $^3J_{FH}$ = 17.1 Hz); HRMS for $C_6H_{11}F_2I$: calc. 247.9833, found 247.9862; CHN for $C_6H_{11}F_2I$: calc. 29.05% C, 4.47% H, found 28.82% C, 4.48% H.

Preparation of 2,2-Difluorohexane (**93**)

1-Bromo-2,2-difluorohexane (**91**) (1.0 g, 4.97 x 10^{-3} mol) was dissolved in 5 mL benzene in a 25 mL round-bottomed flask equipped with septum-capped sidearm inlet and magnetic stir bar, and attached to a small distillation apparatus equipped with with ice water condenser and fractionating column. The bath temperature was raised to 60° C and 1.60 g (5.50 x 10^{-3} mol) nBu_3SnH and 0.01 g (6.09 x 10^{-5} mol) 2,2'-azobisisobutyronitrile (AIBN) dissolved in 0.5 mL benzene was added slowly via syringe through the rubber septum. When the addition was complete, the mixture was stirred for an additional 30 minutes and the bath temperature quickly raised to 150° C. All volatile material was flash distilled and subjected to preparative GC separation which afforded analytically pure **93** as a colorless liquid.

2,2-Difluorohexane (**93**): ^{1}H NMR: δ 0.92 (3H, t, $^3J_{HH}$ = 7.2 Hz), 1.42 (4H, m), 1.58 (3H, t, $^3J_{HF}$ = 18.3 Hz), 1.83 (2H, m); ^{13}C NMR: δ 13.8, 22.5, 23.2 (t, $^2J_{CF}$ = 28.1 Hz), 24.9 (t, $^3J_{CF}$ = 4.5 Hz), 37.7 (t, $^2J_{CF}$ = 25.1 Hz), 124.5 (t, $^1J_{CF}$ = 236.4 Hz); ^{19}F NMR: ϕ -90.9 (m); HRMS for $C_6H_{12}F_2$: calc. 122.0907, calc. (M-HF) 102.0845, found 102.0822.

Preparation of 1-Phenyloctan-4-ol (**96**)

In a manner similar to that of the preparation of **86**, 10.0 g (5.02 x 10^{-2} mol) of 1-bromo-3-phenylpropane dissolved in 100 mL anhydrous ether was added to 3.67 g (1.51 x 10^{-1} mol) Mg turnings to which a crystal of iodine had been added. Subsequent addition of 4.54 g (5.27 x 10^{-2} mol) of valeraldehyde dissolved in 50 mL anhydrous ether followed by workup in the usual way afforded 7.36 g (71.1%) **96**, bp 102-103° C / 0.05 mm Hg.

1-Phenyloctan-4-ol (**96**): ^{1}H NMR: δ 0.91 (3H, t, $^3J_{HH}$ = 6.6 Hz), 1.52 (10H, overlapping m), 2.65 (2H, t, $^3J_{HH}$ = 7.5 Hz), 3.62 (1H, m), 7.24 (5H, m); ^{13}C NMR: 14.0, 22.7, 27.4, 27.8, 35.9, 37.0, 37.1, 71.7, 125.7, 128.2, 128.3, 142.4; HRMS for $C_{14}H_{22}O$:

calc. 206.1671, found 206.1671; CHN for $C_{14}H_{22}O$: calc. 81.50% C, 10.75% H, found 81.72% C, 10.92% H.

Preparation of 1-Phenyloctan-4-one (**97**)

In a manner similar to that of the preparation of **87**, 15 mL of Jones' reagent was added to 5.0 g (2.42 x 10^{-2} mol) 1-phenyloctan-4-ol (**96**) in 25 mL ether. Workup in the usual way followed by distillation at reduced pressure yielded 4.14 g (83.7%) **97**, bp 123-125° C / 0.4 mm Hg.

1-Phenyloctan-4-one (**97**): ^{1}H NMR: δ 0.96 (3H, t, $^3J_{HH}$ = 7.2 Hz), 1.36 (2H, m), 1.60 (2H, m), 1.97 (2H, overlapping tt, $^3J_{HH}$ = 7.5 Hz), 2.46 (4H, m), 2.69 (2H, t, $^3J_{HH}$ = 7.2 Hz), 7.30 (5H, m); ^{13}C NMR: 13.8, 22.3, 25.2, 25.8, 35.0, 41.8, 42.5, 125.8, 128.3, 128.4, 141.6, 211.0; HRMS for $C_{14}H_{20}O$: calc. 204.1514, found 204.1576; CHN $C_{14}H_{20}O$: calc. 82.30% C, 9.87% H, found 82.40% C, 9.83% H.

Preparation of 4,4-Difluoro-1-phenyloctane (**98**)

In a manner similar to the preparation of **83**, 2.5 g (1.22 x 10^{-2} mol) 1-phenyloctan-4-one (**97**) and 3.93 g (2.44 x 10^{-2} mol) DAST in 25 mL CH_2Cl_2 were refluxed for 48 hours. Workup in the usual way afforded 1.83 g (66.3%) **98**, bp 85-88° C / 0.1 mm Hg.

4,4-Difluoro-1-phenyloctane (**98**): ^{1}H NMR: δ 0.89 (3H, t, $^3J_{HH}$ = 6.9 Hz), 1.34 (4H, m), 1.80 (6H, m), 2.63 (2H, t, $^3J_{HH}$ = 6.9 Hz), 7.22 (5H, m); ^{13}C NMR: δ 13.8, 22.5, 24.0 (t, $^3J_{CF}$ = 4.5 Hz), 24.38 (t, $^3J_{CF}$ = 4.7 Hz), 35.4, 35.7 (t, $^2J_{CF}$ = 26.0 Hz), 36.1 (t, $^2J_{CF}$ = 25.1 Hz), 125.2 (t, $^1J_{CF}$ = 238.9 Hz), 125.9, 128.4 (2C, overlapping), 141.5; ^{19}F NMR: ϕ -98.3 (overlapping tt, $^3J_{FH}$ = 17.1 Hz); HRMS for $C_{14}H_{20}F_2$: calc. 226.1533, found 226.1533; CHN for $C_{14}H_{20}F_2$: calc. 74.30% C, 8.91% H, found 74.40%C, 8.85% H.

Preparation of 1-Bromo-1,1,2,2-tetrafluorohexane (**102**)

Into a 250-mL three-necked round-bottomed flask equipped with a magnetic stir bar, rubber septum, and condenser equipped with an argon inlet was added 36 mL tetraglyme and 30.0 g (1.28 x 10^{-1} mol) of 6-bromo-5,5,6,6-tetrafluorohex-1-ene (**101**). A 2.0 M solution of borane · dimethyl sulfide in diethyl ether (24 mL, 4.80 x 10^{-2} mol) was slowly injected into the flask through the septum. Some bubbling was evident and the flask became slightly warm. This mixture was stirred for two hours at room temperature then heated at reflux with stirring overnight. The flask was then cooled to room temperature and 64 mL (59.3 g, 5.11 x 10^{-1} mol) of hexanoic acid was slowly injected into the reaction mixture with stirring. Vigorous bubbling was evident and the flask became warm. Stirring was continued for 2 hours at room temperature then at reflux overnight. The mixture was distilled through a 15 cm Vigreux column at ambient pressure until the head temperature reached 140° C, at which time distillation ceased. The distillate was diluted with 50 mL of ether, washed with two 10 mL portions of saturated aqueous sodium bicarbonate and two 10 mL portions of water, dried, and the resulting solution distilled at ambient pressure. After removal of ether and residual dimethyl sulfide in this way, 24.16 g (79.6%) **102** was obtained as a colorless liquid boiling at 122-124° C.

1-Bromo-1,1,2,2-tetrafluorohexane (**102**): ^{1}H NMR: δ 0.95 (3H, t, $^{3}J_{HH}$ = 7.2 Hz), 1.41 (2H, m), 1.59 (2H, m), 2.07 (2H, m); ^{13}C NMR: δ 13.7, 22.3, 22.6, 30.1 (t, $^{2}J_{CF}$ = 22.5 Hz), 117.5 (tt, $^{2}J_{CF}$ = 31.1 Hz, $^{1}J_{CF}$ = 251.8 Hz,), 118.0 (tt, $^{2}J_{CF}$ = 39.6 Hz, $^{1}J_{CF}$ = 309.5 Hz,); ^{19}F NMR: ϕ -65.9 (2F, s), -112.6 (2F, t, $^{3}J_{FH}$ = 19.5 Hz); HRMS for $C_6H_9F_4Br$: calc. 235.9823, calc. (M+H) 236.9902, found 236.9738; CHN for $C_6H_9F_4Br$: calc. 30.40% C, 3.83% H, found 30.72% C, 3.46% H.

Attempted Transhalogenation Reactions of **102** via Lithium-Halogen Exchange and Formation of 1,1,2-Trifluoro-1-hexene (**103**)

In each instance, 1.0 g (4.22 x 10^{-3} mol) **102** was dissolved in 25 mL dry diethyl ether and cooled in a bath of liquid nitrogen / pentane. A slight excess (1.1 equivalents; 2.2 in the case of *t*-butyllithium) of the desired alkyllithium as a solution in diethyl ether was added very slowly to the reaction mixture via syringe. An solution of excess iodine in diethyl ether was then added dropwise to the mixture and allowed to warm to room temperature and stir overnight in each case. ^{19}F NMR analysis showed in all cases quantitative formation of **103**. Use of carbon dioxide as an alternative electrophile was not successful; β-fluoride elimination of the lithiated species was too rapid, even at -100° C, to be successfully trapped.

1,1,2-Trifluoro-1-hexene (**103**): ^{19}F NMR ($CDCl_3$): δ -106.9 (1F, dd, $^2J_{FF}$ = 90 Hz, $^3J_{FF}$ = 32 Hz), -125.9 (1F, dd, $^2J_{FF}$ = 90 Hz, $^3J_{FF}$ = 112 Hz), -174 .8 (1F, dtd, $^3J_{FF}$ = 112 Hz, $^3J_{FF}$ = 32 Hz, $^3J_{FH}$ = 22 Hz).

Attempted Iodofluorination of **103**.

To a solution of 1,1,2-trifluoro-1-hexene (**103**) (containing 9.04 x 10^{-3} mol as judged by a ^{19}F NMR standard of hexafluorobenzene) in 10 mL of diethyl ether at 0° C was added 3.7 mL (3.65 g, 2.27 x 10^{-2} mol) of triethylamine trihydrofluoride. N-iodosuccinimide (2.24 g, 9.94 x 10^{-3} mol) was added in portions, the mixture warmed to room temperature, and stirred overnight. ^{19}F NMR analysis of the mixture showed no change in the spectrum from that of the starting material. The mixture was then heated at reflux for an additional 24 hours, at which time ^{19}F NMR analysis indicated no reaction.

Preparation of 1,1,2,2-Tetrafluoro-1,4-diiodobutane (**105**)

Into a stainless steel pressure reactor of approximately 700 mL capacity was added 100 g (2.83 x 10^{-1} mol) of 1,2-diiodotetrafluoroethane and 0.5 g (3.67 x 10^{-3} mol)

of *d*-limonene. The reactor was tightly sealed, connected to a vacuum line, immersed in a liquid nitrogen bath, and subjected to three successive freeze-pump-thaw cycles to remove oxygen. A total of 15.86 g (5.65 x 10^{-1} mol) of ethylene was transferred into the bomb, which was then sealed and placed into a heating manifold. *(Caution: the following is performed behind a safety shield.)* The thermostat was then set at 210° C, and with constant stirring the reaction mixture was heated for 8 hours. After cooling in an ice bath, venting, and opening, the contents (a dark violet liquid and dark solid) were diluted with 50 mL $CHCl_3$, transferred to a 250 mL Erlenmeyer flask, and chilled in a freezer at -20° C, which caused precipitation of a large amount of dark solid. The mixture was filtered, the solid washed with three 20 mL portions of cold $CHCl_3$, and the combined organic liquids rotary evaporated at room temperature. The remaining liquid was fractionally distilled at reduced pressure through a 15 cm Vigreux column. A total of 43.36 g (40.1%) **105** was obtained as a violet liquid, bp 82-85° C / 22 mm Hg.

1,1,2,2-Tetrafluoro-1,4-diiodobutane (**105**): ^{1}H NMR: δ 2.70 (2H, m), 3.24 (2H, m); ^{13}C NMR: δ -10.5, 34.7 (t, $^2J_{CF}$ = 22.7 Hz), 96.7 (tt, $^2J_{CF}$ = 42.8 Hz, $^1J_{CF}$ = 315.9 Hz), 116.5 (tt, $^2J_{CF}$ = 30.9 Hz, $^1J_{CF}$ = 253.1 Hz); ^{19}F NMR: ϕ -60.8 (2F, t, $^3J_{FF}$ = 4.9 Hz), -108.9 (2F, tt, $^3J_{FF}$ = 4.9 Hz, $^3J_{FH}$ = 17.0 Hz).

Preparation of 3,3,4,4-Tetrafluoro-4-iodobut-1-ene (**106**)

Into a 250 mL three-necked round-bottomed flask equipped with magnetic stir bar, argon inlet, and pressure-equalizing addition funnel was added 30.69 g (8.03 x 10^{-2} mol) 1,1,2,2-tetrafluoro-1,4-diiodobutane (**105**) dissolved in 60 mL anhydrous ether. DBU (26.88 g, 1.77 x 10^{-1} mol) dissolved in 50 mL anydrous ether was added dropwise at room temperature and allowed to stir for an additional 6 hours; at this time, ^{19}F NMR analysis of a small aliquot of the reaction mixture showed complete consumption of starting material. The mixture was poured into 50 mL of 5% aqueous HCl, the layers separated, and the aqueous phase extracted with three 10 mL portions of ether. The

combined organic fractions were washed once with 20 mL of saturated $NaHCO_3$ solution, once with 10 mL of water, dried over $MgSO_4$, and the ether carefully removed by gentle, ambient pressure distillation through a 15 cm Vigreux column. Upon removal of most of the solvent in this way, the bath temperature was increased and 13.46 g (66.0%) **106** was collected over a range of 90-92° C.

3,3,4,4-Tetrafluoro-4-iodobut-1-ene (**106**): ^1H NMR: δ 5.83 (1H, m), 5.99 (2H, m); ^{13}C NMR: δ 97.3 (tt, $^2J_{CF}$ = 44.1 Hz, $^1J_{CF}$ = 316.5 Hz), 113.5 (tt, $^2J_{CF}$ = 30.1 Hz, $^1J_{CF}$ = 249.9 Hz), 124.2 (t, $^2J_{CF}$ = 26.1 Hz), 126.0 (t, $^3J_{CF}$ = 8.6 Hz); ^{19}F NMR: ϕ -60.7 (2F, t, $^3J_{FH}$ = 7.3 Hz), -108.7 (2F, m).

Preparation of 1,1,2,2-Tetrafluoro-1-iodobutane (**107**)

Into a 250 mL three-necked round-bottomed flask equipped with reflux condenser, pressure-equalizing addition funnel and magnetic stir bar was added 10.0 g (3.94 x 10^{-2} mol) of 3,3,4,4-tetrafluoro-4-iodobut-1-ene (**106**) dissolved in 50 mL of dry methanol, 3.20 g (9.98 x 10^{-2} mol) anhydrous hydrazine, and 0.1 g (1.01 x 10^{-3} mol) cuprous chloride. The flask was cooled to 0° C, and 14.2 g of a 30% aqueous solution of hydrogen peroxide was delivered dropwise over a period of 20 minutes, over which time the color of the reaction mixture changed to powder blue then to a dark amber as the H_2O_2 addition neared completion. The cooling bath was then removed, the mixture allowed to stir at room temperature for an additional 2 hours, and the contents poured into a solution of 1 mL of concentrated HCl in 200 mL of water. The mixture was extracted with six 10 mL portions of 1,2-dichlorobenzene, dried over Na_2SO_4, and transferred to a 100 mL flask attached to a 15 cm Vigreux column. A vacuum adapter attached to small trap (immersed in a dry ice-isopropanol slush) was attached, the pressure lowered to 100 mm Hg, and the flask heated with vigorous stirring until the contents began to boil. At this time, it was observed that approximately 1 mL of material

had accumulated in the trap, which was subjected to preparative GC separation. A total of 1.08 g (10.7%) **107** was collected as a colorless liquid.

1,1,2,2-Tetrafluoro-1-iodobutane (**107**): ^{1}H NMR: δ 1.15 (3H, t, $^{3}J_{HH}$ = 7.5 Hz), 2.11 (2H, m); ^{13}C NMR: 5.05, 23.0 (t, $^{2}J_{CF}$ = 23.6 Hz); 98.5 (tt, $^{2}J_{CF}$ = 43.5 Hz, $^{1}J_{CF}$ = 315.9 Hz); 117.5 (tt, $^{2}J_{CF}$ = 29.6 Hz, $^{1}J_{CF}$ = 250.9 Hz); ^{19}F NMR: ϕ -59.9 (2F, t, $^{3}J_{FF}$ = 4.9 Hz), -110.4 (2F, tt, $^{3}J_{FF}$ = 4.9 Hz, $^{3}J_{FH}$ = 17.1 Hz).

Preparation of 1,1,2,2-Tetrafluorohexane (**108**)

1-Bromo-1,1,2,2-tetrafluorohexane (**102**) (2.0 g, 8.44 x 10^{-3} mol) was dissolved in 5 mL of benzene in a 25 mL round-bottomed flask equipped with septum-capped sidearm inlet and stir bar, and attached to a small distillation apparatus equipped with ice water condenser and fractionating column. The bath temperature was raised to 60° C and 2.95 g (1.01 x 10^{-2} mol) nBu_3SnH and 0.01 g (6.09 x 10^{-5} mol) AIBN dissolved in 0.5 mL benzene was added slowly via syringe through the rubber septum. When the addition was complete, the mixture was stirred for an additional 30 minutes and the bath temperature quickly raised to 150° C. All volatile material was flash distilled and subjected to preparative GC separation, which afforded pure **108** as a colorless liquid.

1,1,2,2-Tetrafluorohexane (**108**): ^{1}H NMR: δ 0.95 (3H, t, $^{3}J_{HH}$ = 7.5 Hz), 1.40 (2H, m), 1.55 (2H, m), 1.95 (2H, m), 5.70 (1H, tt, $^{3}J_{HF}$ = 3.0 Hz, $^{2}J_{HF}$ = 54.0 Hz); ^{13}C NMR: 13.6, 22.4 (2C, overlapping), 29.6 (t, $^{2}J_{CF}$ = 22.5 Hz), 110.4 (tt, $^{2}J_{CF}$ = 41.1 Hz, $^{1}J_{CF}$ = 248.4 Hz), 118.1 (tt, $^{2}J_{CF}$ = 28.5 Hz, $^{1}J_{CF}$ = 243.8 Hz); ^{19}F NMR: ϕ -116.8 (2F, t, $^{3}J_{FH}$ = 19.5 Hz), -136.1 (2F, d, $^{2}J_{FH}$ = 53.7 Hz); HRMS for $C_6H_{10}F_4$: calc. 158.0719, calc. (M-H) 157.0640, found 157.0648.

Preparation of 3,3,4,4-Tetrafluoro-1-phenyloctane (**110**)

1-Bromo-1,1,2,2-tetrafluorohexane (**102**) (2.0 g, 8.44 x 10^{-3} mol) and 1.76 g (1.69 x 10^{-2} mol) styrene dissolved in 25 mL benzene were added to a 100 mL three-necked round-bottomed flask fitted with rubber septum, condenser with argon inlet, and

magnetic stirrer. A total of 4.90 g (1.68 x 10^{-2} mol) nBu_3SnH and 0.05 g (3.04 x 10^{-4} mol) AIBN were dissolved in 5 mL benzene and taken up in a syringe. A 150 W flood lamp was placed at a distance of approximately 15 cm from the flask, and with irradiation (at this distance, sufficient heat was generated to cause the solvent to reflux as well) the nBu_3SnH solution was delivered to the reaction mixture via syringe pump over a 36 hour period. After rotary evaporation at elevated temperature, column chromatography (silica gel, hexanes) afforded four fractions of **110** free from organotin contaminants.

3,3,4,4-Tetrafluoro-1-phenyloctane (**110**): ^1H NMR: δ 0.96 (3H, t, $^3J_{HH}$ = 7.2 Hz), 1.41 (2H, m), 1.57 (2H, m), 2.02 (2H, m), 2.31 (2H, m), 2.90 (2H, m), 7.28 (5H, m) ^{13}C NMR: 1.0, 13.8, 22.5, 26.9, 29.7 (t, $^2J_{CF}$ = 22.7 Hz), 32.1 (t, $^2J_{CF}$ = 22.8 Hz), 118.8 (tt, $^2J_{CF}$ = 37.6 Hz, $^1J_{CF}$ = 250.4 Hz); 119.3 (tt, $^2J_{CF}$ = 34.1 Hz, $^1J_{CF}$ = 245.9 Hz), 126.3, 128.3, 128.6, 140.3); ^{19}F NMR: ϕ -116.0 (2F, m), -116.4 (2F, m); HRMS for $C_{14}H_{18}F_4$: calc. 262.1345, found 262.1307.

Preparation of 1-[Perfluorohexyl]ethane (**113**)

Into a 25 mL round-bottomed flask equipped with septum-capped sidearm inlet and magnetic stir bar was placed 4.22 g (8.90 x 10^{-3} mol) 2-[perfluorohexyl]-1-iodoethane (**112**.) The flask was attached to a distillation apparatus equipped with a small fractionating column and ice water condenser. The bath temperature was raised to 80° C and 3.11 g (1.07 x 10^{-2} mol) nBu_3SnH was slowly injected into the flask with stirring. After 30 minutes at this temperature, the bath temperature was raised to 150° C and the product distilled over a range of 81-82° C. Preparative GC purification afforded pure **113**.

1-[Perfluorohexyl]ethane (**113**): ^1H NMR: δ 1.14 (3H, m), 2.10 (2H, m); ^{19}F NMR: ϕ -81.5 (3F, t, $^3J_{FF}$ = 9.8 Hz), -117.0 (2F, m), -122.5 (2F, br s), -123.4 (2F, br m), -124.2 (2F, br m), -126.8 (2F, m); HRMS for $C_8H_5F_{13}$: calc. 348.0183, calc. (M-F) 329.0200, found 329.0280.

Preparation of 2-Iodo-1-[perfluorohexyl]-4-phenylbutane (**116**)

Into a 50 mL three-necked round-bottomed flask equipped with argon inlet, rubber septum and stir bar was added 0.5 g (3.78 x 10^{-3} mol) 4-phenyl-1-butene and 2.02 g (4.53 x 10^{-3} mol) perfluorohexyl iodide dissolved in 20 mL of hexanes. A 1.0 M solution of triethylborane in hexanes (0.4 mL, 4 x 10^{-4} mol) was slowly injected through the septum, and the reaction allowed to stir for 6 hours at room temperature. The mixture was washed twice with 10 mL water, the solvent rotary evaporated, and the remaining liquid subject to reduced pressure fractional distillation. A total of 1.81 g (82.8%) **116** was collected as a light violet liquid, bp 125-127° C / 1 mm Hg.

2-Iodo-1-[perfluorohexyl]-4-phenylbutane (**116**): ^{1}H NMR: δ 2.12 (2H, m), 2.75 (2H, m), 2.92 (2H, m), 4.27 (1H, m), 7.27 (5H, m); ^{19}F NMR: ϕ -81.3 (3F, t, $^3J_{FF}$ = 9.8 Hz), -111.8 (1F, dm, $^2J_{FF}$ = 275.9 Hz), -115.2 (1F, dm, $^2J_{FF}$ = 267.3 Hz), -122.3 (2F, br s), -123.3 (2F, s), -124.2 (2F, br s), -126.7 (2F, m); HRMS for $C_{16}H_{12}F_{13}I$: calc. 577.9776, found 577.9815.

Preparation 1-[Perfluorohexyl]-4-phenylbutane (**117**)

Into a 50 mL three-necked round-bottomed flask equipped with argon inlet and magnetic stirrer was added 1.5 g (2.59 x 10^{-3} mol) 2-iodo-1-[perfluorohexyl]-4-phenylbutane (**116**) dissolved in 10 mL DMSO. The bath temperature was raised to 70° C and 0.39 g (1.03 x 10^{-2} mol) sodium borohydride was added in portions to the reaction mixure. Stirring was continued for an additional 6 hours, at which time the mixture was poured into 50 mL of ice water, and carefully acidified with 6 M HCl. 10 mL ether was added, the layers separated, and the aqueous layer extracted with three 10 mL portions of ether. The combined organic layers were washed once with 10 mL 5% aqueous $NaHCO_3$ and twice with 10 mL of water, dried over $MgSO_4$, and the solvent rotary evaporated. Reduced pressure fractional distillation afforded 0.82 g (70.0 %) **117**, bp 83-85° C / 0.25 mm Hg.

1-[Perfluorohexyl]-4-phenylbutane (**117**): ^{1}H NMR: δ 1.67 (4H, m), 2.06 (2H, m), 2.64 (2H, t, $^3J_{HH}$ = 6.9 Hz), 7.24 (5H, m); ^{19}F NMR: ϕ -81.4 (3F, t, $^3J_{FF}$ = 9.8 Hz), -114.9 (2F, m), -122.5 (2F, br s), -123.4 (2F, s), -124.1 (2F, s), -126.7 (2F, m); HRMS for $C_{16}H_{13}F_{13}$: calc. 452.0810, found 452.0797.

Preparation of Pentafluoroethane (**120**)

Iodopentafluoroethane (2.16 g, 8.78 x 10^{-3} mol) was condensed into a Pyrex tube equipped with a Rotaflo stopcock, rubber septum, and immersed in a dry ice-isopropanol slush. In one portion, 3.07 g (1.05 x 10^{-2} mol) nBu_3SnH was injected into the tube and the stopcock closed. The tube was then subjected to photolysis in a Rayonet reactor for 30 minutes at room temperature with periodic shaking. The tube was cooled to -20° C in a dry ice-isopropanol bath, a rubber hose connected to the Rotaflo tube and to a trap immersed in a liquid nitrogen-ether slush, and the stopcock opened. After trap-to-trap transfer in this way, an NMR tube containing ca. 1 mL $CDCl_3$, capped with a rubber septum, and immersed in a liquid-nitrogen-ether slush was connected via cannula. The trap was warmed to -20° C as a sample of **120** collected in the tube, which was flame sealed and taken for NMR analysis.

Pentafluoroethane (**120**): ^{1}H NMR: δ 5.88 (tq, $^3J_{HF}$ = 2.4 Hz, $^2J_{HF}$ = 52.2 Hz); ^{19}F NMR: ϕ -86.1 (3F, s), -138.5 (2F, d, $^2J_{FH}$ = 51.3 Hz).

Preparation of 1,1,1,2,2-Pentafluoro-4-phenylbutane (**122**)

Iodopentafluoroethane (5.47 g, 2.22 x 10^{-2} mol) of was condensed into a Pyrex Rotaflo tube containing 2.12 g (2.04 x 10^{-2} mol) styrene, 5.92 g (2.03 x 10^{-2} mol) nBu_3SnH, 5 mL benzene and a small sir bar. The stopcock was closed and the tube irradiated with a 150 W flood lamp with stirring for 72 hours. Volatiles were removed by rotary evaporation and the residue subject to flash vaccuum distillation at 100 mm Hg (bath temperature 150° C) during which time the distillate temperature reached 69° C. Preparative GC purification of the distillate yielded an analytically pure sample of **122**.

1,1,1,2,2-Pentafluoro-4-phenylbutane (**122**): ^{1}H NMR: δ 2.38 (2H, m), 2.95 (2H, m), 7.31 (5H, m); ^{13}C NMR: δ 26.6, 32.7 (t, $^2J_{CF}$ = 21.5 Hz), 115.5 (tq, $^2J_{CF}$ = 37.6 Hz, $^1J_{CF}$ = 250.4 Hz), 119.3 (qt, $^2J_{CF}$ = 36.1 Hz, $^1J_{CF}$ = 283.4 Hz), 126.7, 128.2, 128.8, 139.2; ^{19}F NMR: ϕ -85.9 (3F, s), -119.1 (2F, t, $^3J_{FH}$ = 19.5 Hz); HRMS for $C_{10}H_9F_5$: calc. 224.0624, found 224.0670; CHN for $C_{10}H_9F_5$: calc. 53.58% C, 4.05% H, found 53.42%C, 3.97% H.

Preparation of 1-(*tert*-Butyldimethylsiloxyl)-3-butene (**130**)

Into a 250-mL three-necked round-bottomed flask equipped with a condenser and argon inlet was placed 9.60 g (1.33 x 10^{-1} mol) of 3-buten-1-ol, 20 mL DMF, 24.1 g (1.60 x 10^{-1} mol) *tert*-butyldimethylsilyl chloride, and 22.7 g (3.33 x 10^{-1} mol) imidazole. This was stirred for 48 hours at room temperature under an argon atmosphere. The contents of the flask were then poured into 250 mL of pentane, and washed with three 50 mL portions of water followed by three 50 mL portions of saturated aqueous sodium chloride. The organic phase was dried, the solvent rotary evaporated, and the resulting liquid subjected to fractional reduced pressure distillation through a 15 cm vigreaux column. A total of 22.08 g (89.3%) of pure **130** was obtained in 4 fractions as a colorless liquid boiling at 102-105° C / 75 mm Hg.

1-(*tert*-Butyldimethylsiloxyl)-3-butene (**130**): ^{1}H NMR ($CDCl_3$): δ 0.05 (6H, s), 0.90 (9H, s), 2.27 (2H, dt, $^3J_{HH}$ = 7 Hz, $^3J_{HH}$ = 3 Hz), 3.66 (2H, t, $^3J_{HH}$ = 7 Hz), 5.02 (1H, m), 5.10 (1H, m), 5.81 (1H, m); ^{13}C NMR ($CDCl_3$): δ -5.27, 18.3, 25.9, 37.5, 62.8, 116.2, 135.4; HRMS for $C_{10}H_{22}SiO$: calc. 186.1440, found (M+H) 187.1561; CHN for $C_{10}H_{22}SiO$: calc. 64.45% C, 11.90% H, found 64.32%C, 12.03 % H.

Preparation of 1,3-Dibromo-5-(*tert*-butyldimethylsiloxyl)-1,1-difluoropentane (**131**)

Cuprous chloride (0.10 g, 1.25 x 10^{-3} mol), along with 12.5 mL *tert*-butanol, 3.83 g (6.26 x 10^{-2} mol) ethanolamine, 23.30 g (1.25 x 10^{-1} mol) 1-(*tert*-butyldimethylsiloxyl)-3-butene (**130**), and 52.60 g (2.51 x 10^{-1} mol) CF_2Br_2 were added

to a Carius tube. A small stir bar was added and the tube flame-sealed. After stirring at 85° C for 96 hours (*performed behind a safety shield*) the tube was cooled in an ice bath, opened, and the contents transferred to a 500 mL Erlenmeyer flask. The tube was rinsed with four 50 mL portions of hexanes, and the combined organic material filtered through a 50 mL pad of silica gel, which was rinsed with three additional 50 mL portions of hexanes. Rotary evaporation of the solvent afforded a colorless liquid judged by ^{1}H NMR to contain some unreacted starting material, 2.78 g of which was successfully recovered by reduced pressure distillation at 102-105° C / 75 mm Hg. High vacuum was then applied and a total of 35.83 g (72.4%, 82.0% based on consumed **130**) **131** was obtained as a colorless liquid boiling at 75-79° C / 0.09 mm Hg.

1,3-Dibromo-5-(*tert*-butyldimethylsiloxyl)-1,1-difluoropentane (**131**): ^{1}H NMR: δ 0.07 (3H, s), 0.08 (3H, s), 0.90 (9H, s), 1.95 (1H, m), 2.15 (1H, m), 3.08 (2H, m), 3.80 (2H, m), 4.46 (1H, m); ^{13}C NMR: δ -5.5, 18.2, 25.9, 41.3, 43.8, 52.9 (t, $^2J_{CF}$ = 19 Hz), 60.2, 120.64 (t, $^1J_{CF}$ = 306 Hz); ^{19}F NMR: ϕ -43.1 (m); HRMS for $C_{11}H_{22}SiOF_2Br_2$: calc. 393.9774, calc. (M-*t*-C_4H_9) 336.9070, found 336.905; CHN for $C_{11}H_{22}SiOF_2Br_2$: calc. 33.35% C, 5.60% H, found 33.62% C, 5.62% H.

Preparation of 1-Bromo-5-(*tert*-butyldimethylsiloxyl)-1,1-difluoropentane (**132**)

1,3-Dibromo-5-(*tert*-butyldimethylsiloxyl)-1,1-difluoropentane (**131**) (30.15 g, 7.60 x 10^{-2} mol) was dissolved in 150 mL of dry DMSO in a 500 mL three-necked round-bottomed flask equipped with an argon inlet and strong magnetic stir bar. Sodium borohydride (11.5 g, 3.04 x 10^{-1} mol) was then added in portions with vigorous stirring. After the addition was complete, the temperature was raised to 70-75° C over the course of one hour and stirring continued for an additional 6 hours, at which time analysis of the reaction mixture by ^{19}F NMR demonstrated complete consumption of starting material. The flask was cooled and carefully quenched with ca. 100 g of ice, and the contents carefully acidified with concentrated hydrochloric acid and transferred to a 1 liter

separatory funnel. After extraction with three 100 mL portions of ether, the combined extracts were washed with two 25 mL portions of water, dried over $MgSO_4$, and rotary evaporated. The remaining liquid was distilled at reduced pressure through a 15 cm vigreaux column, affording 21.70 g (90.0%) **132** as a colorless liquid, bp 108-111° C / 10 mm Hg.

1-Bromo-5-(*tert*-butyldimethylsiloxyl)-1,1-difluoropentane (**132**): ^{1}H NMR: δ 0.05 (6H, s), 0.90 (9H, s), 1.63 (4H, m), 2.38 (2H, m), 3.63 (2H, t, $^3J_{HH}$ = 6 Hz); ^{13}C NMR: δ 18.3, 20.7, 25.9 (2C, overlapping), 31.4, 44.1 (t, $^2J_{CF}$ = 22.5 Hz), 62.4, 123.2 (t, $^1J_{CF}$ = 304 Hz); ^{19}F NMR: ϕ -44.0 (m); HRMS for $C_{11}H_{23}SiOF_2Br$: calc. 316.0669, found (M+H) 317.0630.

Preparation of 5-Bromo-5,5-difluoropentan-1-ol (**133**)

Into a 250-mL round-bottomed flask was placed 15.04 g (4.74 x 10^{-2} mol) 1-bromo-5-(*tert*-butyldimethylsiloxyl)-1,1-difluoropentane (**132**) along with 41 mL of acetonitrile. To this was slowly added with stirring 7.70 g (4.75 x 10^{-2} mol) ferric chloride. The reaction mixture turned a brick-red color and became slightly warm. The reaction was allowed to stir for 3 hours at room temperature, at which time the contents of the flask were poured into 250 mL of water and 100 mL of chloroform was added. The chloroform layer was drained and the aqueous layer extracted with three 50 mL portions of chloroform. These combined extracts were washed twice with 25 mL of water, dried over $MgSO_4$ and the solvent rotary evaporated. A total of 9.41 g (97.7%) **132** was collected by fractional reduced pressure distillation, bp 80-82° C / 10 mm Hg.

5-Bromo-5,5-difluoropentan-1-ol (**133**): ^{1}H NMR: δ 1.39 (1H, s), 1.69 (4H, m), 2.40 (2H, m), 3.69 (2H, t, $^3J_{HH}$ = 6 Hz); ^{13}C NMR: δ 20.5, 31.3, 44.0 (t, $^2J_{CF}$ = 21.5 Hz), 62.2, 123.0 (t, $^1J_{CF}$ = 303.5 Hz); ^{19}F NMR: ϕ -44.1 (t, $^3J_{FH}$ = 14.7 Hz); HRMS for $C_5H_9F_2BrO$: calc. 201.9804, found (M+H) 202.9957; CHN for $C_5H_9F_2BrO$: calc. 29.58% C, 4.47% H, found 29.71% C, 4.46% H.

Preparation of 5-Bromo-5,5-difluoropentanal (**134**)

Into a 250-mL round-bottomed flask equipped with a magnetic stir bar was added 8.5 g (4.18 x 10^{-2} mol) 5-bromo-5,5-difluoropentan-1-ol (**133**) dissolved in 85 mL of dichloromethane. PCC (13.53 g, 6.28 x 10^{-2} mol) was added slowly in portions with vigorous stirring. After the addition was complete, the mixture was allowed to stir at room temperature for an additional 6 hours. The darkened reaction mixture (which demonstrated complete consumption of starting material by TLC analysis) was filtered through a pad of silica gel, which was rinsed with an additional three 10 mL portions of CH_2Cl_2. Rotary evaporation of the solvent followed by fractional distillation at reduced pressure afforded 4.46 g (53.1%) **134** as a colorless liquid, bp 100-102° C / 50 mm Hg.

5-Bromo-5,5-difluoropentanal (**134**): ^{1}H NMR: δ 1.97 (2H, m), 2.41 (2H, m), 2.59 (2H, t, $^3J_{HH}$ = 7.2 Hz), 9.80 (1H, s); ^{13}C NMR: δ 16.6 (t, $^3J_{CF}$ = 3.5 Hz), 42.1, 43.2 (t, $^2J_{CF}$ = 22.0 Hz); 122.5 (t, $^1J_{CF}$ = 303.4 Hz), 200.5; ^{19}F NMR: ϕ -44.4 (t, $^3J_{FH}$ = 14.4 Hz); HRMS for $C_5H_7F_2BrO$: calc. 199.9648, found (M+H) 200.9726.

Preparation of 6-Bromo-6,6-difluorohex-1-ene (**135**)

A 100 mL three-necked round-bottomed flask equipped with self-equalizing addition funnel, argon inlet and magnetic stir bar was charged with 9.12 g (2.55 x 10^{-2} mol) of methyltriphenylphosphonium bromide and 20 mL anhydrous THF. The flask was cooled to 0° C and 9.4 mL of a 2.5 M solution of butyllithium in hexanes (2.35 x 10^{-2} mol) was added dropwise. After addition was complete, the mixture was stirred for an additional 30 minutes at 0° C. 5-Bromo-5,5-difluoropentanal (**134**) (4.28 g, 2.13 x 10^{-2} mol) was dissolved in 20 mL anhydrous THF and added dropwise to the reaction mixture. After addition the mixture was allowed to warm to room temperature and stir for an additional 6 hours. The contents were poured into 50 mL of water and extracted with five 20-mL portions of ether. The combined ether fractions were dried over $MgSO_4$, filtered, and the solution concentrated by distillation through a 15 cm vigreaux column.

Upon removal of most of the ether and residual THF the product was distilled at ambient pressure, yielding 2.04 g (48.1%) **135**, bp 120-123° C. An analytically pure sample was obtained by preparative GC for spectroscopic analysis and kinetic experiments.

6-Bromo-6,6-difluorohex-1-ene (**135**): ^{1}H NMR: δ 1.74 (2H, m), 2.15 (2H, overlapping dt, J = 7 Hz), 2.35 (2H, m), 5.05 (2H, m), 5.77 (1H, m); ^{13}C NMR: δ 23.1, 32.3, 43.6 (t, $^{2}J_{CF}$ = 21.6 Hz), 115.9, 123.1 (t, $^{1}J_{CF}$ = 303.5 Hz), 137.0; ^{19}F NMR: ϕ -43.9 (t, $^{3}J_{FH}$ = 14.7 Hz); HRMS for $C_6H_9F_2Br$: calc. 197.9855, calc (M-Br) 119.0672, found 119.0667; CHN for $C_5H_9F_2Br$: calc. 36.21% C, 4.56% H, found 36.28% C, 4.56% H.

Preparation of 6,6-Difluorohex-1-ene (**136**)

6-Bromo-6,6-difluorohex-1-ene (**135**) (1.0 g, 5.02 x 10^{-3} mol) was dissolved in mesitylene (1 mL) in a 10 mL round-bottomed flask equipped with a septum-capped sidearm inlet and small stir bar. This was attached to an ice-water-cooled micro distillation apparatus. Tributyltin hydride (1.6 g, 5.50 x 10^{-3} mol) was slowly injected into the flask through the septum. When the addition was complete, heating was begun with an oil bath. After 15 minutes at 50° C, the temperature was quickly raised and all volatile material was flash distilled until the bath temperature reached 150° C. The distillate was subjected to preparative GC separation, affording pure **136**.

6,6-Difluorohex-1-ene (**136**): ^{1}H NMR: δ 1.57 (2H, m), 1.83 (2H, m), 2.12 (2H, overlapping dt, J = 7 Hz), 5.00 (2H, m), 5.79 (1H, m), 5.81 (1H, tt, $^{3}J_{HH}$ = 4 Hz, $^{2}J_{HF}$ = 57 Hz); ^{13}C NMR: δ 21.3, 32.9, 33.8 (t, $^{2}J_{CF}$ = 20.5 Hz), 115.4, 117.3 (t, $^{1}J_{CF}$ = 237.6 Hz), 120.5; ^{19}F NMR: ϕ -116.4 (dt, $^{3}J_{FH}$ = 14.6 Hz, $^{2}J_{FH}$ = 59.8 Hz); HRMS for $C_6H_{10}F_2$: calc. 120.0751, found 120.0756; CHN for $C_6H_{10}F_2$: calc. 59.98% C, 8.39% H, found 59.96% C, 8.47% H.

Preparation of 1,1-Difluoro-2-methylcyclopentane (**138**)

Into a 50 mL three-necked round-bottomed flask equipped with magnetic stirrer and septum was placed 0.5 g (5.09 x 10^{-3} mol) 2-methylcyclopentanone dissolved in 10

mL of anhydrous CH_2Cl_2. DAST (0.9 g, 5.58 x 10^{-3} mol) was then injected and the mixture stirred at room temperature overnight. The reaction was dispensed onto ca. 2 g of ice, the layers separated, and the organic layer washed with 1 mL of saturated aqueous $NaHCO_3$. After drying, all volatile material was flash distilled and subjected to preparative GC, affording pure **138**.

1,1-Difluoro-2-methylcyclopentane (**138**): ^{1}H NMR: δ 1.04 (3H, d, $^3J_{HH}$ = 7 Hz), 1.40 (1H, m), 1.73 (2H, m), 2.04 (4H, overlapping m); ^{13}C NMR: δ 12.1, 19.9, 30.9, 34.4 (t, $^2J_{CF}$ = 25.1 Hz), 40.7 (t, $^2J_{CF}$ = 23.5 Hz), 132.4 (t, $^1J_{CF}$ = 249.4 Hz); ^{19}F NMR: ϕ -100.2 (1F, d of overlapping dt, $^3J_{FH}$ = 12.2 Hz, $^2J_{FF}$ = 225.8 Hz), -107.6 (1F, d of overlapping dt, $^3J_{FH}$ = 17.1 Hz, $^2J_{FF}$ = 224.6 Hz); HRMS for $C_6H_{10}F_2$: calc. 120.0751, found 120.0748.

Preparation of 6-Bromohex-1-en-5-ol (**142**)

To a 500 mL three-necked round-bottomed flask equipped with magnetic stirrer was added 100 mL acetic acid, 50 mL of saturated aqueous potassium bromide, and 50 mL THF. The flask was cooled to 0° C and 5.0 g (5.09 x 10^{-2} mol) of 1,2-epoxy-5-hexene dissolved in 10 mL of THF was added dropwise with stirring. The heterogeneous mixture was stirred at 0° C for an additional two hours, then allowed to warm to room temperature and stir overnight. Most of the THF was removed by rotary evaporation, 100 mL of ether and 50 mL of water was added, and the aqueous layer washed with saturated aqueous $NaHCO_3$ until the acetic acid was removed. Drying over $MgSO_4$ followed by rotary evaporation of the solvent afforded 8.03 g (88.1%) **142** which was used in the next step without further purification.

6-Bromohex-1-en-5-ol (**142**): ^{1}H NMR: δ 1.61 (2H, overlapping dt, J = 8 Hz), 2.15 (2H, m), 2.67 (1H, s), 3.35 (1H, m), 3.48 (1H, m), 3.76 (1H, m), 4.99 (2H, m), 5.77 (1H, m); ^{13}C NMR: δ 29.6, 34.0, 40.0, 70.2, 115.2, 137.5; HRMS for $C_6H_{11}BrO$: calc. 177.9993, calc (M+H) 178.9993, found 179.0058.

Preparation of 1-Bromo-5-hexen-2-one (**143**)

6-Bromohex-1-en-5-ol (**142**) (7.25 g, 4.05 x 10^{-2} mol) dissolved in 10 mL ether was added dropwise to a mixture of 60 mL of Jones' reagent and 25 mL ether at room temperature with stirring. After 4 hours the dark green reaction mixture was diluted with 50 mL of water. The layers were separated and the aqueous layer extracted with three 20 mL portions of ether. The combined organic extracts were washed twice with 20 mL of saturated aqueous $NaHCO_3$ and once with 20 mL of water. Drying and rotary evaporation of the solvent afforded 5.92 g (82.6%) **143** which was used without further purification.

1-Bromo-5-hexen-2-one (**143**): ^{1}H NMR: δ 2.35 (2H, overlapping dt, J = 6 Hz), 2.74 (2H, t, $^3J_{HH}$ = 7 Hz), 3.88 (2H, s), 5.01 (2H, m), 5.78 (1H, m); ^{13}C NMR: δ 27.7, 34.2, 38.8, 115.7, 136.3, 201.2; HRMS for C_6H_9BrO: calc. 175.9836, found 175.9850.

Preparation of 6-Bromo-5,5-difluorohex-1-ene (**144**)

A 100 mL three-necked round-bottomed flask equipped with an argon inlet, rubber septum, and magnetic stirrer was charged with 2.1 g (1.19 x 10^{-2} mol) 1-bromo-5-hexen-2-one (**143**) in 20 mL of anhydrous CH_2Cl_2. The flask was cooled to 0° C and 1.9 mL (2.32 g, 1.44 x 10^{-2} mol) of diethylaminosulfurtrifluoride was slowly injected into the reaction mixture with stirring. After two hours at 0° C, the flask was allowed to warm to room temperature and stirring continued for an additional 48 hours. The contents were carefully dispensed onto 20 g of ice, the layers separated, and the aqueous layer extracted twice with 5 mL CH_2Cl_2. The combined organic extracts were washed once with 10 mL of saturated aqueous $NaHCO_3$ and once with 10 mL of water. After drying over MgSO4 the solution was carefully concentrated via gentle ambient pressure distillation. A total of 1.33 g (56.2%) **144** was obtained as a colorless liquid, bp 117-119° C, which was further purified by preparative GC for spectroscopic analysis and kinetic experiments.

6-Bromo-5,5-difluorohex-1-ene (**144**): ^{1}H NMR: δ 2.06 - 2.31 (4H, m), 3.53 (2H, t, $^3J_{HF}$ = 13 Hz), 5.07 (2H, m), 5.82 (1H, m); ^{13}C NMR: δ 26.2 (t, $^3J_{CF}$ = 4.5 Hz), 31.3 (t, $^2J_{CF}$ = 33.6 Hz), 33.8 (t, $^2J_{CF}$ = 24.1 Hz), 115.8, 121.1 (t, $^1J_{CF}$ = 241.4 Hz), 136.2; ^{19}F NMR: ϕ -99.3 (m); HRMS for $C_6H_9F_2Br$: calc. 197.9855, found 197.9850; CHN for $C_6H_9F_2Br$: calc. 36.21% C, 4.56% H, found 36.16% C, 4.57% H.

Preparation of 5,5-Difluorohex-1-ene (**144**)

6-Bromo-5,5-difluoro-1-hexene (**144**) (1.0 g, 5.02 x 10^{-3} mol) was treated with 1.6 g (5.50 x 10^{-3} mol) of tributyltin hydride in a manner identical to the independent preparation of **136**. Flash distillation followed by preparative GC separation afforded pure **144**.

5,5-Difluorohex-1-ene (**144**): ^{1}H NMR: δ 1.60 (3H, t, $^3J_{HF}$ = 18 Hz), 1.94 (2H, m), 2.24 (2H, m), 5.03 (2H, m), 5.83 (2H, m); ^{13}C NMR: δ 23.3 (t, $^2J_{CF}$ = 28.1 Hz), 26.9 (t, $^3J_{CF}$ = 5.0 Hz), 37.2 (t, $^2J_{CF}$ = 25.1 Hz), 115.2, 123.9 (t, $^1J_{CF}$ = 236.4 Hz), 136.9; ^{19}F NMR: ϕ -91.3 (m); HRMS for $C_6H_{10}F_2$: calc. 120.0751, found 120.0743.

Preparation of 1,1-Difluoro-3-methylcyclopentane (**147**)

3-Methylcyclopentanone (0.5 g, 5.09 x 10^{-3} mol) and 0.9 g (5.58 x 10^{-3} mol) DAST were reacted in 10 mL of anhydrous CH_2Cl_2 in a manner identical to the preparation of **138**. Flash distillation and preparative GC separation afforded pure **147**.

1,1-Difluoro-3-methylcyclopentane (**147**): ^{1}H NMR: δ 1.05 (3H, d, $^3J_{HH}$ = 6Hz), 1.36 (1H, m), 1.61 (1H, m), 1.87 - 2.31 (5H, m); ^{13}C NMR: δ 20.0, 31.6, 32.0 (t, $^3J_{CF}$ = 4.3 Hz), 36.0 (t, $^2J_{CF}$ = 25.0 Hz), 44.0 (t, $^2J_{CF}$ = 23.6 Hz), 133.0 (t, $^1J_{CF}$ = 246.9 Hz); ^{19}F NMR: ϕ -88.9 (1F, dm, $^2J_{FF}$ = 217.1 Hz), -90.2 (1F, dm, $^2J_{FF}$ = 227.1 Hz); HRMS for $C_6H_{10}F_2$: calc. 120.0751, found 120.0759.

Preparation of 1,1-Difluorocyclohexane (**149**)

Cyclohexanone (0.5 g, 5.09 x 10^{-3} mol) and 0.9 g (5.58 x 10^{-3} mol) DAST were reacted in 10 mL of anhydrous CH_2Cl_2 in a manner identical to the preparation of **138**. Preparation and flash distillation afforded pure **149**.

1,1-Difluorocyclohexane (**149**): ^{1}H NMR: δ 0.97 (2H, m), 1.29 (4H, q, $^3J_{HH}$ = 6 Hz), 1.58 (4H, m); ^{13}C NMR: δ 22.8, 24.4, 34.1 (t, $^2J_{CF}$ = 23.5 Hz), 123.6 (t, $^1J_{CF}$ = 239.9 Hz); ^{19}F NMR: ϕ -95.7 (2F, br s).

Preparation of 5,5,6,6-Tetrafluorohex-1-ene (**153**), 1,1,2,2-Tetrafluoro-3-methylcyclopentane (**155**), and 1,1,2,2-Tetrafluorocyclohexane (**157**)

6-Bromo-5,5,6,6-tetrafluorohex-1-ene (**101**) (5.0 g, 2.13 x 10^{-2} mol) dissolved in 5 mL of mesitylene was added to a 50 mL three-necked round-bottomed flask equipped with ice water condenser, argon inlet, magnetic stir bar and rubber septum. Tributyltin hydride (7.5 g, 2.58 x 10^{-2} mol) and 0.05 g (3.04 x 10^{-4} mol) 2,2'-azobisisobutyronitrile (AIBN) in 5 mL of mesitylene were taken up into a syringe. The flask was heated at 50° C and irradiated with a 150 W flood lamp placed at a distance of ca. 1 m while the nBu_3SnH solution was delivered to the reaction mixture, via syringe pump, over a 24 hour period. After the addition was complete, all volatile material was flash distilled from the reaction mixture until the bath temperature reached 150° C. Purification by preparative GC afforded pure samples of **153**, **155**, and **157.**

5,5,6,6-Tetrafluorohex-1-ene (**153**): ^{1}H NMR: δ 2.06 (2H, m), 2.33 (2H, m), 5.08 (2H, m), 5.72 (1H, tt, $^3J_{HF}$ = 3 Hz, $^2J_{HF}$ = 54 Hz), 5.84 (1H, m); ^{13}C NMR: δ 24.6 (t, $^3J_{CF}$ = 4.0 Hz), 29.2 (t, $^2J_{CF}$ = 22.1 Hz), 110.3 (tt, $^2J_{CF}$ = 41.1 Hz, $^1J_{CF}$ = 247.7 Hz), 115.9, 117.8 (tt, $^2J_{CF}$ = 29.0 Hz, $^1J_{CF}$ = 244.8 Hz), 136.1; ^{19}F NMR: ϕ -116.7 (2F, t, $^3J_{FH}$ = 17.1 Hz), -136.0 (2F, d, $^2J_{FH}$ = 56.2 Hz); HRMS for $C_6H_8F_4$: calc. 156.0562, found 156.0562.

1,1,2,2-Tetrafluoro-3-methylcyclopentane (**155**): ^{1}H NMR δ 1.12 (3H, d, $^3J_{HH}$ = 7 Hz), 1.47 (1H, m), 2.00 (1H, m), 2.07 - 2.49 (3H, m); ^{13}C NMR: δ 11.4, 23.7 (m), 29.8 (t, $^2J_{CF}$ = 22.8 Hz), 36.2 (t, $^2J_{CF}$ = 21.0 Hz), 117.6 - 125.8 (2C, m); ^{19}F NMR: ϕ -110.1 (1F,

dm, $^2J_{FF}$ = 234.4 Hz), -120.7 (1F, dm, $^2J_{FF}$ = 239.3 Hz), -126.0 (1F, dt, $^3J_{FH}$ = 12.2 Hz, $^2J_{FF}$ = 236.8 Hz), -132.9 (1F, dm, $^2J_{FF}$ = 235.6); HRMS for $C_6H_8F_4$: calc. 156.0562, found 156.0563; CHN for $C_6H_8F_4$: calc. 46.16% C, 5.16% H, found 46.17% C, 5.35% H.

1,1,2,2-Tetrafluorocyclohexane (**157**): ^{1}H NMR: δ 1.69 (4H, br s), 2.06 (4H, br s); ^{13}C NMR: δ 21.0, 31.7 (t, $^2J_{CF}$ = 22.1 Hz), 117.0 (tt, $^2J_{CF}$ = 28.1 Hz, $^1J_{CF}$ = 250.4 Hz); ^{19}F NMR: ϕ -119.7 (4F, br s); HRMS for $C_6H_8F_4$: calc. 156.0562, found 156.0571.

Competitive Kinetic Procedures

Competition Kinetics: Hydrogen Atom Abstraction (k_H) versus Addition (k_{add}) and Hydrogen Atom Abstraction versus Cyclization (k_{Cn})- General Procedure.

Into each of a set of six Pyrex NMR tubes were added a known amount of C_6D_6, varying, known amounts of trapping agent or trapping agent and styrene, and a known amount of trifluorotoluene as an internal ^{19}F NMR standard. Each tube was sealed with rubber septa secured with PTFE tape, frozen in a dry ice-isopropanol slush, and subjected to three successive freeze-pump-thaw cycles followed by pressurization with argon. Into each frozen tube was then injected a known amount of the radical precursor (in the case of **119**, a stock solution in degassed C_6D_6) followed by warming to room temperature (in the case of **119**, the tubes were flame-sealed before warming) with vigorous shaking. The tubes were then subjected to UV photolysis in a Rayonet reactor (254 nm lamps) until complete consumption of starting material was demonstrated by ^{19}F NMR analysis. Product ratios for varied concentrations of trapping agent or ratios of trapping agent to styrene allow determination of the ratios k_H / k_{Cn} or k_H / k_{add}. Yields are determined by integration of product resonances versus that of internal standard (ϕ -63.24) in the ^{19}F NMR.

1,1-Difluorohex-1-yl Radical (**77**)

Ratios of [**81**] / [**83**] were determined by integration of the -CF_2H and -CF_2- resonances (at ϕ -116.0 and -99.1, respectively) in the ^{19}F NMR.

Table 5-1. Data for Competitive Determination of k_H (nBu_3SnH) / k_{add} (Styrene) for 1,1-Difluorohex-1-yl Radical (**77**).

[**80**]	[$C_6H_5CH=CH_2$]	[nBu_3SnH] / [$C_6H_5CH=CH_2$]	[**81**] / [**83**]	% Yield
0.094	2.01	0.719	2.30	95
0.094	1.81	0.847	2.73	95
0.094	1.61	1.01	3.26	96
0.094	1.41	1.21	3.93	97
0.094	1.21	1.49	4.88	96
0.094	1.01	1.87	6.21	95

Slope = k_H / k_{add} = 3.39 ± 0.02

k_H (nBu_3SnH) = 9.1 (± 1.7) x 10^6 M^{-1} s^{-1}

2,2-Difluorohex-1-yl Radical (**88**)

Ratios of [**93**] / [**98**] were obtained by integration of the respective -CF_2- resonances at ϕ -91.0 and -98.6.

Table 5-2. Data for Competitive Determination of k_H (nBu_3SnH) / k_{add} (Styrene) for 2,2-Difluorohex-1-yl Radical (**88**).

[**92**]	[$C_6H_5CH=CH_2$]	[nBu_3SnH] / [$C_6H_5CH=CH_2$]	[**93**] / [**98**]	% Yield
0.087	4.08	0.223	5.96	96
0.087	3.97	0.243	6.62	98
0.087	3.85	0.263	7.16	97
0.087	3.73	0.285	7.79	98
0.087	3.62	0.308	8.33	97
0.087	3.50	0.333	9.01	100

Slope = k_H / k_{add} = 27.3 ± 0.6

k_H (nBu_3SnH) = 1.4 (± 0.5) x 10^7 M^{-1} s^{-1}

1,1,2,2-Tetrafluorohex-1-yl Radical (**100**)

Ratios of [**108**] / [**110**] were obtained by the sum of integrals of the $-CF_2-$ and $-CF_2H$ resonances of **108** (at ϕ -117.1 and -136.1, respectively) versus that of the two $-CF_2-$ resonances of **110** (at ϕ -116.0 and -116.4, respectively).

Table 5-3. Data for Competitive Determination of k_H (nBu_3SnH) / k_{add} (Styrene) for 1,1-2,2-Tetrafluorohex-1-yl Radical (**100**).

[**102**]	[$C_6H_5CH=CH_2$]	[nBu_3SnH] / [$C_6H_5CH=CH_2$]	[**108**] / [**110**]	% Yield
0.085	1.86	0.506	2.33	98
0.085	1.68	0.611	2.90	97
0.085	1.49	0.741	3.56	97
0.085	1.30	0.909	4.30	97
0.085	1.12	1.13	5.34	97
0.085	0.931	1.45	6.65	99

Slope = k_H / k_{add} = 4.56 ± 0.10

k_H (nBu_3SnH) = 9.2 (± 0.8) x 10^7 M^{-1} s^{-1}

Table 5-4. Data for Competitive Determination of k_H ($(TMS)_3SiH$) / k_{add} (Styrene) for 1,1-2,2-Tetrafluorohex-1-yl Radical (**100**).

[**102**]	[$C_6H_5CH=CH_2$]	[$(TMS)_3SiH$] / [$C_6H_5CH=CH_2$]	[**108**] / [**110**]	% Yield
0.074	1.29	0.988	1.10	90
0.074	1.19	1.11	1.20	92
0.074	1.08	1.26	1.32	93
0.074	0.970	1.44	1.52	94
0.074	0.863	1.67	1.71	92
0.074	0.755	1.96	1.98	95

Slope = k_H / k_{add} = 0.913 ± 0.017.

k_H ($(TMS)_3SiH$) = 1.8 (±0.1) x 10^7 M^{-1} s^{-1}

2-[Perfluorohexyl]eth-1-yl Radical (**111**)

Ratios of **[113] / [117]** were determined by integration of the respective $-CF_2-$ resonances at ϕ -117.1 and -115.0.

Table 5-5. Data for Competitive Determination of k_H (nBu_3SnH) / k_{add} (Styrene) for 2-[Perfluorohexyl]eth-1-yl Radical (**111**).

[**112**]	[$C_6H_5CH=CH_2$]	[nBu_3SnH] / [$C_6H_5CH=CH_2$]	[**113**] / [**117**]	% Yield
0.064	2.96	0.217	3.11	100
0.064	2.83	0.248	3.58	100
0.064	2.69	0.283	4.13	100
0.064	2.56	0.320	4.72	100
0.064	2.42	0.362	5.44	100
0.064	2.29	0.408	6.14	100

Slope = k_H / k_{add} = 16.0 $\pm$ 0.1

k_H (nBu_3SnH) = 2.1 ($\pm$ 0.3) x 10^6 M^{-1} s^{-1}

Pentafluoroethyl Radical (**118**)

Ratios of **120 / 122** were determined the sum of integrals of the CF_3- and $-CF_2H$ resonances of **120** (at ϕ -86.6 and -138.6, respectively) versus that of the CF_3- and $-CF_2-$ resonances of **122** (at ϕ -86.1 and -119.2, respectively).

Table 5-6. Data for Competitive Determination of k_H (nBu_3SnH) / k_{add} (Styrene) for Pentafluoroethyl Radical (**118**).

[**119**]	[$C_6H_5CH=CH_2$]	[nBu_3SnH] / [$C_6H_5CH=CH_2$]	[**120**] / [**122**]	% Yield
0.082	2.20	0.434	1.15	89
0.082	2.08	0.485	1.31	85
0.082	1.96	0.542	1.46	85
0.082	1.84	0.608	1.62	82
0.082	1.71	0.682	1.79	83

Table 5-6-- continued

[**119**]	[$C_6H_5CH=CH_2$]	[nBu_3SnH] / [$C_6H_5CH=CH_2$]	[**120**] / [**122**]	% Yield
0.082	1.59	0.768	2.05	83

Slope = k_H / k_{add} = 2.62 ± 0.06

k_H (nBu_3SnH) = 3.2 (± 0.3) x 10^8 M^{-1} s^{-1}

1,1-Difluorohex-5-en-1-yl Radical (**128**)

Ratios of **136** to **138** were determined by integration of the -CF_2H resonance of **136** (at ϕ -116.2) versus the sum of integrals for the diastereotopic -CF_2- resonances of **138** (at ϕ -100.3 and -107.8) in the ^{19}F NMR.

Table 5-7. Data for Competitive Determination of k_H (nBu_3SnH) / k_{C5} for 1,1-Difluorohex-5-en-1-yl Radical (**128**).

[**135**]	[nBu_3SnH]	[**136**] / [**138**]	% Yield
0.054	0.673	1.53	88
0.054	0.807	1.91	100
0.054	0.942	2.28	89
0.054	1.08	2.57	94
0.054	1.21	2.93	95
0.054	1.35	3.29	92

Slope = k_H / k_{C5} = 2.57 ± 0.05.

k_{C5} = 3.5 (± 0.6) x 10^6 s^{-1}

2,2-Difluorohex-5-en-1-yl Radical (**140**)

Ratios of **145** to **147** and **145** to **149** were determined by integration of the -$CH_2CF_2CH_3$ resonance of **145** (at ϕ -91.5) versus the sum of integrals for the diastereotopic -CF_2- resonances of **147** (at ϕ -88.9 and -90.4) and the -CF_2- resonance of **149** (at ϕ -95.8) in the ^{19}F NMR.

Table 5-8. Data for Competitive Determination of k_H (nBu_3SnH) / k_{C5} and k_H (nBu_3SnH) / k_{C6} for 2,2-Difluorohex-5-en-1-yl Radical (**140**).

[**144**]	[nBu_3SnH]	[**145**] / [**147**]	[**145**] / [**149**]	% Yield
0.053	0.286	2.64	24.3	98
0.053	0.343	3.40	30.9	100
0.053	0.400	4.03	37.8	100
0.053	0.457	4.71	48.2	99
0.053	0.514	5.44	54.4	98
0.053	0.572	6.26	61.1	98

For C_5: Slope = k_H / k_{C5} = 12.5 ± 0.2.

k_{C5} = 1.1 (± 0.38) x 10^6 s^{-1}

For C_6: Slope = k_H / k_{C6} = 132 ± 5.

k_{C6} = 1.1 (± 0.34) x 10^5 s^{-1}

1,1,2,2-Tetrafluorohex-5-en-1-yl Radical (**152**)

Ratios of **153** to **155** and **153** to **157** were determined by the sum of integrals of the $-CF_2-$ and $-CF_2H$ resonances of **153** (at ϕ -116.7 and -135.9, respectively) versus the sum of integrals for the diastereotopic $-CF_2-$ resonances of **155** (at ϕ -109.9, -120.8, -126.0, and -132.9) and the $-CF_2-$ resonance of **157** (at ϕ -119.6, for k_{C6}) in the ^{19}F NMR.

Table 5-9. Data for Competitive Determination of k_H ($(TMS)_3SiH$) / k_{C5} and k_H ($(TMS)_3SiH$) / k_{C6} for 1,1,2,2-Tetrafluorohex-5-en-1-yl Radical (**152**).

[**101**]	[$(TMS)_3SiH$]	[**153**] / [**155**]	[**153**] / [**157**]	% Yield
0.052	0.581	0.988	4.35	96
0.052	0.686	1.19	5.28	95
0.052	0.792	1.44	6.39	94
0.052	0.897	1.67	7.36	95
0.052	1.00	1.84	8.21	98
0.052	1.11	2.11	9.37	99

For C_5: Slope = k_H / k_{C5} = 2.11 ± 0.05.

k_{C5} = 8.7 (± 0.41) x 10^6 s^{-1}

For C_6: Slope = k_H / k_{C6} = 9.44 ± 0.14.

k_{C6} = 1.9 (± 0.11) x 10^6 s^{-1}

APPENDIX A

SELECTED ^{19}F NMR SPECTRA

The ^{19}F NMR spectra of radical precursors, a representative sample from each kinetic run, and isolated products of addition, hydrogen abstraction, and cyclization are graphically illustrated in this appendix. Full spectral characterization data are presented numerically in their respective areas of Chapter 5.

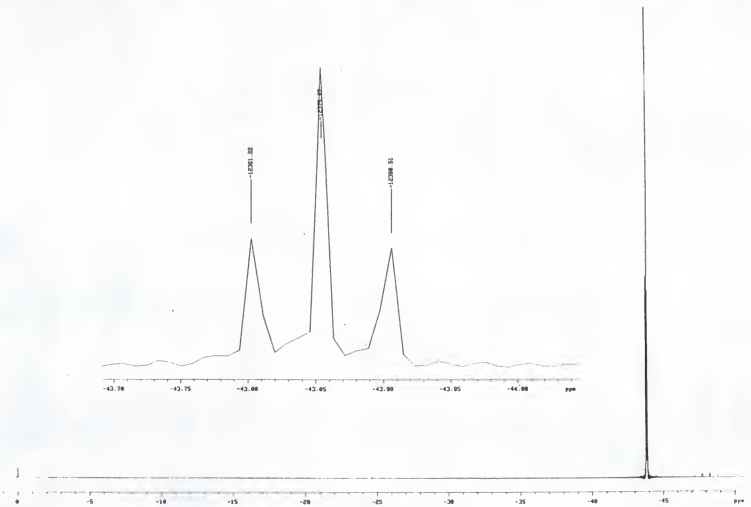

Figure A-1. 1-Bromo-1,1-difluorohexane (**80**).

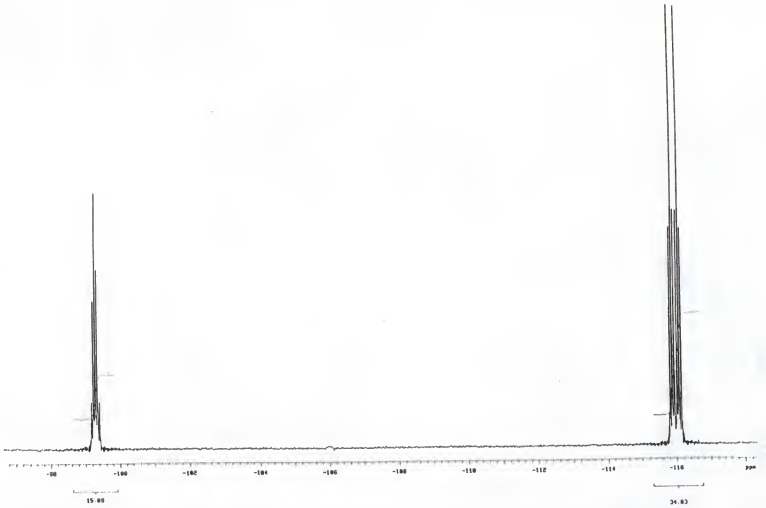

Figure A-2. Data Point 1 of k_H / k_{add} Determination for 1,1-Difluorohex-1-yl Radical (**77**).

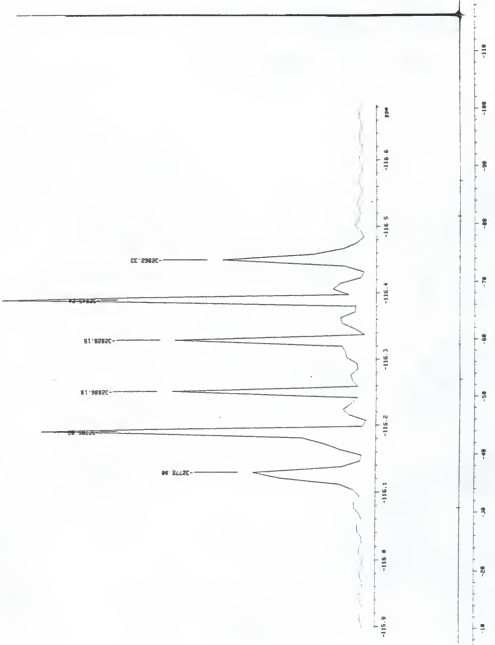

Figure A-3. 1,1-Difluorohexane (**81**).

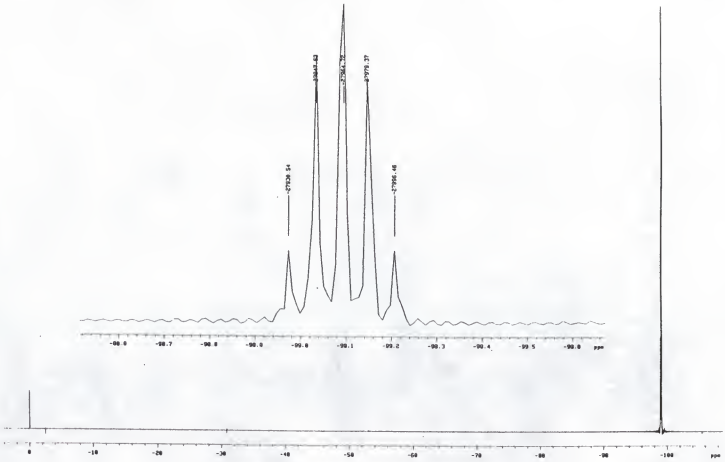

Figure A-4. 3,3-Difluoro-1-phenyloctane (**83**).

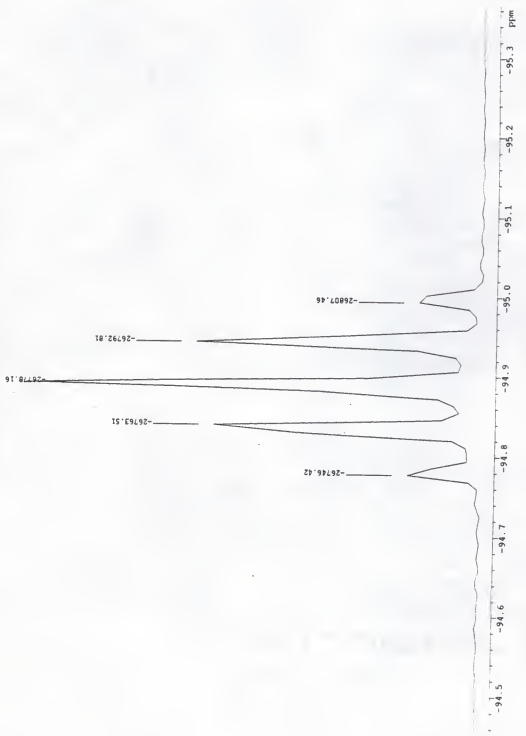

Figure A-5. 1-Iodo-2,2-difluorohexane (**92**).

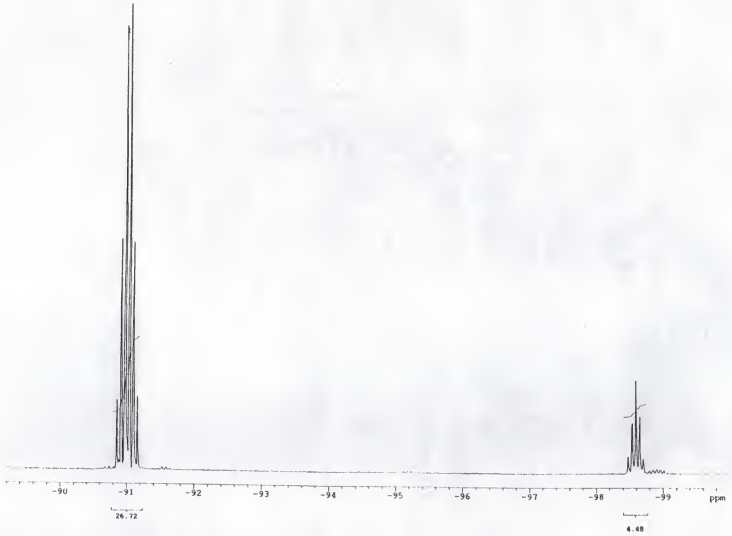

Figure A-6. Data Point 1 of k_H / k_{add} Determination for 2,2-Difluorohex-1-yl Radical (**88**).

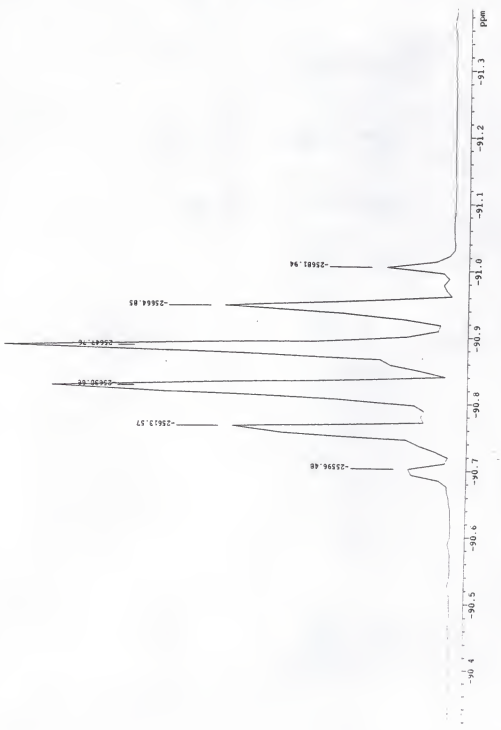

Figure A-7. 2,2-Difluorohexane (**93**).

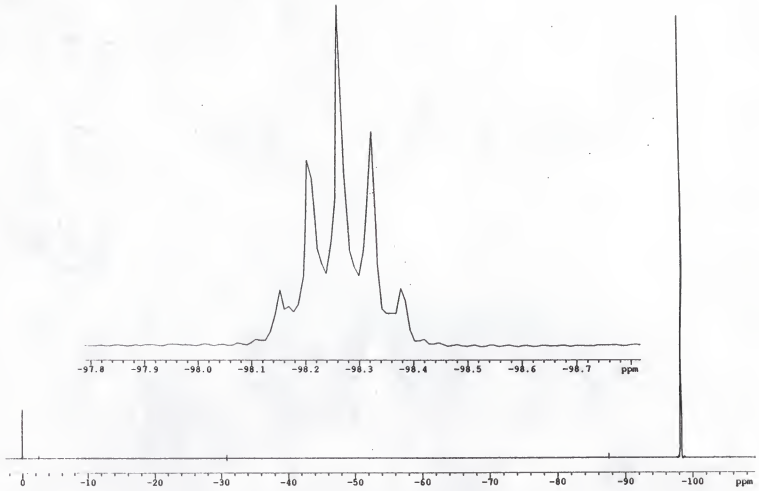

Figure A-8. 4,4-Difluoro-1-phenyloctane (**98**).

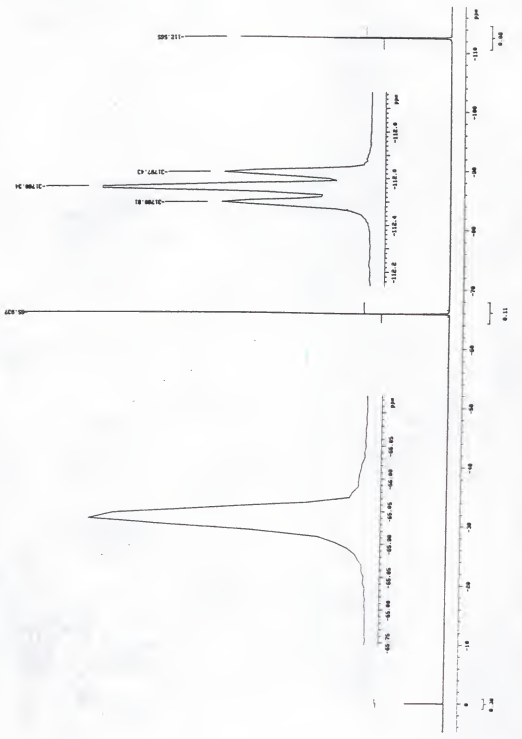

Figure A-9. 1-Bromo-1,1,2,2-tetrafluorohexane (**102**).

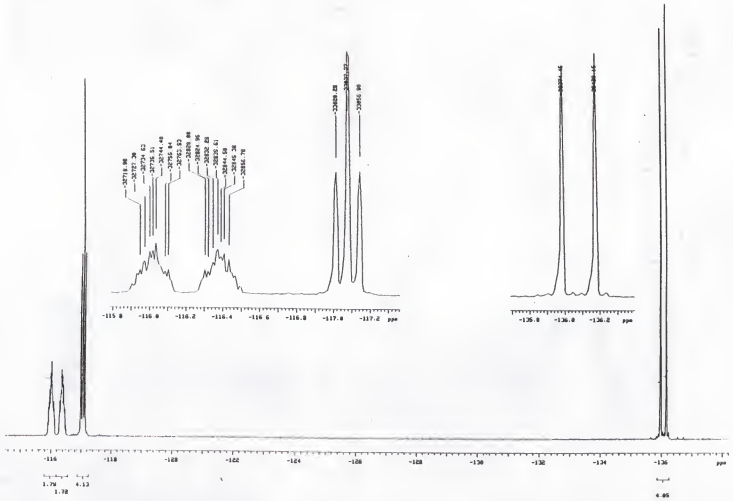

Figure A-10. Data Point 1 of k_H / k_{add} Determination for 1,1,2,2-Tetrafluorohex-1-yl Radical (**100**).

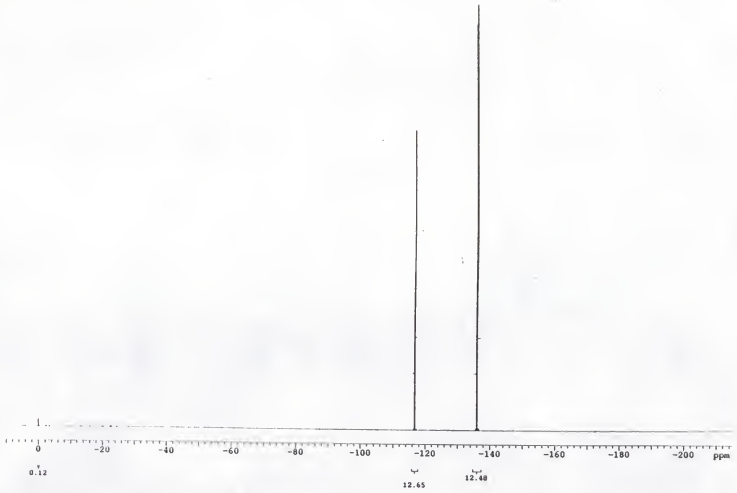

Figure A-11. 1,1,2,2-Tetrafluorohexane (**108**).

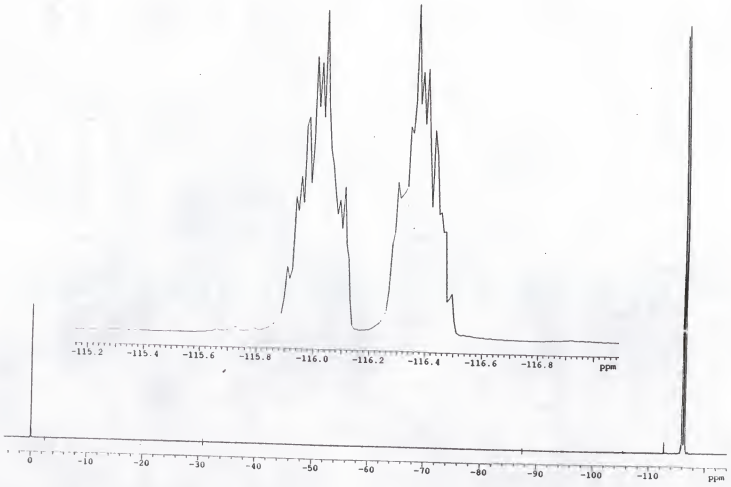

Figure A-12. 3,3,4,4-Tetrafluoro-1-phenyloctane (**110**).

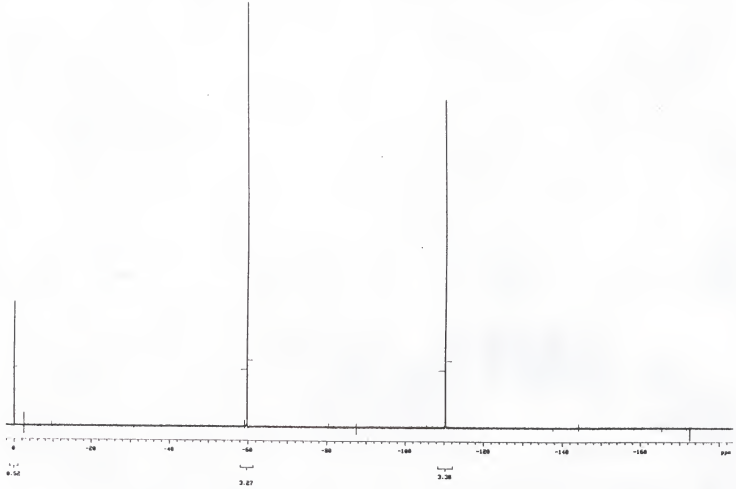

Figure A-13. 1,1,2,2-Tetrafluoro-1-iodobutane (**107**).

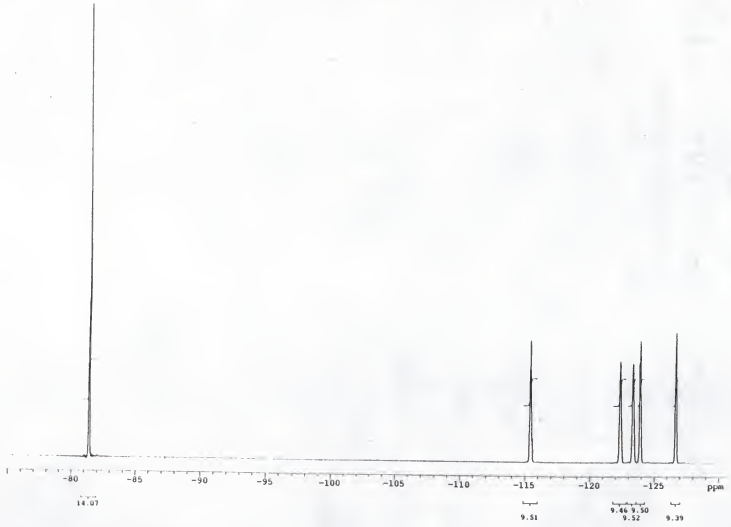

Figure A-14. I-Iodo-2-[perfluorohexyl]ethane (**112**).

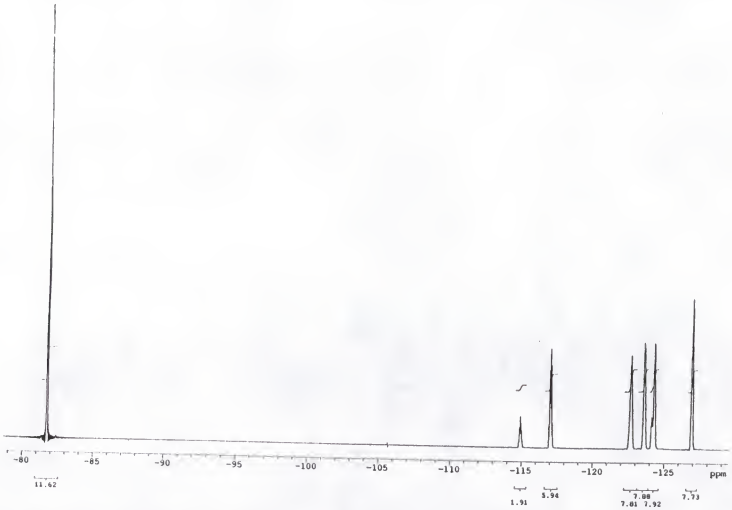

Figure A-15. Data Point 1 of k_H / k_{add} Determination for 2-[Perfluorohexyl]eth-1-yl Radical (**111**).

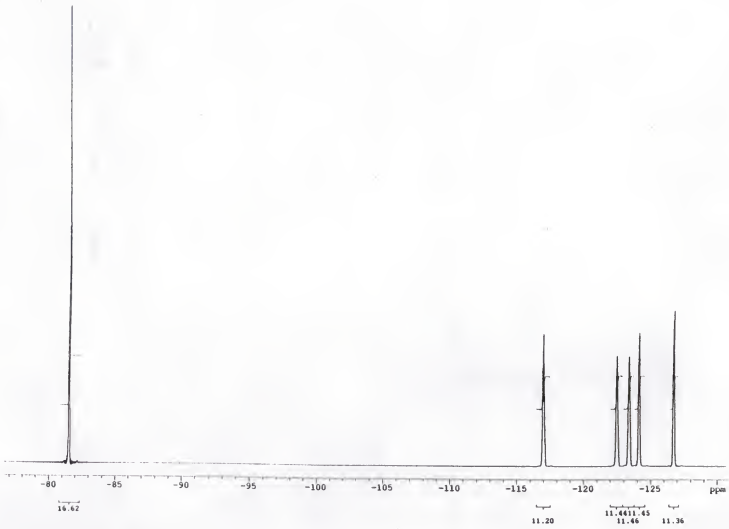

Figure A-16. 1-[Perfluorohexyl]ethane (**113**).

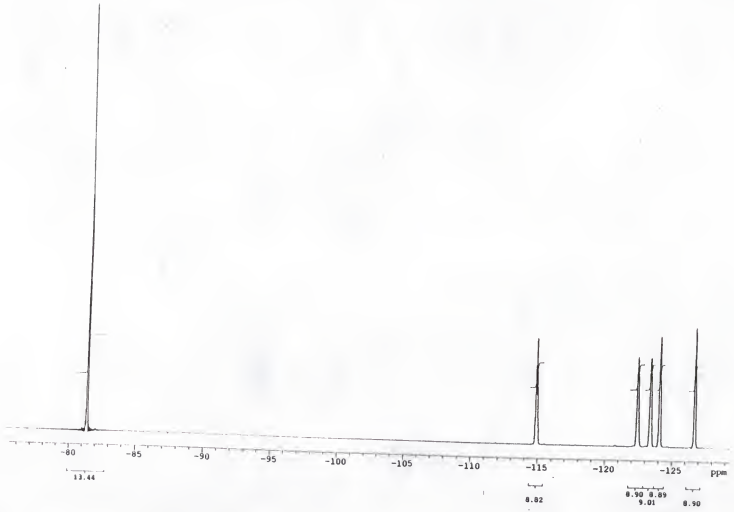

Figure A-17. 1-[Perfluorohexyl]-4-phenylbutane (**117**).

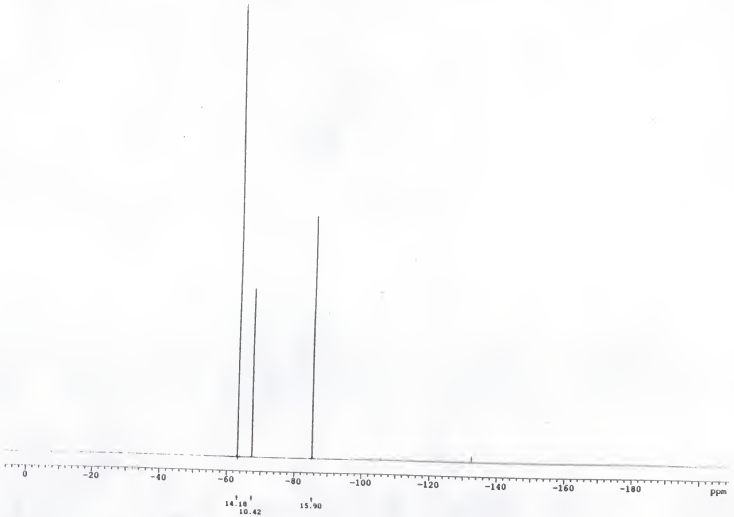

Figure A-18. Iodopentafluoroethane (**119**).

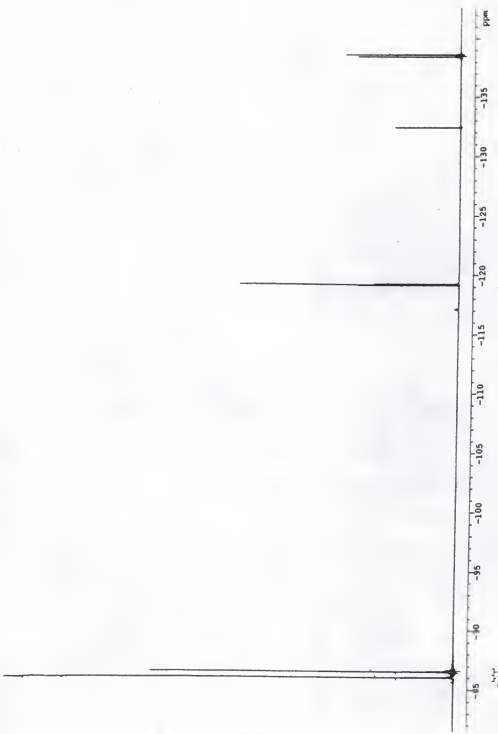

Figure A-19. Data Point 1 of k_H / k_{add} Determination for Pentafluoroethyl Radical (**118**).

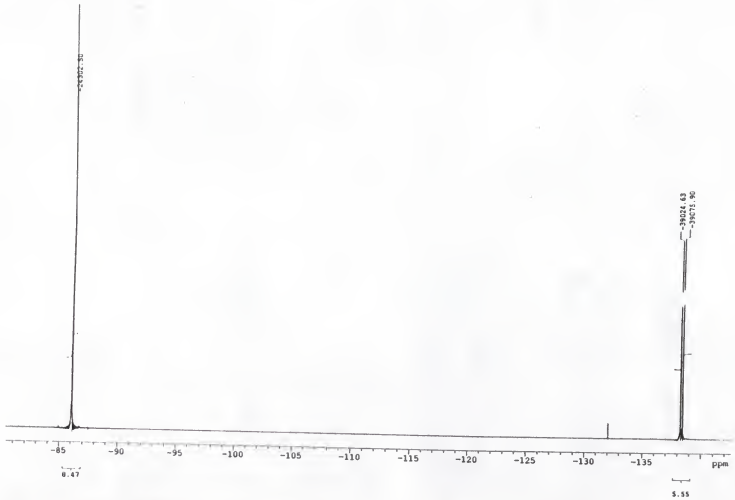

Figure A-20. Pentafluoroethane (**120**).

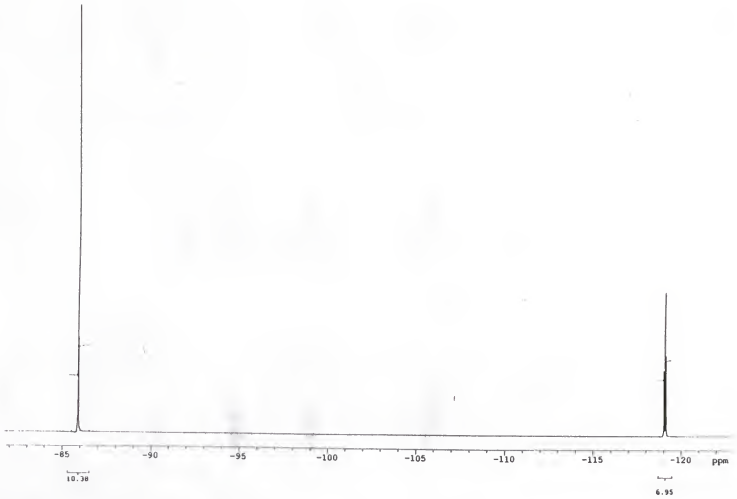

Figure A-21. 1,1,1,2,2-Pentafluoro-4-phenylbutane (**122**).

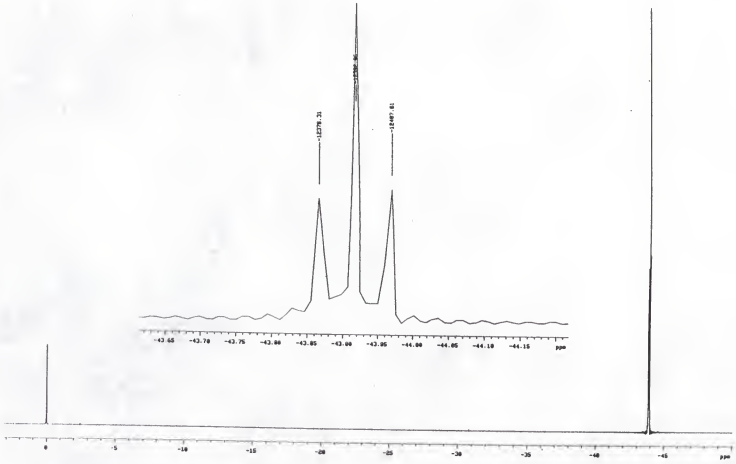

Figure A-22. 6-Bromo-6,6-difluorohex-1-ene (**135**).

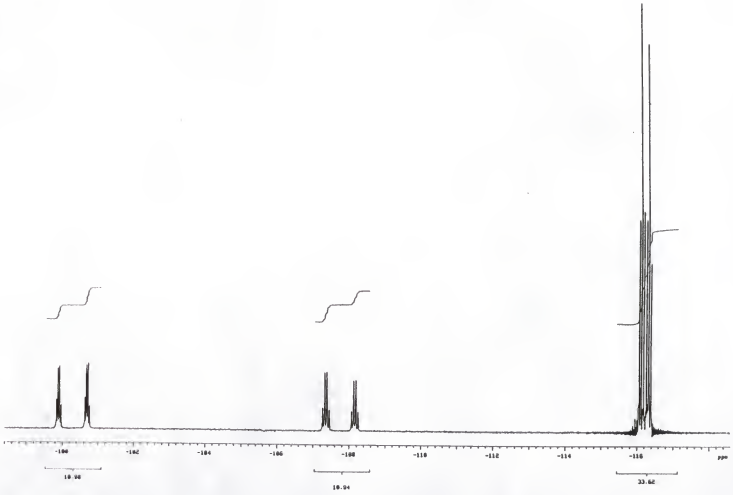

Figure A-23. Data Point 1 of k_H / k_C Determination for 1,1-Difluorohex-5-en-1-yl Radical (**128**).

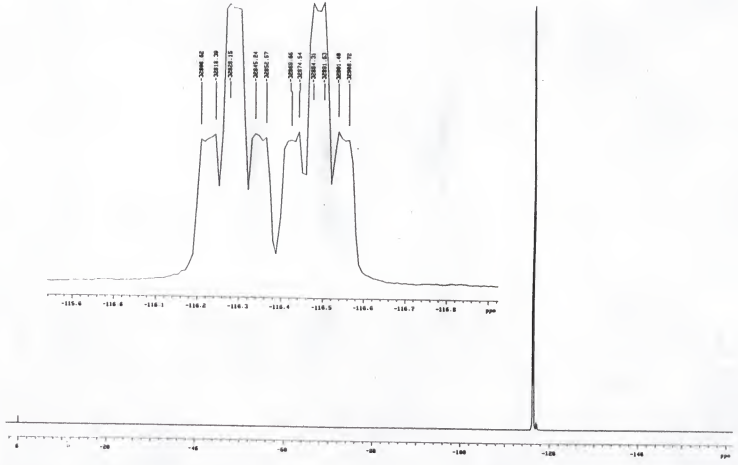

Figure A-24. 6,6-Difluorohex-1-ene (**136**).

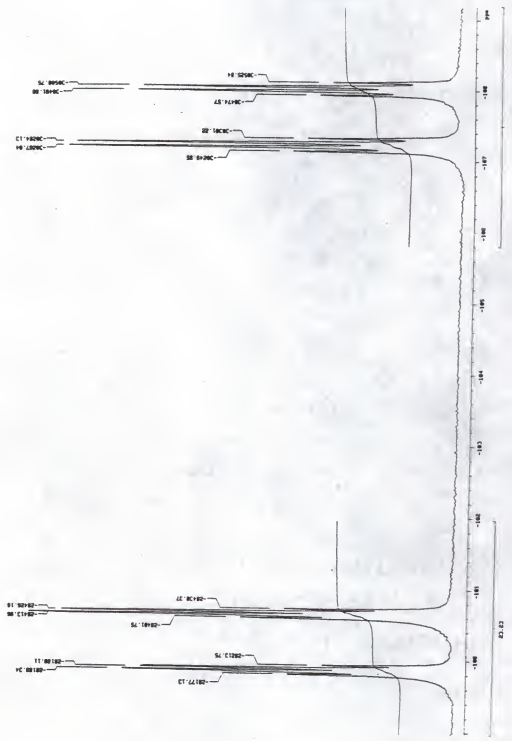

Figure A-25. 1,1-Difluoro-2-methylcyclopentane (**138**).

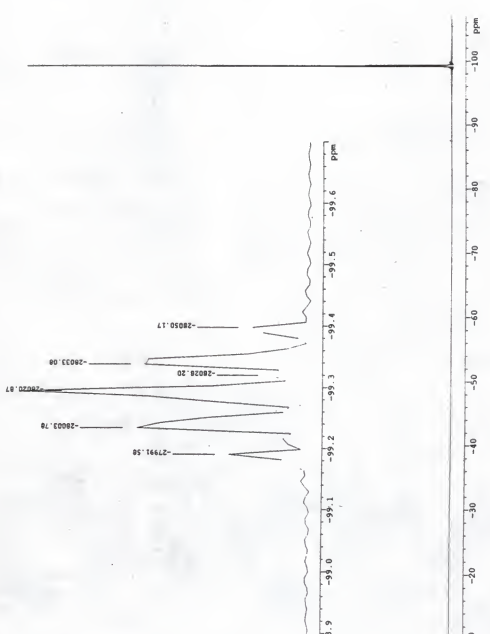

Figure A-26. 6-Bromo-5,5-difluorohex-1-ene (**144**).

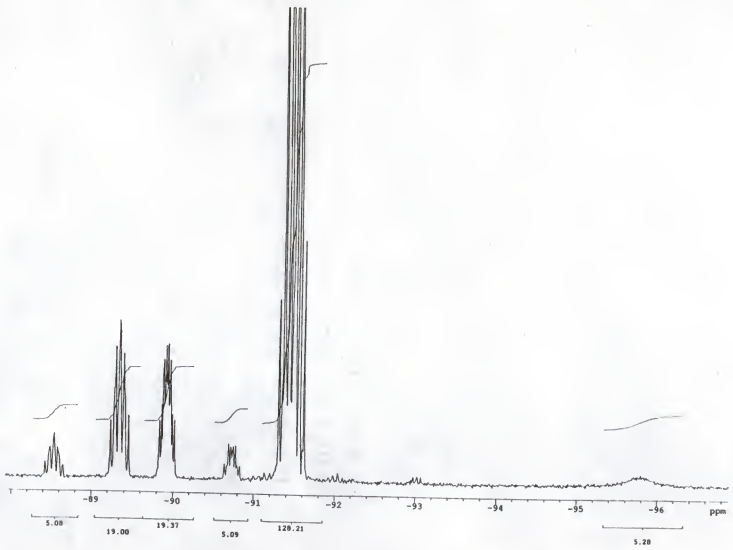

Figure A-27. Data Point 1 of k_H / k_C Determination for 2,2-Difluorohex-5-en-1-yl Radical (**140**).

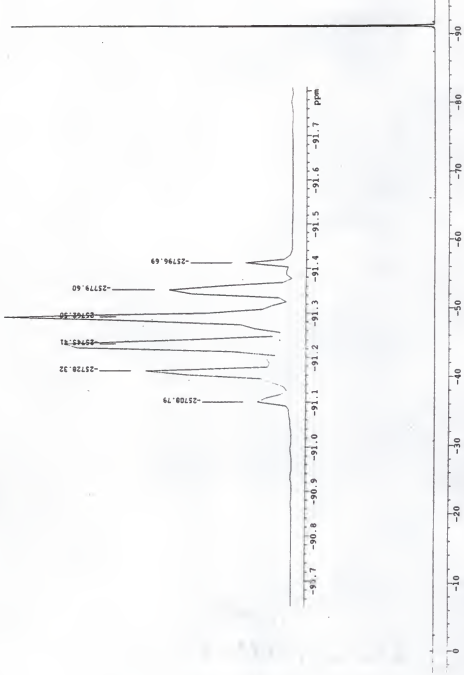

Figure A-28. 5,5-Difluorohex-1-ene (**145**).

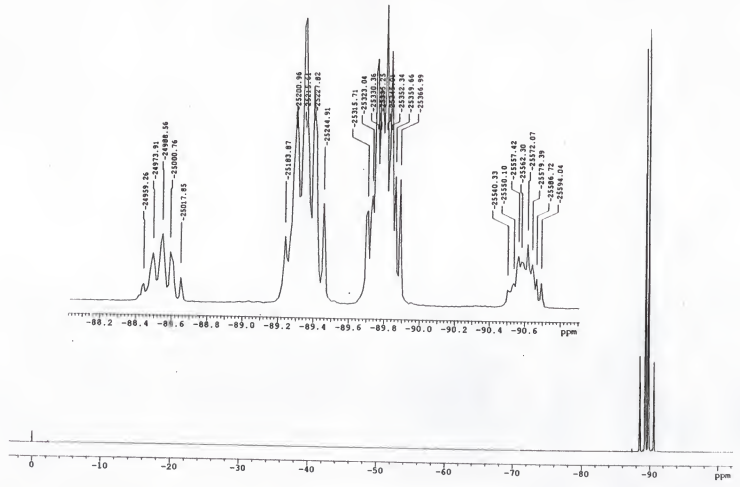

Figure A-29. 1,1-Difluoro-3-methylcyclopentane (**147**).

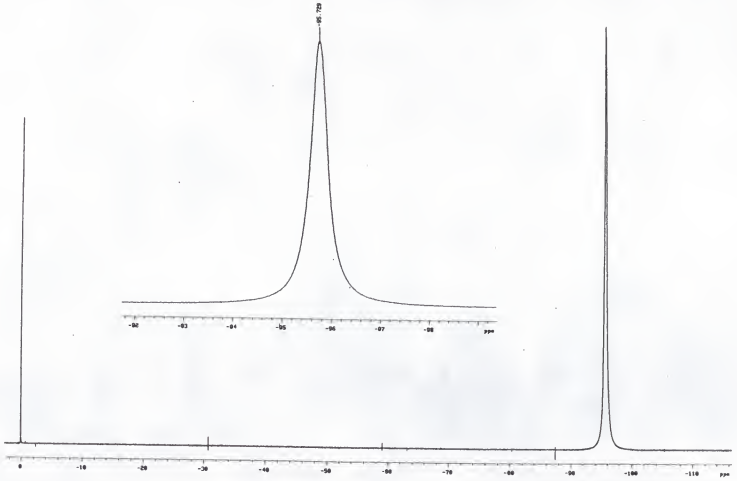

Figure A-30. 1,1-Difluorocyclohexane (**149**).

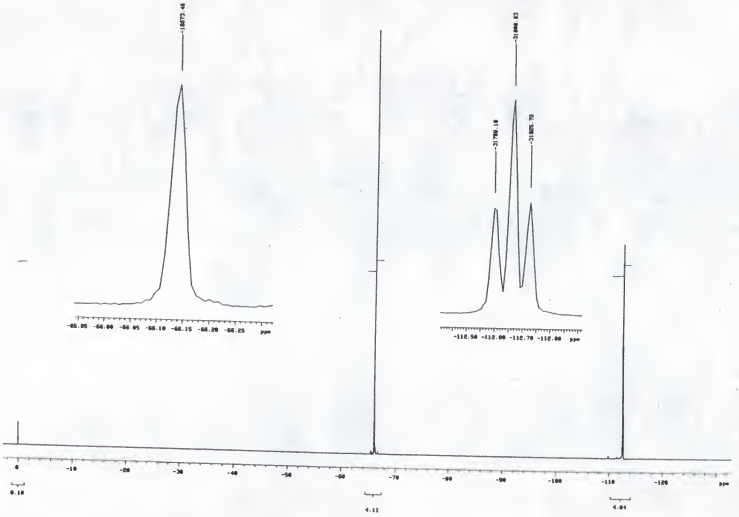

Figure A-31. 6-Bromo-5,5,6,6-tetrafluorohex-1-ene (**101**).

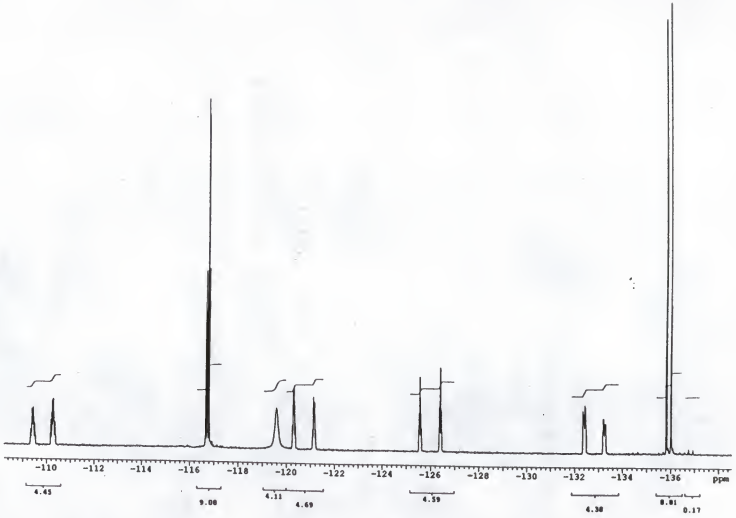

Figure A-32. Data Point 1 of k_H / k_C Determination for 1,1,2,2-Tetrafluorohex-5-en-1-yl Radical (**152**).

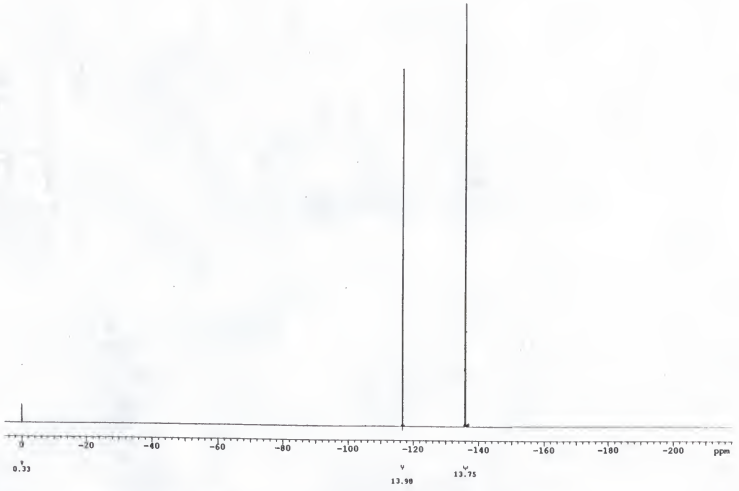

Figure A-33. 5,5,6,6-Tetrafluorohex-1-ene (**153**).

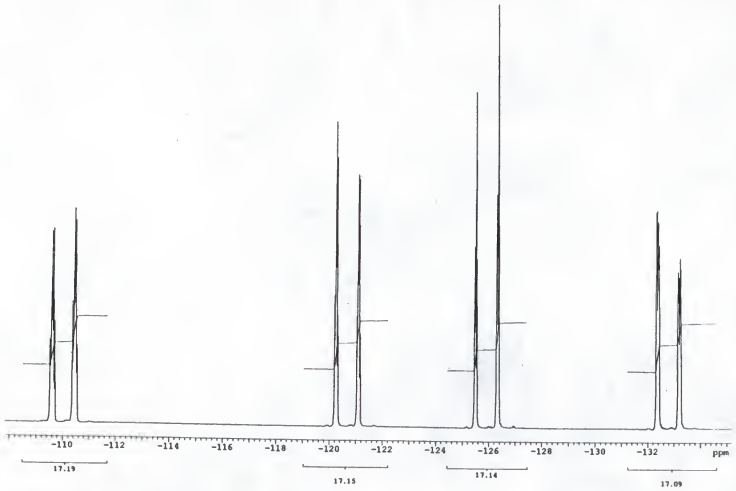

Figure A-34. 1,1,2,2-Tetrafluoro-3-methylcyclopentane (**155**).

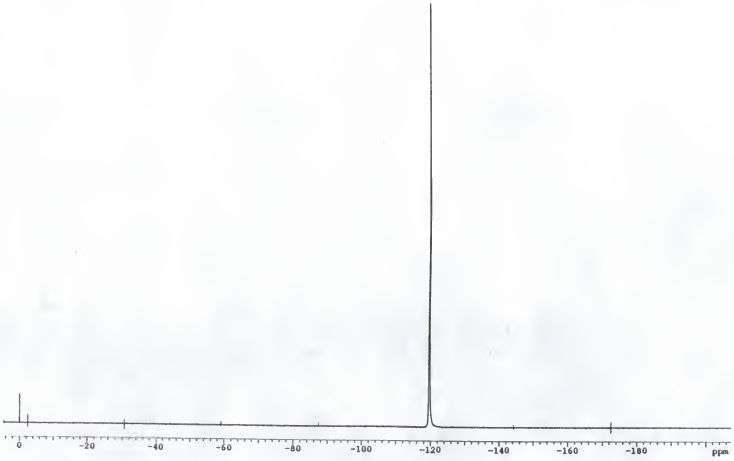

Figure A-35. 1,1,2,2-Tetrafluorocyclohexane (**157**).

APPENDIX B

B3LYP/6-31G(d) TOTAL AND ZERO-POINT ENERGIES
FOR DATA IN TABLES 3-3 AND 3-4

The total electronic and unscaled zero-point energies for hydrofluorocarbon radicals and closed shell species used in the determination of the bond dissociation energies reported in Tables 3-3 and 3-4 are provided in this appendix. In instances where more than one conformer is provided, that of lowest energy was used in the C-C and C-H BDE computation.

Table B-1. Total and (Unscaled) Zero-Point Energies for Fluorinated Alkanes.

Species	E(B3LYP/6-31G(d)), a.u.	ZPE, a.u.
CH_3CH_3	-79.8304 167	0.075231
CH_3CF_3	-377.5549 235	0.052872
CH_3CF_2H	-278.3015 940	0.061076
CF_3CF_2H	-576.0077 790	0.037905
$CH_3CH_2CH_3$	-119.1442 464	0.104110
$CH_3CF_2CH_3$	-317.6263 447	0.088479
$CF_3CH_2CH_3$	-416.8699 039	0.081649
$CF_3CF_2CH_3$	-615.3356 199	0.065266
$CH_3CH_2CF_2H$ [a]	-317.6163 135	0.089851
$CH_3CH_2CF_2H$ [b]	-317.6162 650	0.090006
$CH_3CF_2CF_2H$ [b]	-516.0884 655	0.073687
$CH_3CF_2CF_2H$ [a]	-516.0853 571	0.073705
$CH_3CH_2CH_2CH_3$ [c]	-158.4580 400	0.132860

Table B-1-- continued

Species	E(B3LYP/6-31G(d)), a.u.	ZPE, a.u.
$CH_3CH_2CH_2CH_3$ [d]	-158.4567 065	0.132957
$CH_3CH_2CF_2CH_3$ [c]	-356.9408 361	0.117249
$CH_3CH_2CF_2CH_3$ [d]	-356.9401 189	0.117349
$CH_3CF_2CF_2CH_3$ [c]	-555.4151 664	0.101158
$CH_3CF_2CF_2CH_3$ [d]	-555.4110 960	0.101141
$CF_3CH_2CH_2CH_3$ [c]	-456.1836 478	0.110224
$CF_3CH_2CH_2CH_3$ [d]	-456.1826 866	0.110445

[a] Methyl and Hydrogen Gauche. [b] Methyl and Hydrogen Anti. [c] Methyl (or Methyl and Trifluoromethyl) Groups Anti. [d] Methyl (or Methyl and Trifluoromethyl) Groups Gauche.

Table B-2. Total and (Unscaled) Zero-Point Energies for Fluorinated Radicals.

Species	E(B3LYP/6-31G(d)), a.u.	ZPE, a.u.
H·	-0.5002 728	0
CH_3·	-39.8382 909	0.029849
CF_3·	-337.5509 879	0.012153
CH_3CH_2·	-79.1578 663	0.059647
CH_3CF_2·	-277.6352 216	0.047481
CF_3CH_2·	-376.8760 847	0.037830
CF_3CF_2·	-575.3382 007	0.024522
$CH_3CH_2CH_2$· [a]	-118.4713 699	0.088731
$CH_3CH_2CH_2$· [b]	-118.4711 179	0.088945
$CH_3CH_2CF_2$· [b]	-316.9496 940	0.076574
$CH_3CH_2CF_2$· [a]	-316.9496 712	0.076368
$CH_3CF_2CH_2$· [c]	-316.9493 447	0.073435
$CH_3CF_2CH_2$· [b]	-316.9489 182	0.073225

Table B-2-- continued

Species	E(B3LYP/6-31G(d)), a.u.	ZPE, a.u.
$CH_3CF_2CF_2^{\cdot}$ [b]	-515.4178 170	0.060271
$CH_3CF_2CF_2^{\cdot}$ [c]	-515.4173 201	0.060276
$CF_3CH_2CH_2^{\cdot}$ [a]	-416.1952 103	0.066154
$CF_3CH_2CH_2^{\cdot}$ [b]	-416.1951 213	0.066242

[a] Radical p Orbital Aligned with β C-H Bond. [B] β C-C Bond Alignment. [C] β C-F bond alignment.

REFERENCES

1. Gomberg, M. *J. Am. Chem. Soc.* **1900**, *22*, 757.
2. Waters, W. A. *The Chemistry of Free Radicals*; Clarendon Press: Oxford, **1946**.
3. Walling, C. *Free Radicals in Solution*; Wiley: New York, **1957**.
4. *Free Radicals*; Kochi, J. K., Ed.; Wiley: New York, **1973**.
5. Kharasch, M. S.; Jensen, E. V.; Urry, W. H. *Science* **1945**, *102*, 128.
6. Kharasch, M. S.; Jensen, E. V.; Urry, W. H. *J. Am. Chem. Soc.* **1946**, *68*, 1100.
7. Kharasch, M. S.; Jensen, E. V.; Urry, W. H. *J. Am. Chem. Soc.* **1947**, *69*, 1105.
8. Beckwith, A. L. J. *Chem. Soc. Rev.* **1993**, 143.
9. Hart, D. J. *Science* **1984**, *223*, 883.
10. Giese, B. *Radicals in Organic Synthesis: Formation of Carbon-Carbon Bonds*; Pergamon Press: Oxford, **1986**.
11. Curran, D. P. *Synthesis* **1988**, 417.
12. Curran, D. P. *Synthesis* **1988**, 489.
13. Jasperse, C. P.; Curran, D. P.; Feviz, T. L. *Chem. Rev.* **1991**, *91*, 1237.
14. Dowd, P.; Zhang, W. *Chem. Rev.* **1993**, *93*, 2091.
15. Stork, G. In *Selectivity– A Goal for Synthetic Efficiency*; Bartmann, W., Trost, B. M., Eds.; Verlag Chemie: Basel, **1984**.
16. Newcomb, M. *Tetrahedron* **1993**, *49*, 1151.
17. Kuivila, H. G. *Accts. Chem. Res.* **1968**, *1*, 299.
18. Neumann, W. P. *Synthesis* **1987**, 665.
19. Tedder, J. M.; Walton, J. C. *Accts. Chem. Res.* **1976**, *9*, 183.
20. Benson, S. W. *Thermochemical Kinetics*; Wiley: New York, **1973**.
21. Fischer, H. In *Substituent Effects in Radical Chemistry*; Viehe, H. G., Janousek, Z., Merényi, R., Eds.; Reidel: Dordrecht; **1986**; NATO ASI Series C, *189*, 123.

22. Beckwith, A. L. J.; Pigou, P. E. *Aust. J. Chem.* **1986**, *39*, 77.

23. Chatgilialoglu, C. *Accts. Chem. Res.* **1992**, *25*, 188.

24. Fukui, K. *Fortsch. Chem. Forsch.* **1970**, *15*, 1.

25. Fleming, I. *Frontier Orbitals and Organic Chemical Reactions*; Wiley: London, **1976**.

26. Burkey, T. J.; Majewski, M.; D. *J. Am. Chem. Soc.* **1986**, *108*, 2218.

27. Chatgilialoglu, C.; Ingold, K. U.; Scaiano, J. C. *J. Am. Chem. Soc.* **1981**, *103*, 7739.

28. Chatgilialoglu, C.; Dickhaut, J.; Giese, B. *J. Org. Chem.* **1991**, *56*, 6399.

29. Kanabus-Kaminska, J. M.; Hawari, J. A.; Griller, D.; Chatgililoglu, C. *J. Am. Chem. Soc.* **1987**, *109*, 5267.

30. Lusztyk, J.; Maillard, B.; Lindsay, D. A.; Ingold, K. U. *J. Am. Chem. Soc.* **1983**, *105*, 3578.

31. Clark, K. B.; Griller, D. *Organometallics* **1991**, *10*, 746.

32. Chatgilialoglu, C.; Guerrini, A.; Lucarini, M. *J. Org. Chem.* **1992**, *57*, 3405.

33. Franz, J. A.; Bushaw, B. A.; Alnajjar, M. S. *J. Am. Chem. Soc.* **1989**, *111*, 268.

34. Newcomb, M.; Manek, M. B. *J. Am. Chem. Soc.* **1990**, *112*, 9662.

35. Griller, D.; Kanabus-Kaminska, J. M.; Maccoll, A. *J. Mol. Struct.* **1988**, *163*, 125.

36. Chatgilialoglu, C.; Scaiano, J. C.; Ingold, K. U. *Organometallics* **1982**, *1*, 466.

37. Chatgilialoglu, C.; Ingold, K. U.; Lusztyk, J.; Nazran, A. S.; Scaiano, J. C. *Organometallics* **1983**, *2*, 1332.

38. Momillen, D. F.; Golden, D. M. *Ann. Rev. Phys. Chem.* **1982**, *33*, 493.

39. Hartung, J.; Gallou, F. *J. Org. Chem.* **1995**, *60*, 6706.

40. Laidler, K. *Chemical Kinetics*; Harper and Row: New York, **1987**.

41. Wong, M. W.; Radom, L. *J. Phys. Chem.* **1995**, *99*, 8582.

42. Lias, S. G.; Bartmess, J. E.; Liebman, J. F.; Holmes, J. L.; Levin, R. D.; Mallard, W. G. *J. Phys. Chem. Ref. Data* **1988**, *17*, Suppl. 1.

43. Hammond, G. S. *J. Am. Chem. Soc.* **1955**, *77*, 334.

44. Abell, P. I. In *Comprehensive Chemical Kinetics*; Bamford, C.H., Tipper, C. F. H., Eds.; Elsevier: Amsterdam, **1976**, *18*, Ch. 3, 111.

45. Hoyland, J. R. *Helv. Chim. Acta* **1971**, *22*, 229.

46. Houk, K. N.; Paddon-Row, M. N.; Spellmeyer, D. C.; Rondan, N. G.; Nagase, S. *J. Org. Chem.* **1986**, *51*, 2874.

47. Zipse, H.; He, J.; Houk, K. N.; Giese, B. *J. Am. Chem. Soc.* **1991**, *113*, 4324.

48. Wong, M. W.; Pross, A.; Radom, L. *J. Am. Chem. Soc.* **1994**, *116*, 6284.

49. Wong, M. W.; Pross, A.; Radom, L. *J. Am. Chem. Soc.* **1994**, *116*, 11938.

50. Houk, K. N. *Accts. Chem. Res.* **1975**, *8*, 361.

51. Héberger, K.; Walbiner, M.; Fischer, H. *Angew. Chem., Int. Ed. Engl.* **1992**, *31*, 635.

52. Tedder, J. M.; Walton, J. C. *Tetrahedron* **1980**, *36*, 701.

53. Riemenschneider, K.; Bartlels, H. M.; Dornow, R.; Drechsel-Grau, E.; Eichel, W.; Luthe, H.; Matter, Y. M.; Michaelis, W.; Boldt, P. *J. Org. Chem.* **1987**, *52*, 205.

54. Avila, D. V.; Ingold, K. U.; Lusztyk, J.; Dolbier, W. R., Jr.; Pan, H.-Q.; Muir, M. *J. Am. Chem. Soc.* **1994**, *116*, 99.

55. Giese, B.; He, J.; Mehl, W. *Chem. Ber.* **1988**, *121*, 2063.

56. Santi, R.; Bergamini, F.; Citterio, A.; Sebastiano, R.; Nicolini, M. *J. Org. Chem.* **1992**, *57*, 4250.

57. Beranek, I.; Fischer. In *Free Radicals in Synthesis and Biology*; Minisci, F., Ed.; Kluwer: Dordrecht, **1989**, NATO ASI Series C, *260*, 303.

58. Lamb, R. C.; Ayers, P. W.; Toney, M. K. *J. Am. Chem. Soc.* **1963**, *85*, 3483.

59. Baldwin, J. E. *J. Chem. Soc., Chem. Commun.* **1976**, 734.

60. Beckwith, A. L. J.; Moad, G. *J. Chem. Soc., Chem. Commun.* **1974**, 472.

61. Beckwith, A. L. J.; Ingold, K. U. In *Rearrangements in Ground and Excited States*; de Mayo, P., Ed.; Academic Press: New York, **1980**, *1*, Ch. 4, 161.

62. Bischof, P. *Helv. Chim. Acta* **1980**, *63*, 1434.

63. Beckwith, A. L. J.; Schiesser, C. H. *Tet. Lett.* **1985**, *26*, 373.

64. Beckwith, A. L. J.; Schiesser, C. H. *Tetrahedron* **1985**, *41*, 3925.

65. Canadell, E. *J. Chem. Soc., Perkin Trans II* **1985**, 1331.

66. Spellmeyer, D. C.; Houk, K. N. *J. Org. Chem.* **1987**, *52*, 959.

67. Della, E. W.; Knill, A. M. *Aust. J. Chem.* **1995**, *48*, 2047.

68. Hartung, J.; Stowasser, R.; Vitt, D.; Bringmann, G. *Angew. Chem. Int. Ed. Engl.* **1996**, *35*, 2820.

69. Capon, B.; Rees, C. W. *Ann. Rep. Chem. Soc.* **1964**, *61*, 221.

70. Beckwith, A. L. J.; Blair, I. A.; Phillipou, G. *Tet. Lett.* **1974**, 2251.

71. Beckwith, A. L. J.; Easton, C. J.; Lawrence, T.; Serelis, A. K. *Aust. J. Chem.* **1983**, *36*, 545.

72. Allinger, N. L.; Zalkow, J. *J. Org. Chem.* **1960**, *25*, 701.

73. Lusztyk, J.; Maillard, B.; Deycard, S.; Lindsay, D. A.; Ingold, K. U. *J. Org. Chem.* **1987**, *52*, 3509.

74. Park, S.-U.; Chung, S.-K.; Newcomb, M. *J. Am. Chem. Soc.* **1986**, *108*, 240.

75. Johnson, C. C.; Horner, J. H.; Tronche, C.; Newcomb, M. *J. Am. Chem. Soc.* **1995**, *117*, 1684,

76. Newcomb, M.; Horner, J. H.; Filipkowski, M. A.; Ha, C.; Park, S.-U. *J. Am. Chem. Soc.* **1995**, *117*, 3674.

77. Horner, J. H.; Martinez, F. N.; Musa, O. M.; Newcomb, M.; Shahin, H. *J. Am. Chem. Soc.* **1995**, *117*, 11124.

78. Khalil, S. M.; Jarjis, H. M. *Z. Naturforsch., Sec. A.* **1991**, *46*, 898.

79. Korth, H. G.; Lommes, P.; Sustmann, R. *J. Am. Chem. Soc.* **1984**, *106*, 663.

80. Pasto, D. J. *J. Am. Chem. Soc.* **1988**, *110*, 8164.

81. Walling, C.; Cioffari, A. *J. Am. Chem. Soc.* **1972**, *94*, 6064.

82. Julia, M.; Maumy, M. *Bull. Soc. Chim. Fr.* **1966**, 434.

83. Kazanis, S.; Azarani, A.; Johnston, L. *J. Phys. Chem.* **1991**, *95*, 4430.

84. Barton, D. H. R.; Crich, D.; Motherwell, W. B. *Tetrahedron* **1985**, *41*, 3901.

85. Avila, D. V.; Ingold, K. U.; Lusztyk, J.; Dolbier, W. R., Jr.; Pan, H.-Q. *J. Am. Chem. Soc.* **1993**, *115*, 1577.

86. Rong, X. X.; Pan, H.-Q.; Dolbier, W. R., Jr. *J. Am. Chem. Soc.* **1994**, *116*, 4521.

87. Dolbier, W. R., Jr.; Rong, X. X. *J. Fluorine Chem.* **1995**, *72*, 235.

88. Avila, D. V.; Ingold, K. U.; Lusztyk, J.; Dolbier, W. R., Jr.; Pan, H.-Q. *J. Org. Chem.* **1996**, *61*, 2027.

89. Dolbier, W. R., Jr.; Rong, X. X.; Smart, B. E.; Yang, Z.-U. *J. Org. Chem.* **1996**, *61*, 4824.

90. Dolbier, W. R., Jr. *Chem. Rev.* **1996**, *96*, 1557.

91. Bartberger, M. D.; Dolbier, W. R., Jr.; Lusztyk, J.; Ingold, K. U. *Tetrahedron* **1997**, *53*, 9857.

92. *The Chemist's Companion*; Gordon, A. J.; Ford, R. A.; Eds., Wiley: New York, **1972**.

93. Bondi, A. *J. Phys. Chem.* **1964**, *68*, 441.

94. Smart, B. E. In *Organofluorine Chemistry: Principles and Commercial Applications*; Banks, R. E., Smart, B. E., Tatlow, J. C., Eds.; Plenum: New York, **1994**, Ch. 3, 57.

95. Smart, B. E. In *Molecular Structure and Energetics*; Liebman, J. F., Greenberg, A., Eds.; VCH: Deerfield Beach, FL, **1986**, *3*, Ch. 4, 141.

96. Smart, B. E. In *The Chemistry of Functional Groups, Supplement D*; Part 2; Patai, S., Rappoport, Z., Eds.; Wiley: New York, **1983**, 603.

97. Smart, B. E. In *Chemistry of Organic Fluorine Compounds II: A Critical Review*; Hudlický, M., Pavlath, A. E., Eds.; ACS: Washington, **1995**, Ch. 6, 979.

98. Pauling, L. *The Nature of the Chemical Bond*; Cornell University Press: Ithaca, **1960**.

99. Radom, L.; Hehre, W. J.; Pople, J. A. *J. Am. Chem. Soc.* **1971**, *93*, 289.

100. Radom, L.; Stiles, P. J. *Tetrahedron Lett.* **1975**, 789.

101. Baird, N. C. *Can. J. Chem.* **1983**, *61*, 1567.

102. Typke, V.; Dakkouri, M;. Oberhammer, H. *J. Mol. Struct.* **1978**, *44*, 85.

103. Harmony, M. D.; Laurie, V. W.; Kuczkowski, R. L.; Schwendeman, R. H.; Ramsay, D. A.; Lovas, F. J.; Lafferty, W. J.; Maki, A. G. *J. Phys. Chem. Ref. Data* **1979**, *8*, 619.

104. Wiberg, K. B.; Rablen, P. R. *J. Am. Chem. Soc.* **1993**, *115*, 614.

105. Bock, C. W.; George, P.; Mains, G. J.; Trachtman, M. *J. Chem. Soc. Perkin Trans II* **1979**, 814.

106. Facelli, J. C.; Contreras, R. H. *Z. Naturforsch.* **1980**, *35A*, 1350.

107. Bak, B.; Kierkegaard, C.; Pappas, J.; Skaarup, S. *Acta Chem. Scand.* **1973**, *27*, 363.

108. Bernett, W. A. *J. Org. Chem.* **1969**, *34*, 1772.

109. Kollman, P. J. *J. Am. Chem. Soc.* **1974**, *96*, 4363.

110. Epiotis, N. D.; Cherry, W. R.; Shaik, S.; Yates, R. L.; Bernardi, F. *Top. Curr. Chem.* **1977**, *70*, 1.

111. Epiotis, N. D.; Larson, J. R.; Eaton, H. L. *Unified Valence Bond Theory of Electronic Structure*; Springer-Verlag: New York, **1982**, Lecture Notes in Chemistry, *29*.

112. Brundle, C. R.; Robin, M. B.; Kuebler, N. A.; Basch, H. *J. Am. Chem. Soc.* **1972**, *94*, 1451.

113. Chiu, N. S.; Burrow, P. D.; Jordan, K. D. *Chem. Phys. Lett.* **1979**, *68*, 121.

114. Dolbier, W. R.; Jr.; Medinger, K. S. *Tetrahedron* **1982**, *38*, 2415.

115. Chambers, R. D. *Fluorine in Organic Chemistry*; Wiley: New York, **1973**.

116. Bernardi, F.; Mangini, A.; Epiotis, N. D.; Larson, J. R.; Shaik, S. *J. Am. Chem. Soc.* **1977**, *99*, 7465.

117. Blint, R. J.; McMahon, T. B.; Beauchamp, J. L. *J. Am. Chem. Soc.* **1974**, *96*, 1269.

118. Williams, A. D.; Le Breton, P. R.; Beauchamp, J. L. *J. Am. Chem. Soc.* **1976**, *98*, 2705.

119. Olah, G. A.; Mo. Y. K. *Adv. Fluorine Chem.* **1973**, *7*, 69.

120. Prochaska, F. T.; Andrews, L. *J. Am. Chem. Soc.* **1978**, *100*, 2102.

121. Olah, G. A.; Heiliger, L.; Prakash, G. K. S. *J. Am. Chem. Soc.* **1989**, *111*, 8020.

122. Dixon, D. A.; Fukunaga, T.; Smart, B. E. *J. Am. Chem. Soc.* **1986**, *108*, 4027.

123. Dixon, D. A.; Fukunaga, T.; Smart, B. E. *J. Phys. Org. Chem.* **1988**, *1*, 153.

124. Marynick, D. S. *J. Mol. Struct.* **1982**, *87*, 161.

125. Reutov, O. A.; Beletsyaka, I. P.; Butin, K. P. *CH-Acids*; Pergamon: Oxford, **1978**.

126. Streiweiser, A., Jr.; Mares, F. *J. Am. Chem. Soc.* **1968**, *90*, 2444.

127. Farnham, W. B.; Smart, B. E.; Middleton, W. J.; Calabrese, J. C.; Dixon, D. A. *J. Am. Chem. Soc.* **1985**, *107*, 4565.

128. Farnham, W. B.; Dixon, D. A.; Calabrese, J. C. *J. Am. Chem. Soc.* **1988**, *110*, 2607.

129. Cosmo, R.; Sternhell, S. *Aust. J. Chem.* **1987**, *40*, 35.

130. Sherrod, S. A.; daCosta, R. L.; Barnes, R. A.; Boekelheide, V. *J. Am. Chem. Soc.* **1974**, *96*, 1565.

131. Dolbier, W. R., Jr.; Palmer, K. W. *J. Am. Chem. Soc.* **1993**, *115*, 9349.

132. Palmer, K. W. Ph.D. Dissertation, University of Florida, **1993**.

133. Hirsch, J. *Top. Sterochem.* **1967**, *1*, 199.

134. Hansch, C.; Leo, A. *Substituent Constants for Correlation Analysis in Chemistry and Biology*; Wiley: New York, 1979.

135. Dawson, W. H.; Hunter, D. H.; Willis, C. J. *J. Chem. Soc., Chem. Commun.* **1980**, 874.

136. Scherer, K. V., Jr.; Ono, T.; Yamanouchi, R.; Fernandez, R.; Henderson, P.; Goldwhite, H. *J. Am. Chem. Soc.* **1985**, *107*, 718.

137. Haszeldine, R. N. *J. Chem. Soc.* **1949**, 2856.

138. Tarrant, P.; Lovelace, A. M. *J. Am. Chem. Soc.* **1954**, *76*, 3466.

139. Tarrant, P.; Lovelace, A. M. *J. Am. Chem. Soc.* **1955**, *77*, 2783.

140. Stefani, A. P.; Herk, L.; Szwarc, M. *J. Am. Chem. Soc.* **1961**, *83*, 4732.

141. Tedder, J. M.; Walton, J. C.; Winton, K. D. R. *J. Chem. Soc., Faraday Trans. I* **1972**, *68*, 1.

142. Low, H. C.; Tedder, J. M.; Walton, J. C. *J. Chem. Soc., Faraday Trans. I* **1976**, *72*, 1707.

143. Krusic, P. J.; Bingham, R. C. *J. Am. Chem. Soc.* **1976**, *98*, 230.

144. Bernardi, F.; Cherry, W.; Shaik, S.; Epiotis, N. D. *J. Am. Chem. Soc.* **1978**, *100*, 1352.

145. Benzel, M. A.; Maurice, A. M.; Belford, R. L.; Dykstra, C. E. *J. Am. Chem. Soc.* **1983**, *105*, 3802.

146. Paddon-Row, M. N.; Wong, S. S. *J. Mol. Struct.* **1987**, *150*, 109.

147. Pasto, D. J.; Krasnansky, R.; Zercher, C. *J. Org. Chem.* **1987**, *52*, 3062.

148. Wang, S. Y.; Borden, W. T. *J. Am. Chem. Soc.* **1989**, *111*, 7282.

149. Paddon-Row, M. N.; Thomson, C.; Ball, J. R. *J. Mol. Struct.* **1987**, *150*, 93.

150. Paddon-Row, M. N.; Wong, S. S. *J. Mol. Struct.* **1987**, *150*, 109.

151. Chen, Y.; Rauk, A.; Tschuikow-Roux, E. *J. Chem. Phys.* **1990**, *93*, 1187.

152. Chen, Y.; Rauk, A.; Tschuikow-Roux, E. *J. Chem. Phys.* **1990**, *93*, 6620.

153. Paddon-Row, M. N.; Houk, K. N. *J. Phys. Chem.* **1985**, *89*, 3771.

154. Bordwell, F. G.; Zhang, X. M. *Acc. Chem. Res.* **1993**, *26*, 510.

155. Seakins, P. W.; Pilling, M. J.; Niiranen, J. T.; Gutman, D.; Krasnoperov, L. N. *J. Phys. Chem.* **1992**, *96*, 9847.

156. Pickard, J. M.; Rodgers, A. S. *J. Am. Chem. Soc.* **1977**, *99*, 691.

157. Martell, J. M.; Boyd, R. J.; Shi, Z. *J. Phys. Chem.* **1993**, *97*, 7208.

158. Marshall, P.; Schwartz, M. *J. Phys. Chem. A* **1997**, *101*, 2906.

159. Zachariah, M. R.; Westmoreland, P. R.; Burgess, D. R., Jr.; Tsang, W.; Melius, C. F. *J. Phys. Chem.* **1996**, *100*, 8737.

160. Koopmans, T. A. *Physica* **1933**, *1*, 104.

161. Rodriquez, C. F.; Sirois, S.; Hopkinson, A. C. *J. Org. Chem.* **1992**, *57*, 4869.

162. Danovich, D.; Apeloig, Y.; Shaik, S. *J. Chem. Soc., Perkin Trans. II* **1993**, 321.

163. Tedder, J. M. *Tetrahedron* **1982**, *38*, 313.

164. Kim, S. S.; Kim, S. Y.; Ryou, S. S.; Lee, S. S.; Yoo, K. H. *J. Org. Chem.* **1993**, *58*, 192.

165. Brace, N. O. *J. Am. Chem. Soc.* **1964**, *86*, 523.

166. Brace, N. O. *J. Org. Chem.* **1966**, *31*, 2879.

167. Smart, B. E.; Feiring, A. E.; Krespan, C. G.; Yang, Z.-Y.; Hunh, M.-H.; Resnick, P. R.; Dolbier, W. R., Jr.; Rong, X. X. *Macromol. Symp.* **1995**, *98*, 753.

168. Hung, M.-H.; Resnick, P. R.; Smart, B. E.; Buck, W. H. In *Polymeric Materials Encyclopedia*; Salamone, J. C., Ed.; CRC Press: Boca Raton, **1996**, *4*, 2466.

169. *Biomedical Aspects of Fluorine Chemistry*; Filler, R., Kobayashi, Y., Eds.; Kodansha and Elsevier Biomedical: Tokyo, Amsterdam and New York, **1983.**

170. Rong, X. X. Ph.D. Dissertation, University of Florida, **1995**.

171. Gonzalez, J.; Foti, C. J.; Elsheimer, S. *J. Org. Chem.* **1991**, *56*, 4322.

172. Burton, D. J.; Kehoe, L. J. *J. Org. Chem.* **1970**, *35*, 1339.

173. Zav´yalov, S. I.; Ezhova, G. I.; Sitkareva, I. V.; Dorofeeva, O. V.; Zavozin, A. G.; Rumyantseva, E. E. *Isv. Akad. Nauk. SSSR* **1989**, *10*, 2392.

174. Barton, D. H. R.; Lacher, B.; Zard, S. Z. *Tetrahedron* **1986**, *42*, 2325.

175. Hauptschein, M.; Stokes, C. S.; Grosse, A. V. *J. Am. Chem. Soc.* **1952**, *74*, 848.

176. Hauptschein, M.; Kinsman, R. L.; Grosse, A. V. *J. Am. Chem. Soc.* **1952**, *74*, 849.

177. Hudlický, M. *Chemistry of Organic Fluorine Compounds*; Ellis Horwood: Chichester, **1976**, 358.

178. Pierce, O. R.; Meiners, A. F.; McBee, E. T. *J. Am. Chem. Soc.* **1953**, *75*, 2516.

179. Miller, W. T., Jr.; Bergman, E.; Fainberg, A. H. *J. Am. Chem. Soc.* **1957**, *79*, 4159.

180. Alvernhe, G.; Laurent, A.; Haufe, G. *Synthesis* **1987**, 562.

181. Rondestvedt, C. S., Jr. *J. Org. Chem.* **1977**, *42*, 1985.

182. Citterio, A.; Arnoldi, A.; Minisci, F. *J. Org. Chem.* **1979**, *44*, 2674.

183. Johnston, L. J.; Scaiano, J. C.; Ingold, K. U. *J. Am. Chem. Soc.* **1984**, *106*, 4877.

184. Martell, J. M.; Boyd, R. J. *J. Phys. Chem.* **1992**, *96*, 6287.

185. Becke, A. D. *J. Chem. Phys.* **1993**, *98*, 5648.

186. Lee, C.; Yang, W.; Parr, R. G. *Phys. Rev. B* **1988**, *37*, 785.

187. *CRC Handbook of Chemistry and Physics, 76th Edition*; Lide, D. R., Ed.; CRC Press: Boca Raton, **1995-1996**, 9-63-9-67.

188. *NIST Structures Properties Database and Estimation Program 1991*; U.S. Department of Commerce: Gaithersburg, MD, **1991**.

189. Wong, M. W.; Pross, A.; Radom, L. *J. Am. Chem. Soc.* **1993**, *115*, 11050.

190. Wong, M. W.; Pross, A.; Radom, L. *Isr. J. Chem.* **1993**, *33*, 415.

191. Singh, U. C.; Kollman, P. A. *J. Comp. Chem.* **1984**, *5*, 129.

192. Besler, B. H.; Merz, K. M., Jr.; Kollman, P. A. *J. Comp. Chem.* **1990**, *11*, 431.

193. Cort, A. D. *Syn. Comm.* **1990**, *20*, 757.

194. Corey, E. J.; Su, W. *Tet. Lett.* **1984**, *25*, 5119.

195. Morikawa, T.; Kodama, Y.; Uchida, J.; Takano, M.; Washio, Y.; Taguchi, T. *Tetrahedron* **1992**, *48*, 8915.

196. Nobes, R. H.; Pople, J. A.; Radom, L.; Handy, N. C.; Knowles, P. J. *Chem. Phys. Lett.* **1987**, *138*, 481.

197. Stanton, J. F. *J. Chem. Phys.* **1994**, *101*, 371.

198. Chen, W.; Schlegel, H. B. *J. Chem. Phys.* **1994**, *101*, 5957.

199. Frisch, M. J.; Trucks, G. W.; Schlegel, H. B.; Gill, P. M. W.; Johnson, B. G.; Robb, M. A.; Cheeseman, J. R.; Keith T.; Petersson, G. A.; Montgomery, J. A.; Raghavachari, K.; Al-Laham, M. A.; Zakrzewski, V. G.; Ortiz, J. V.; Foresman, J. B.; Cioslowski, J.; Stefanov, B. B.; Nanayakkara, A.; Challacombe, M.; Peng, C. Y.; Ayala, P. Y.; Chen, W.; Wong, M. W.; Andres, J. L.; Replogle, E. S.; Gomperts, R.; Martin, R. L., Fox, D. J., Binkley, J. S.; Defrees, D. J.; Baker, J.; Stewart, J. P.; Head-Gordon, M.; Gonzalez, C.; Pople, J. A. *Gaussian 94*, Revision C.3, Gaussian, Inc., Pittsburgh PA, 1995.

200. Scott, A. P.; Radom, L. *J. Phys. Chem.* **1996**, *100*, 16502.

201. Bauschlicher, C. W., Jr.; Partridge, H. *J. Chem. Phys.* **1995**, *103*, 1788.

202. Hehre, W. J.; Radom, L.; Schleyer, P. v. R.; Pople, J. A. *Ab Initio Molecular Orbital Theory*; Wiley: New York, **1986**.

BIOGRAPHICAL SKETCH

Michael David Bartberger was born September 6, 1970, in Ft. Lauderdale, Florida, the first of two children, and spent his childhood years in the Margate / North Lauderdale area.

Michael received a B.S. degree in chemistry from the University of Central Florida in May of 1992, during which time he was introduced to organic fluorine chemistry by University of Florida alumnus and former Dolbier group member, Professor Seth Elsheimer.

In August of 1992, Michael began graduate study at the University of Florida, having practically joined the research group of Professor William R. Dolbier, Jr. even before moving to Gainesville. In addition to experimental physical organic studies, Michael developed an interest in theoretical methodology, having been exposed to the results of AM1 calculations attractively displayed on a Tektronix CAChe workstation. With a few days of instruction from Dr. Max Muir (a postdoc from another group working on some semiempirical calculations as a favor to the Dolbier group, leaving UF shortly thereafter for a position at MSI) Michael set out to hone his own computational chemistry skills. Spending many late nights at the workstation, he developed his proficiency with the MOPAC, ZINDO, *Gaussian*, ACES II, and GAMESS program systems, leading to a number of productive collaborations with other members of the department, both within and outside the Dolbier group. The highlight of his graduate career came in August of 1996, as an invited participant in the Elucidation of Reaction Mechanisms by *Ab Initio* Methods Symposium held at the 212th National Meeting of the American Chemical Society in Orlando, Florida.

Michael is a recipient of the Department of Chemistry Excellence in Teaching Award, the Shell Foundation Fellowship, and has twice received the Outstanding Presentation Award administered by the Florida Section of the American Chemical Society, once as an undergraduate.

At the time of this writing, Michael had accepted a position as a postdoctoral research associate in the Department of Chemistry and Biochemistry at the University of California, Los Angeles, under the direction of Professor K. N. Houk.

I certify that I have read this study and that in my opinion it conforms to acceptable standards of scholarly presentation and is fully adequate, in scope and quality, as a dissertation for the degree of Doctor of Philosophy.

William R. Dolbier, Jr., Chair
Professor of Chemistry

I certify that I have read this study and that in my opinion it conforms to acceptable standards of scholarly presentation and is fully adequate, in scope and quality, as a dissertation for the degree of Doctor of Philosophy.

Merle A. Battiste
Professor of Chemistry

I certify that I have read this study and that in my opinion it conforms to acceptable standards of scholarly presentation and is fully adequate, in scope and quality, as a dissertation for the degree of Doctor of Philosophy.

Kirk S. Schanze
Professor of Chemistry

I certify that I have read this study and that in my opinion it conforms to acceptable standards of scholarly presentation and is fully adequate, in scope and quality, as a dissertation for the degree of Doctor of Philosophy.

Rodney J. Bartlett
Graduate Research Professor of Chemistry

I certify that I have read this study and that in my opinion it conforms to acceptable standards of scholarly presentation and is fully adequate, in scope and quality, as a dissertation for the degree of Doctor of Philosophy.

John R. Sabin
Professor of Physics

This dissertation was submitted to the Graduate Faculty of the Department of Chemistry in the College of Liberal Arts and Sciences and to the Graduate School and was accepted as partial fulfillment of the requirements for the degree of Doctor of Philosophy.

May, 1998

_____

Dean, Graduate School

LD
1780
1998
.B283